Stockholm University

Transition metal-catalysed hydrogen transfer processes for C–C and C–N bond formation

Synthetic studies and mechanistic investigations

Agnieszka Bartoszewicz

© Agnieszka Bartoszewicz, Stockholm 2012

ISBN 978-91-7447-595-1

Printed in Sweden by US-AB, Stockholm 2012
Distributor: Department of Organic Chemistry, Stockholm University

Abstract

This thesis focusses on synthetic studies and mechanistic investigations of reactions involving hydrogen-transfer processes.

In the first part, the development of an efficient method for the synthesis of β-hydroxy ketones (aldols) and β-amino ketones (Mannich products) from allylic alcohols and aldehydes is described. These reactions use $Ru(\eta^5\text{-}C_5Ph_5)(CO)_2Cl$ as the catalyst. The reaction parameters were optimised in order to suppress the formation of undesired by-products, such as saturated ketones, benzyl alcohols, and α,β-unsaturated ketones. Neutral and mild reaction conditions enabled the synthesis of a variety of aldol products in up to 99% yield, with a good *syn*/*anti* ratio. The influence of the stereoelectronic properties of the catalyst on the reaction outcome was also studied. Based on the results obtained, a plausible reaction mechanism has been proposed, involving as the key steps the 1,4-addition of hydride to α,β-unsaturated ketones and the formation of ruthenium (*Z*)-enolates.

In the second part of this thesis, a ruthenium-catalysed tandem isomerisation/C–H activation reaction is presented. A number of ruthenium complexes, phosphine ligands, and additives were evaluated in order to establish the optimal reaction conditions. It was found that the use of a stable ruthenium catalyst, $Ru(PPh_3)_3Cl_2$, together with P*t*Bu_3 and HCO_2Na resulted in an efficient tandem transformation. Using this procedure, a variety of *ortho*-alkylated aromatic ketones were obtained in excellent yields and in short reaction times. Moreover, homoallylic alcohols could also be used as starting materials for the reaction, which further expands the substrate scope. Mechanistic investigations into the isomerisation part of the process were carried out.

The last project described in the thesis deals with the design and preparation of novel bifunctional iridium complexes containing an *N*-(2-hydroxy-isobutyl)-*N*-Heterocyclic carbene ligand. These complexes were used as catalysts to alkylate amines using alcohols as latent electrophiles. The catalytic system developed here was found to be one of the most active systems reported to date, allowing the reaction to be performed at temperatures as low as 50 °C for the first time. A broad substrate scope was examined, including various primary and secondary alcohols. These alcohols could be efficiently coupled with both primary and secondary aromatic amines. Combined experimental and theoretical studies into the reaction mechanism are consistent with a metal-ligand bifunctional activity of the new catalyst.

List of Publications

This thesis is based on the following publications, referred to in the text by their Roman numerals:

I. **Synthesis of β-Hydroxy Ketones from Allylic Alcohols *via* Catalytic Formation of Ruthenium Enolates**
Agnieszka Bartoszewicz, Madeleine Livendahl, and Belén Martín-Matute
Chemistry – A European Journal **2008**, *14*, 10547-10550.

II. **Synthesis of β–Hydroxy and β–Amino Ketones from Allylic Alcohols Catalysed by Ru η^5-$Ph_5C_5(CO)_2Cl$**
Agnieszka Bartoszewicz, Martina M. Jeżowska, Kévin Laymand, Juri Möbus, and Belén Martín-Matute
*European Journal of Inorganic Chem*istry **2012**, 1517-1530.

III. **Building Molecular Complexity *via* Tandem Ru catalysed Isomerisation/C–H Activation.**
Agnieszka Bartoszewicz and Belén Martín-Matute
Organic Letters **2009**, *11*, 1749-1752.

IV. **A Highly Active Bifunctional Iridium Complex with an Alcohol/Alkoxide-Tethered *N*-Heterocyclic Carbene for Alkylation of Amines with Alcohols**
Agnieszka Bartoszewicz, Rocío Marcos, Suman Sahoo, A. Ken Inge, Xiaodong Zou, and Belén Martín-Matute
Chemistry – A European Journal **2012**, *18*, 14510-14519.

Appendix 1. **Alkylation of Amines with Alcohols Catalysed by a Bifunctional Iridium Complex: A Mechanistic Investigation**
Agnieszka Bartoszewicz, Rocío Marcos, Per-Ola Norrby, and Belén Martín-Matute
Appendix

Reprints were made with kind permission from the publishers.

Publications not included in this thesis:

A Family of Highly Stable Lanthanide Metal−Organic Frameworks: Structural Evolution and Catalytic Activity
Mikaela Gustafsson, Agnieszka Bartoszewicz, Belén Martín-Matute, Junliang Sun, Jekabs Grins, Tony Zhao, Zhongyue Li, Guangshan Zhu, and Xiaodong Zou
Chemistry of Materials **2010**, *22*, 3316-3322.

A Facile Synthesis of α-Fluoroketones Catalysed by $[Cp^*IrCl_2]_2$
Nanna Ahlsten, Agnieszka Bartoszewicz, Santosh Agrawal, and Belén Martín-Matute
Synthesis, **2011**, 2600-2608.

Microporous Aluminoborates with 18- and 24-Octahedral-Atom Channels: Structural and Catalytic Properties
Tao Yang, Agnieszka Bartoszewicz, Jing Ju, Junliang Sun, Zheng Liu, Xiaodong Zou; Yingxia Wang, Guobao Li, Fuhui Liao, Belén Martín-Matute, and Jianhua Lin
Angewandte Chemie International Edition **2011**, *50*, 12555-12558.

Ruthenium Complexation in an Aluminium Metal-Organic Framework and its Application in Alcohol Oxidation Catalysis
Fabian Carson, Santosh Agrawal, Mikaela Gustafsson, Agnieszka Bartoszewicz, Francisca Moraga, Xiaodong Zou, Belén Martín-Matute
Chemistry – A European Journal **2012**,
DOI: 10.1002/chem.201200885

Allylic Alcohols as Synthetic Enoalte Equivalents: Isomerisation and Tandem Reactions Catalysed by Transition Metal Complexes
Nanna Ahlsten, Agnieszka Bartoszewicz, and Belén Martín-Matute
Dalton Transactions **2012**, *41*, 1660-1670. (review)

Enantioselective Synthesis of Alcohols and Amines *via* Iridium-Catalyzed Hydrogenation, Transfer Hydrogenation and Related processes
Agnieszka Bartoszewicz, Nanna Ahlsten, and Belén Martín-Matute
Under revision. (review)

Contents

Abbreviations

The abbreviations and acronyms used are in agreemement with the standards of the subject. [1]

Chapter 1

Introduction

1.1 Multi-component synthesis

Much of the research effort in synthetic organic chemistry is focussed on the development of highly active and selective homogenous or heterogeneous catalysts that are capable of conducting only a single step reaction. The most remarkable examples of synthetic efficiency are, however, multi-component reactions, in which a synthetic sequence is carried out as a 'one-pot' process without isolating any of the intermediates, and preferably using only one catalyst.

This methodology has many advantages, such as reduction of waste and reduction of the number of operations required (*e.g.* isolation of intermediates). From an academic point of view, high molecular complexity can be achieved in a single transformation. This feature leads to shorter synthetic routes, and therefore improved time efficiency. One-pot multi-component reactions have attracted a lot of attention, and the number of recent reviews in this area highlights their increasing popularity.[2]

Multi-component reactions must be carefully designed and optimised to ensure that the correct sequence of events is followed in the right order. Combining two or more elementary reactions is the major challenge in developing new one-pot reactions.

Tandem, domino, cascade, and one-pot reactions are often used as interchangeable synonyms referring to the transformation of a substrate through two or more individual reactions, with just a single work-up step. Although these terms have similar meanings, there are some significant differences between each of the processes they describe. 'One-pot process' is a broad term that can be used as a synonym for all tandem, domino, and cascade transformations. If one of the catalysts is not present in the reaction mixture from the beginning, but is added after the preceding reactions are finished, the process is called a one-pot bicatalytic reaction. Domino and tandem reactions require that all the catalytic species are present from the outset. Domino (cascade) reactions are those in which multiple transformations are effected with a single catalytic mechanism. A more detailed classification of domino reactions has been introduced by Tietze.[2b] According to the definitions proposed by Fogg and Santos,[2g] tandem

catalysis, in contrast to domino catalysis, consists of two or more mechanistically distinct processes.

1.2 Borrowing hydrogen strategy

During the past decade, a variety of catalytic transformations involving the temporary oxidation of an alcohol into the corresponding ketone or aldehyde have been reported (Scheme 1).[3] In these metal-catalysed redox processes, the reactivity of the *in situ* generated carbonyl compound is exploited by its reaction with other reagents. The unsaturated intermediate formed is then reduced in the final step of the transformation, using the hydrogen originating from the starting alcohol substrate. Therefore, the net amount of hydrogen remains constant (Scheme 1). This methodology has been named the "borrowing hydrogen strategy".[3]

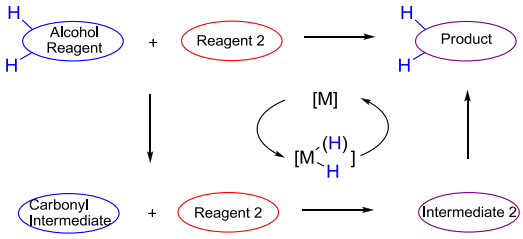

Scheme 1. General mechanism for the reaction involving borrowing hydrogen strategy.

This methodology can be utilised in a number of possible transformations. The most popular examples of functionalisation of the *in situ* formed carbonyl intermediate are: (i) imine formation, followed by hydrogenation (Scheme 2a);[4] (ii) formation of alkanes by an indirect Wittig-type reaction, followed by reduction of the double bond (Scheme 2b);[3] (iii) enolisation, α-functionalisation, and reduction to give a functionalised alcohol (Scheme 2c); or (iv) reaction of the carbonyl compound with carbon nucleophiles, followed by dehydration and reduction of the resulting double bond (Scheme 2d).[3]

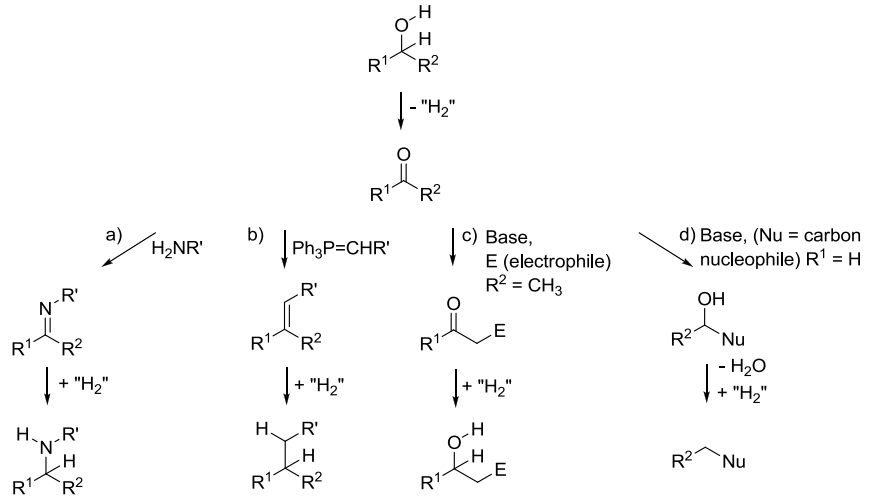

Scheme 2. Selected examples of the functionalisation of alcohols by intramolecular hydrogen transfer strategy.

1.3 Bifunctional catalysis

A bifunctional catalyst contains both Lewis acidic and Lewis basic centres, which simultaneously activate nucleophilic and electrophilic sites of the reagents. In organometallic chemistry, this term most often refers to a specific set of catalysts that are capable of accepting both a proton and a hydride from a reagent, for example from a *sec*-alcohol. Similarly, the reduced form of the catalyst can transfer a proton and a hydride to an unsaturated substrate, for example a carbonyl compound.[5,6]

Two of the most recognised bifunctional catalysts are the Shvo[6] and the Noyori/Ikariya[5] catalysts (Figure 1). These complexes catalyse reactions involving the oxidation of alcohol and amine substrates. In their reduced forms, these complexes catalyse the hydrogenation of carbonyls and imines.

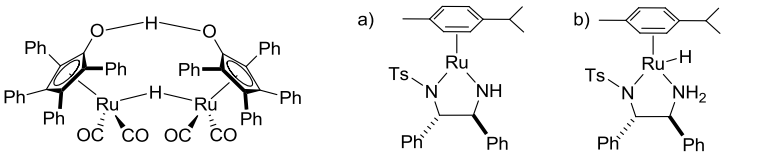

Shvo catalyst

Noyori/Ikariya catalyst: a) amido form, b) hydride form

Figure 1.

A bifunctional catalyst may operate by an outer-sphere or an inner-sphere mechanism (Scheme 3). The outer-sphere mechanism involves a pericyclic six-membered transition state (Scheme 3a) in which both the proton and the hydride are simultaneously transferred from the substrate to

the catalyst (or *vice versa* in the reverse step). The characteristic feature of this mechanism is that it does not involve direct coordination of the reactant to the metal.

The inner-sphere mechanism consists of two consecutive steps. The substrate (*e.g.* a carbonyl compound) coordinates to the metal centre and gets protonated by the Brønsted acidic site of the catalyst. In a second step, the hydride is transferred from the metal to the substrate. Overall, the substrate gets reduced, producing an alcohol in this case. In the reverse step, both the acidic OH proton and the α hydrogen [C*H*(OH)] of an alcohol substrate are transferred to the metal in two consecutive steps. In contrast to the outer-sphere mechanism, both of these steps involve the direct coordination of the substrate to the metal centre (Scheme 3b).

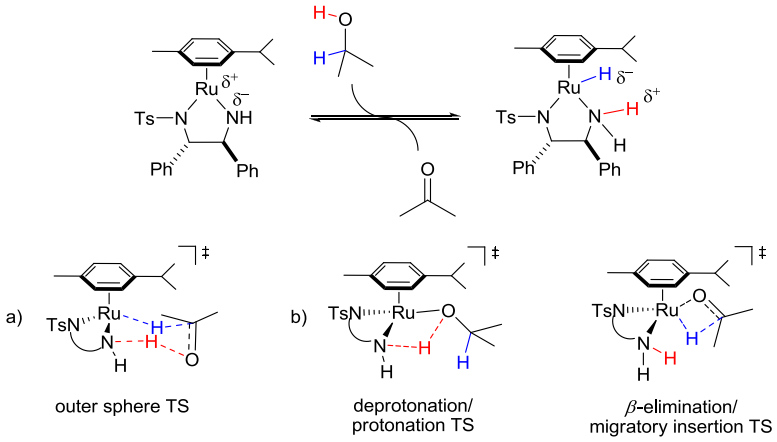

Scheme 3. The modes of action of a metal-ligand bifunctional catalyst. Key transition states of the a) outer-sphere and b) inner-sphere mechanisms.

The catalytic activity of bifunctional complexes is not limited to hydrogen-transfer processes involving alcohols/ketones or amines/imines. In principle, the Lewis acidic and basic sites should be capable of reacting with other polar reagents. This is indeed the case, and for instance, the addition of malonates to Michael acceptors as nitro olefins or cyclic enones, catalysed by the Noyori/Ikariya complex has been reported (Scheme 4).[5f]

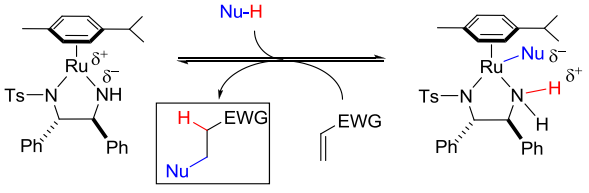

Scheme 4. Michael addition with a bifunctional catalyst (EWG = electron withdrawing group).

1.4 Isomerisation of allylic alcohols to ketones

The conversion of allylic and other unsaturated alcohols into saturated carbonyl compounds is a useful synthetic transformation.[7,8] Conventionally, such a reaction would require a two-step, sequential oxidation and reduction (or *vice versa*), that are fundamentally opposite processes (Scheme 5a). Transition-metal complexes allow a one-pot catalytic internal redox reaction that leads to the same overall outcome (Scheme 5b). The reaction is highly thermodynamically favoured – the energy of a C=O plus a C–C bond compared to a C=C plus a C–O bond is lower by 125 kJ/mol (30 kcal/mol) in favour of the carbonyl compound.[9]

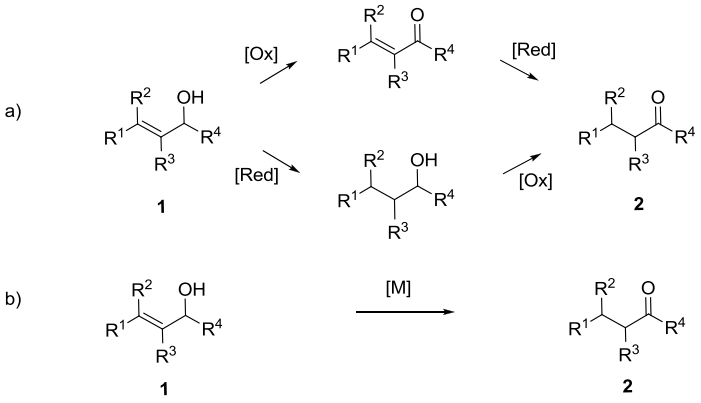

Scheme 5. a) Transformation of allylic alcohols into saturated carbonyl compounds using a two-step sequence; b) direct transition-metal-catalysed redox isomerisation of allylic alcohols.

From an atom economy point of view,[10] isomerisation can be a highly efficient process, without any by-product formation. Another advantage is that the stoichiometric use of expensive and usually toxic reagents, especially in the oxidation reactions, is avoided. From a total synthesis perspective, one can treat an allylic alcohol as the synthetic equivalent of a carbonyl group. This is indeed an advantage in cases where a specific allylic alcohol is cheaper or more readily available than its ketone equivalent.[11]

Various complexes of Ru, Rh, Fe, Co, Ni, Mo, Os, Ir, Pd, and Pt have been used for the isomerisation of allylic alcohols into ketones and aldehydes.[7] Some of them have limited scope due to the harsh reaction conditions required. Also, most of the catalytic systems do not tolerate all the possible substitution patterns of the substrate (R^1, R^2, R^3, R^4). When R^1 and R^2 are different groups and the catalyst is chiral, an asymmetric version of this reaction is possible.[7d,12]

1.4.1 The isomerisation mechanisms

Three mechanisms have been proposed for the isomerisation of allylic alcohols into aldehydes or ketones, catalysed by metal complexes.[7] All of them involve metal monohydride intermediates.

In the first mechanism (Scheme 6), the catalyst is a metal hydride, either isolated or generated *in situ*. Upon coordination of the substrate, reversible insertion of the alkene into the M–H bond occurs, followed by β-hydride elimination of the hydrogen atom adjacent to the OH group. This step generates an enol. After decoordination from the metal, the enol tautomerises to the carbonyl derivative.

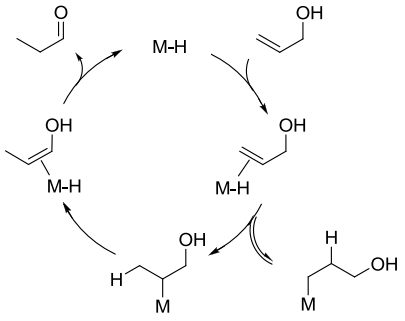

Scheme 6. Metal-hydride-catalysed isomerisation *via* olefin migratory insertion / β-hydride elimination.

In the second isomerisation mechanism (Scheme 7), a π-allyl metal hydride complex is formed by coordination of the metal complex (which does not contain a hydride ligand) to the double bond, followed by oxidative addition of a C–H bond. A shift of the hydride to the other side of the allylic system (by reductive elimination) leads to an enol complex.

In contrast to the first isomerisation mechanism (Scheme 6), in the π-allyl mechanism, the hydrogen transfer is entirely intramolecular. This isomerisation mechanism has been proposed for some low-valent metal complexes, since during the course of this mechanism, the oxidation state of the metal must be increased by two.[8f,8i,8s]

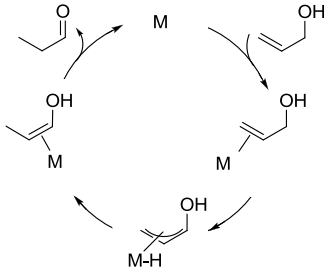

Scheme 7. Isomerisation *via* π-allyl metal-hydride intermediates.

In the third isomerisation mechanism, in contrast to the previously described cases, the metal species coordinates preferentially to the oxygen rather than to the olefin (Scheme 8). The reaction usually involves metal halides as catalyst precursors, and catalytic amounts of base, which allows the generation of metal-alkoxide intermediates.[13] The alkoxide undergoes a β-hydride elimination producing an α,β-unsaturated ketone. Next, reduction of the double bond of this intermediate can occur by 1,4-addition of hydride to the double bond *via* a six-membered transition state, forming a metal enolate (Scheme 8, path a).[8m,8w] Alternatively, a migratory insertion of the olefin into the metal hydride bond (*via* a metal olefin complex) would generate a C-bound transition-metal enolate (Scheme 8, path b).[8o] Crossover experiments have shown that the hydride transfer can occur in an intramolecular fashion when the reaction is run under mild conditions. However, with higher reaction temperatures or with more sterically crowded substrates, the enone intermediate may decoordinate, resulting in an intermolecular hydrogen transfer.[8m] Finally, the metal enolate undergoes protonation by another allylic alcohol molecule, and the released enol readily tautomerises into the saturated carbonyl compound.

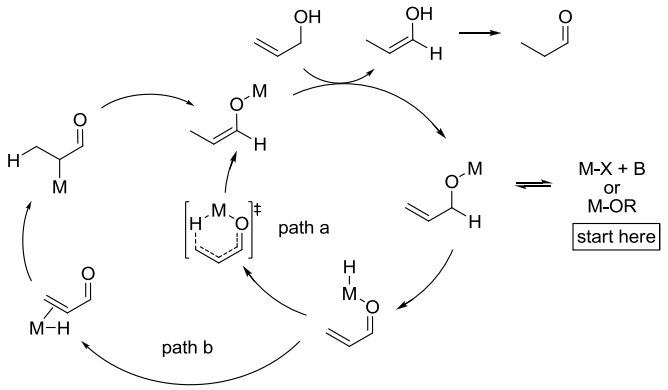

Scheme 8. Isomerisation by β-hydride elimination from metal alkoxide complexes.

A special variant of the isomerisation mechanism shown in Scheme 8 uses metal–ligand bifunctional catalysts. This is the case, for instance, with the Cp*Ru(PN) family of complexes, which have the general structure shown in Scheme 9a, as reported by Ikariya.[12b] The unsaturated 16-electron Ru complex dehydrogenates an allylic alcohol through a six-membered concerted transition state, in which the proton from the OH group and the α-hydride are transferred regiospecifically to the NH group and the metal, respectively (Scheme 9a). The second step in this mechanism is a hydrogenation of the α,β-unsaturated ketone, again in a regiospecific manner.[14] The substrate scope for this transformation is quite broad, and additional unsaturations are tolerated.

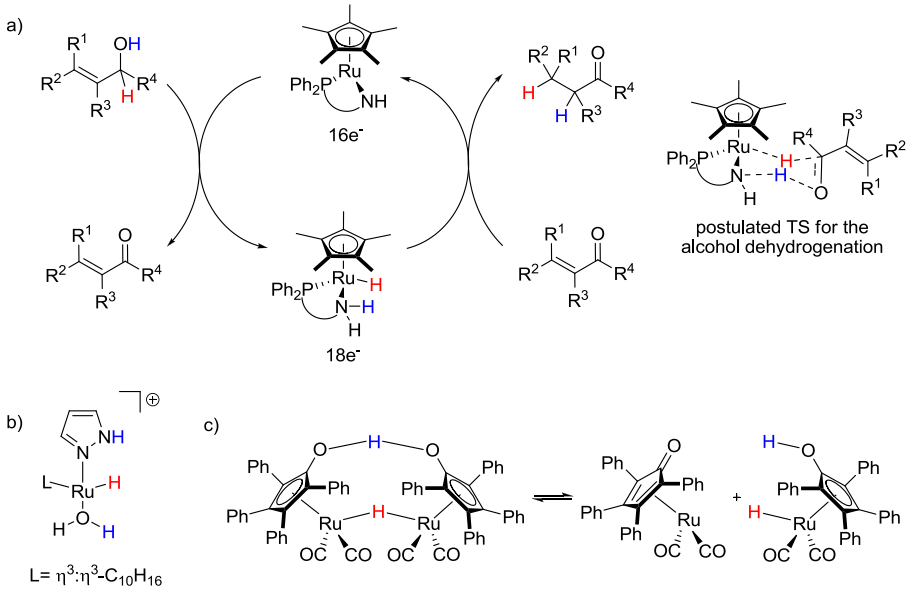

Scheme 9. Isomerisation with bifunctional catalysts a) general isomerisation scheme and postulated transition state with Ikariya catalyst; b) Gimeno's catalyst; c) Shvo's catalyst and its monomeric forms.

Other examples using bifunctional catalysts for allylic alcohol isomerisation have been reported by Gimeno and Lledós (a Ru(IV) complex, Scheme 9b),[8y,8z] and Bäckvall (Shvo's catalyst,[6a,6b] Scheme 9c).[8d] In the former case, it was shown that a water molecule coordinated to the metal centre acts as a proton donor/acceptor site. Shvo's catalyst, on the other hand, dissociates into two monomeric forms that are the saturated and unsaturated forms of the bifunctional complex. The carbonyl moiety on the cyclopentadienone ruthenium complex acts as a proton acceptor.

1.5 Tandem isomerisation/enolate intermediate trapping

As described in the previous section, the transition-metal-catalysed isomerisation of allylic alcohols can proceed *via* enolate or enol intermediates. This can be exploited by trapping these species with a suitable electrophile, thus resulting in an overall tandem process (Scheme 10). For instance, enols/enolates formed by the isomerisation were intercepted with aldehydes or imines, yielding aldols or Mannich-type products, respectively.[15] The use of less common electrophiles such as electrophilic heteroatomic species ('F^+', 'Cl^+' and 'Br^+') for this coupling reaction was recently achieved in our group.[16]

The tandem reactions involving the initial formation of metal enolates from allylic alcohols are good alternatives to the most commonly used

approaches to aldol and Mannich-type reactions. The big advantage of this methodology is that the regioselectivity in the enol/enolate formation step is, except for a few cases,[15b] fully controlled. Also generation of enols/enolates from allylic alcohols overcomes some of the limitations of the ordinary used methods (Scheme 10). For example, stoichiometric amounts of strong bases or stoichiometric formation of enol derivatives are not necessary. Also, self-condensation is not observed due to the neutral reaction conditions used.

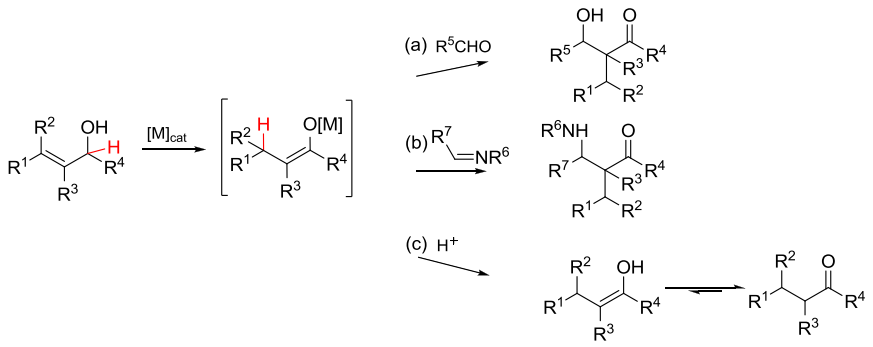

Scheme 10. a) Formation of aldols from allylic alcohols using a catalytic amount of a transition metal complex; b) formation of Mannich-type products; c) protonation of transition metal enolates leading to unwanted carbonyl compounds. Note that the key intermediate shown in the scheme is an O-bound enolate, but it may also be a C-bound enolate or free enol, depending on the catalytic system and the exact isomerisation mechanism (*cf.* Schemes 6–8).

A number of research groups have attempted the transition-metal-catalysed coupling of allylic alcohols with aldehydes with some success. Among them, the groups of Li[15d-f,h] and Grée[15b,c,g,i,j,l,m,q] have made major contributions to this field. However, a limitation encountered in many instances has been the formation of ketones by isomerisation, which is an undesired side-reaction in the tandem process (Scheme 10c). The success of the tandem reaction relies on efficient trapping of the enolate intermediate with the electrophile before it can be protonated.

Li *et al*. used $Ru(PPh_3)_3Cl_2$ in toluene/H_2O mixtures at 100 ºC to obtain aldols in moderate yields (27–72%).[15d,15e] The yield of the aldol products increased in the presence of $In(OAc)_3$ as a Lewis acid additive. The same catalyst and similar reaction conditions were used in a *one-pot* three-component Mannich-type reaction, in which 1-buten-3-ol was successfully coupled with imines, generated *in situ* from various aromatic aldehydes and 4-methoxy-aniline, to give the coupling products in 44–70% yield.[15e]

Grée and co-workers used $Rh(PPh)_3Cl$ and $Ru(PPh_3)_3Cl_2$, activated with Grignard or organolithium reagents, to synthesise aldols in up to 75% yield, albeit accompanied by significant amounts of the ketone by-products (5–52%).[15c] They also used $Fe(CO)_5$ activated under irradiation conditions.[15b] Mechanistic studies revealed that under these conditions, isomerisation of

allylic alcohols to enols occurs *via* π-allyl species (Scheme 5). Small amounts of regioisomeric aldols were observed due to further 1,3-hydride shift, which led to the formation of small amounts of a constitutional isomer of the aldol product (Scheme 11).

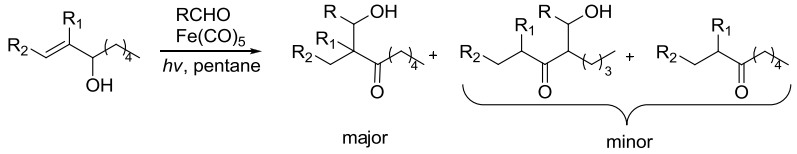

Scheme 11. Tandem aldol-type reaction catalysed by $Fe(CO)_5$.

So far, the best results have been achieved with Ni complexes and Mg salts as co-catalysts, reported by Grée and co-workers; aldol products were formed in high yields, together with small amounts of ketones (2–15%).[15m] Isomerisation to the enolate in this case was proposed to occur by a mechanism involving Ni-alkoxides (Scheme 8).

In the course of the aldol and Mannich reactions, one or two new stereogenic centres are created. In most examples, low diastereoselectivities were obtained. Depending on the starting allylic alcohol and the electrophile used, *syn*/*anti* ratios from 1:1 to 4:1 have been observed. Only for allylic alcohols containing a bulky substituent next to the OH functional group (group R^4 = *t*Bu or $C(Me)_2CO_2Et$ in Scheme 10) could an excellent diastereoisomeric ratio of 19:1 be obtained using the above-mentioned Ni catalyst.[15m]

As for the enantioselectivity, in contrast to the classical aldol[17] and reductive aldol and Mannich-type reactions,[18] no efficient chiral catalyst for the tandem isomerisation/aldol or Mannich-type reaction of allylic alcohols has been developed. Two unsuccessful attempts using chiral ruthenium and nickel complexes have been reported.[8k,15m] Recently, Grée's group used enantiopure *N*-*tert*-butylsulfinimines as electrophiles in a diastereoselective synthesis of *β*-amino ketones and *β*-amino ketones with the $NiHCl(dppe)/MgBr_2$ catalytic system (Scheme 12).[15q]

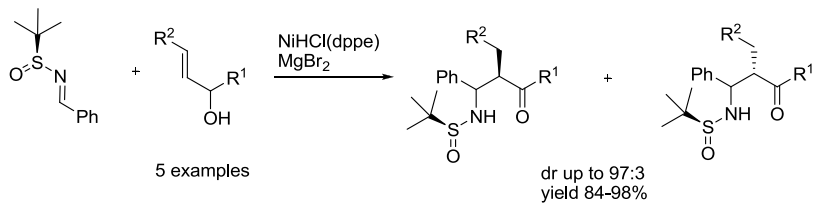

Scheme 12. Diastereoselective tandem isomerisation/Mannich-type reaction.

In most cases, intermediate O-bound metal enolates and a Zimmerman–Traxler cyclic six-membered transition state model[19] were proposed for the C–C coupling step (Scheme 13). However, it is difficult to be certain that it

is the transition metal that is binding to the enolate and the electrophile in the transition state. Possibly, it could also be any alkali metal cation, which are often present in the reaction mixture, or alternatively, a proton of the free enol. Theoretical investigations have shown that the latter is the case in the reaction involving an $Fe(CO)_5$ catalyst.[15j] The fact that no enantioselectivity was observed with chiral Ni complexes was used as an argument against the involvement of the transition metal in the C–C bond-forming step.[15m] The authors of this study also excluded the involvement of magnesium enolates as possible intermediates, since such enolates when prepared independently gave no C–C bond formation upon treatment with aldehydes.

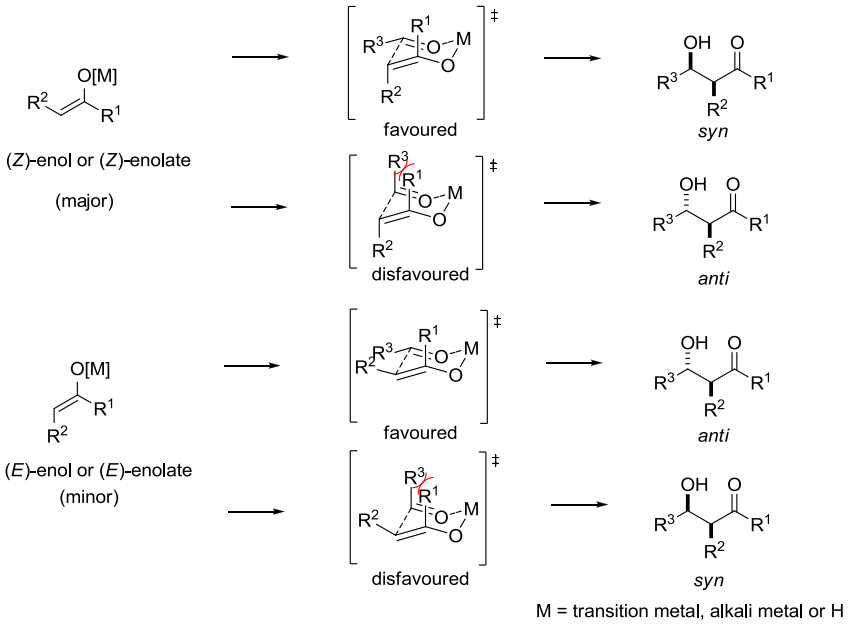

Scheme 13. Aldol couplings from (*Z*)- and (*E*)- enols/enolates.

In the tandem aldol and Mannich-type reactions described above, the *syn* diastereomer was usually the major product. Since the Zimmerman–Traxler model predicts formation of the *syn* aldol from (*Z*)-enolate, the observed product distribution could be accounted for by preferential formation of (*Z*)-enol/enolate complexes during the isomerisation. In specific cases, the reaction mechanism allows only the formation of (*Z*)-enolates (Scheme 6, path a),[8m] and in general, (*Z*)-enolates should be favoured due to steric reasons (allylic strain may occur in the (*E*)-enolate).

According to the model, the *syn*/*anti* diastereoisomeric ratio should increase with larger R^1 substituents on the alcohol and R^3 on the aldehyde, and this was indeed observed for the Ni complex.[15m] However, it is also

possible that the C–C bond formation takes places according to a transition state other than the Zimmerman–Traxler one, and the observed diastereoselectivity may not originate from preferential (*Z*)-enolate formation.

1.6 Transition-metal-catalysed C(sp^2)–H cleavage

Catalytic processes involving functionalisation of unreactive C–H bonds are highly desirable and useful, both within the research and industrial areas of organic synthesis, since they fulfill the requirements of atom economy.[10] Therefore, much research effort has been devoted to the design and synthesis of new catalytic systems that can effect the C–H activation efficiently under mild reaction conditions.[20]

There are four generally accepted mechanisms proposed for aromatic C–H bond cleavage by transition metal complexes: oxidative addition, σ-bond metathesis, electrophilic substitution and ligand-assisted concerted metallation-deprotonation (Scheme 14).[20] Two additional mechanisms: 1,2 C–H addition to metal carbenoids and metalloradical C–H activations are much more common for C(sp^3)–H bond activations, and thus will not be discussed here.[21,22]

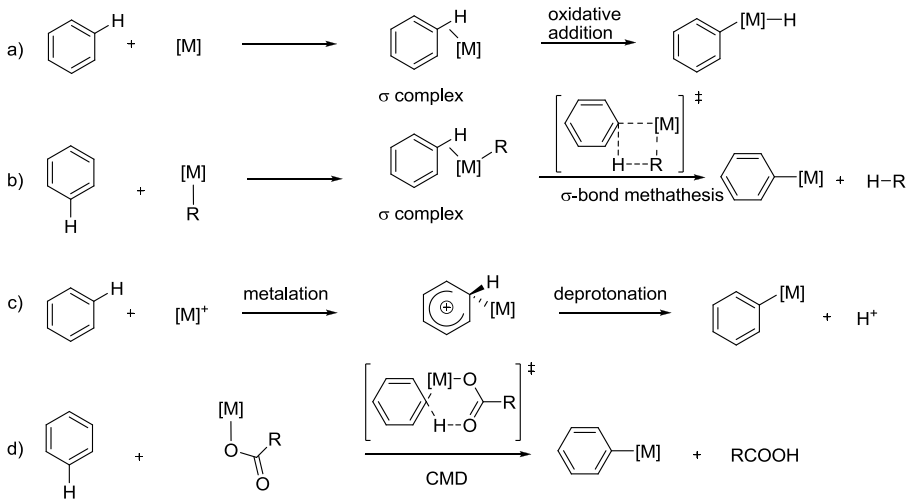

Scheme 14. Mechanisms of arene C–H bond activation: a) oxidative addition; b) σ-bond metathesis; c) electrophilic metallation; d) ligand-assisted concerted metallation-deprotonation.

Oxidative addition reactions are typical for electron-rich, low-valent complexes of late transition metals such as Re, Fe, Ru, Os, Rh, Ir, Pd, and Pt. In this reaction type (Scheme 14a), the reactive species [M] is a coordinatively unsaturated metal complex, in most cases generated *in situ*

by thermal or photochemical activation of a suitable precursor. Since two electrons of the metal are used for breaking the C–H bond, the oxidation state of the metal increases by two. Importantly, a metal hydride is formed, although the hydride may be transferred immediately to another ligand on the metal.

The σ-bond metathesis[23] mechanism involves transfer of a hydrogen atom from the aryl group to another ligand in a concerted fashion *via* a four-membered, four-electron transition state that leaves the oxidation state of the metal unchanged (Scheme 14b). This mechanism is characteristic of electron-deficient metal complexes, in particular d^0 complexes, in which the metal centre cannot be further oxidised. This applies especially to early transition metals from groups 4 and 5 in high oxidation states, as well as to lanthanide and actinide complexes. The ligand R on the metal is usually a halide or a triflate.

C–H activation by electrophilic substitution mechanisms requires an electrophilic late- or a post-transition metal in a high oxidation state (Pd^{2+}, Pt^{2+}, Pt^{4+}, Hg^{2+}, Tl^{3+}). Usually the reaction requires a polar solvent such as DMF or NMP. Electrophilic aromatic substitution involves a rate-limiting metallation step to form a Wheland-type intermediate. That step is followed by a rapid deprotonation leading to the rearomatisation of the system and the generation of the metal-aryl product.

The last mechanism, called metal/ligand activation or concerted metallation–deprotonation, uses metals bearing carboxylate (acetate, pivalate, mesitylate, adamantylate), carbonate, or phosphine oxide ligands. Recently, this mechanism has attracted much attention, as a number of C–H activations catalysed by late transition metal complexes (Pd(II), Ru(II), Rh(I)) previously believed to proceed by electrophilic aromatic substitution, turned out to involve this pathway.[24]

1.7 The Murai reaction

In 1993, Murai reported a highly efficient ruthenium-catalysed coupling reaction between aromatic compounds and olefins (Scheme 15).[20a] The key feature of this reaction is a regioselective C–H activation controlled by coordination of the metal complex to a directing group.

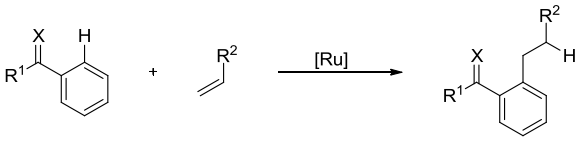

Scheme 15. The Murai reaction.

Originally, the Murai protocol used ketones as the directing groups. Later, it was found that a variety of other coordinating groups containing N or O atoms, such as other carbonyls (in esters, amides), cyano groups, imino groups, and heteroaromatic rings containing sp^2-hybridised nitrogens (pyridines, imidazoles, oxazolidines) are also efficient in this respect.[25] Both electron-withdrawing and electron-donating substituents are tolerated in the aromatic ring. Steric hindrance and the possibility of chelation can influence the regioselectivity of the reaction, as shown in Figure 1.[26] Regarding the scope of the unsaturated substrate, terminal olefins, strained internal alkenes, such as cyclopentenes and norbornenes, and disubstituted alkynes can be used.

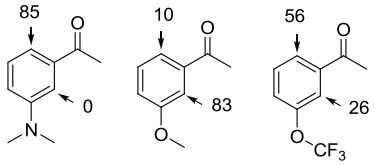

Figure 1. Effect of substituents on the selectivity of the Murai reaction (reaction with triethoxy(vinyl)silane, isolated yields of coupling products in %).

A variety of commercially available Ru complexes, such as $RuH_2(CO)(PPh_3)_3$, $RuH_2(PPh_3)_4$, $Ru(CO)_2(PPh_3)_3$, and $Ru_3(CO)_{12}$ have been used in the Murai reaction. Also $[Ru(p\text{-cymene})Cl_2]_2$ and $RuCl_3$ were used as precursors of the active Ru species generated *in situ*.[27] Dihydrogen-containing $RuH_2(H_2)(CO)(PCy_3)_2$ and structurally related complexes were found to be exceptionally good catalysts for the Murai reaction, active even at room temperature.[28]

Many attempts have been made to obtain insights into the mechanism of the Murai reaction. A plausible catalytic cycle is shown in Scheme 16. It is believed that, upon heating, Ru(0) species are formed from the catalyst precursors. The generated unsaturated Ru(0) complexes can coordinate to the carbonyl group and undergo *ortho* C–H oxidative addition. Computational studies by Koga and co-workers revealed that coordination of the carbonyl group of benzaldehyde to $Ru(CO)(PH_3)_n$ significantly decreases the activation energy barrier of the C–H activation step.[29] A number of [Ru–H] complexes that are possible reaction intermediates (C–H activation products) were isolated and characterised.[30] The next postulated step of the catalytic cycle is migratory insertion of the olefin into the Ru–H bond. It is usually regioselective for steric and electronic reasons.

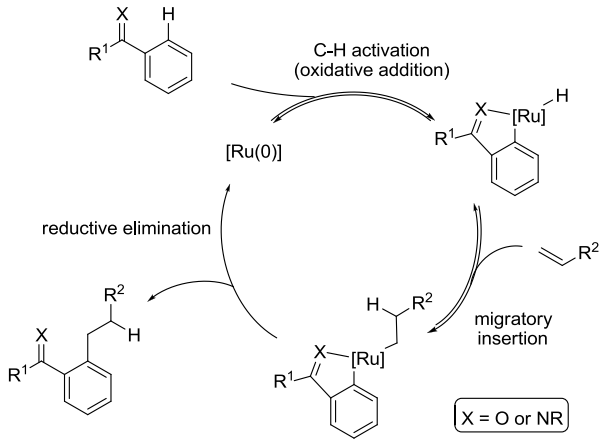

Scheme 16. Plausible mechanism of the Murai reaction.

The last step is a reductive elimination, which results in the C–C bond formation. This process is accelerated by the presence of electron-withdrawing groups in the aromatic ring. The reductive elimination was shown, using both experimental studies and theoretical calculations, to be the turnover-limiting step of the reaction.[19,29] In particular, deuterium labelling studies showed that all the steps preceding the reductive elimination are reversible.[31]

Recently, for the specific case of $RuH_2(H_2)_2(PX_3)_2$ and similar complexes, a significantly different mechanism has been suggested, based on the results of theoretical calculations.[28f] The main feature of this mechanism is a Ru(II)/Ru(IV) catalytic cycle in which the dihydrogen ligand has an active role.[28e] This mechanism rationalises the above-mentioned excellent performance of these catalysts.

1.8 Alkylation of amines with alcohols

There are a number of methods for the synthesis of *N*-substituted amines.[32] Among them, the catalytic redox condensation between alcohols and amines to produce higher order amines is an attractive alternative.[4] A wide variety of inexpensive alcohols are commercially available, and water is the sole by-product of the reaction. These features make this method atom economical and environmentally friendly.

The reaction is typically catalysed by complexes of Ru, Ir, and Pd. It was reported for the first time independently by Grigg[33] and Watanabe[34] in the 1980s. Since then, a number of successful examples have been described, with the major contributions in this field coming from the groups of Fujita, Williams, Beller, Kempe, Crabtree, Peris, and Madsen.[4] High activity has

been achieved with commercially available iridium and ruthenium complexes $[IrCp^*Cl_2]_2$, $RuCl_2(PPh_3)_3$, and $[RuCl_2(p\text{-cymene})]_2$ and also with the systems reported by Kempe,[35] Crabtree,[36] and Peris[37] (Figure 2).

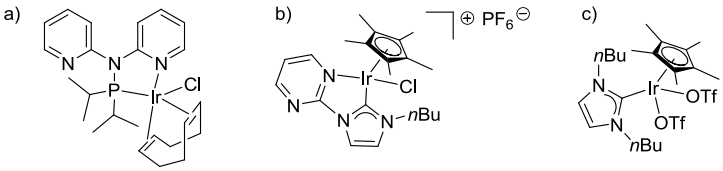

Figure 2. Selected structures of iridium complexes catalysing the alkylation of amines with alcohols. a) Kempe catalyst, b) Crabtree catalyst, c) Peris catalyst.

Our group has used this reaction for the synthesis of aminosugars (iridium catalyst) and aminoferrocenes (ruthenium catalyst).[38]

The general mechanism of the reaction involves a hydrogen transfer, and consists of three steps (Scheme 17): (i) oxidation of the alcohol with concomitant formation of a metal hydride; (ii) formation of an imine from the resulting carbonyl compound and the amine substrate; and (iii) re-hydrogenation of the imine and catalyst regeneration.[4,39]

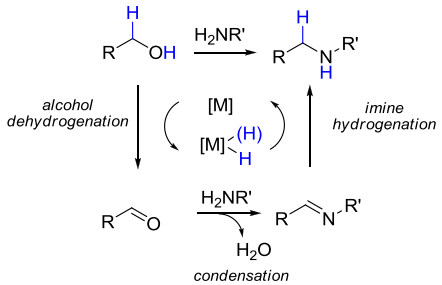

Scheme 17. General mechanism for the alkylation of amines with alcohols, involving hydrogen transfer.

1.9 *N*-Heterocyclic carbenes as ligands for transition metal catalysts

N-heterocyclic carbenes (NHCs) are one of the most popular classes of ligands nowadays. The success of NHCs is often attributed to their excellent σ-donating properties, which result in a strong metal–NHC bond. This feature makes carbene complexes more stable to heat, oxygen, and moisture, and in some instances more active in comparison to complexes containing phosphine ligands.[40]

Initially, only imidazole-derived: imidazolidin-2-ylidenes and imidazolin-2-ylidenes of the Wanzlick[41] and Arduengo[42] ligand families

were used in metal complexes. It was realised later that other heterocyclic structures such as pyrazoles, triazoles, thiazoles, and other scaffolds could also be used. The substituents on the nitrogen atoms might be identical or different. The possibility of choosing the appropriate heterocyclic ring and the nitrogen-substituents, together with the great number of possible synthetic pathways makes the potential structural diversity of this type of ligands unlimited.

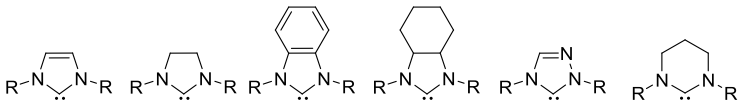

Figure 3. Representative examples of NHC ligands.

1.10 Objectives of the thesis

This thesis aims for the development of new, efficient methods and catalytic systems for the functionalisation of C(sp^2)–H and C(sp^3)–O bonds using tandem redox hydrogen-transfer reactions based on ruthenium and iridium catalysis.

The first aim of the thesis (Chapter 2), was to develop an efficient catalytic system for the synthesis of β-hydroxy ketones and β-amino ketones from allylic alcohols. The aldol and Mannich-type products were expected to be formed by trapping enolate intermediates formed during the isomerisation of allylic alcohols by transition metal complexes.

The second goal of the thesis was to combine Ru catalysed tandem isomerisations with C–H activation and C–C coupling processes (Chapter 3). In this case, we wanted to use allylic alcohol substrates as ketone synthetic equivalents. The carbonyl group formed in the first step would serve as a directing group for a further C–H activation/C–C bond formation reaction.

Finally, in the last part of the thesis (Chapter 4) the aim was to design, prepare, and apply a new metal-ligand bifunctional iridium(III) catalyst having the alcohol/alkoxide functionality.

Chapter 2

Efficient synthesis of β-hydroxy ketones and β-amino ketones from allylic alcohols by catalytic formation of ruthenium enolates. (Paper I and II)

2.1 Introduction

Since the beginning of organic chemistry, enolates have been very important intermediates in synthetic transformations.[43] In recent decades, enolates of transition metals have emerged as synthetically appealing alternatives to enolates of the main group metals.[44] Methods to prepare transition metal enolates include the reduction of enones by hydrogen or silanes, mediated by rhodium and other transition metals.[45] Alternatively, these intermediates can also be prepared from allylic alcohols, by an internal redox process catalysed by a metal complex.[7,8] Enolates formed by either of these methods can be trapped by electrophiles, such as aldehydes or imines.[15] (Scheme 18).

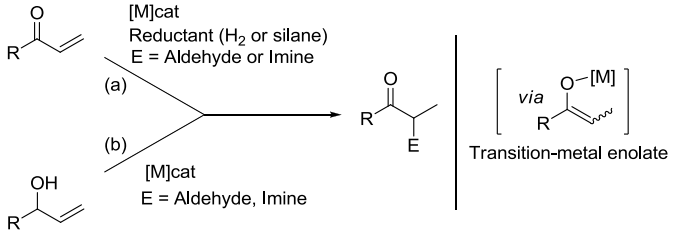

Scheme 18. Synthesis of α-substituted ketones from enones or allylic alcohols catalysed by transition metal complexes.

While reductive aldol/Mannich type reactions (Scheme 18a) have been extensively studied, tandem processes combining allylic alcohol isomerisation with aldol or Mannich-type couplings (Scheme 18b) remain still largely unexplored.[15] The main achievements in this field were summarised in Section 1.5. As mentioned above, two major problems remain unsolved; these are: (i) low yields due to the formation of isomerisation product (ketone), and (ii) a low *syn*/*anti* diastereoselectivity.

The aim of this project was to search for a catalytic system that would perform the isomerisation/aldol and Mannich-type tandem processes with a high efficiency and diastereoselectivity, and ideally under mild reaction conditions. Due to the high activity of ruthenium complex **1a** (Figure 4) in the isomerisation of allylic alcohols, we focussed on evaluating the performance of this complex and other structurally related ruthenium complexes in the tandem reactions. In parallel to this project, our group has developed a rhodium system, $[Rh(COD)Cl]_2/PPh_3$, that efficiently catalyses the coupling of allylic and homoallylic alcohols with aromatic aldehydes and imines.[15o]

2.2 Catalyst screening and optimisation of reaction conditions

In order to find the optimal catalyst for the reaction, we examined the activity of a variety of ruthenium halide complexes (Figure 4, **1a–i**) in the reaction between α-vinylbenzyl alcohol (**2a**) and *p*-chlorobenzaldehyde (**3a**) (Table 1).

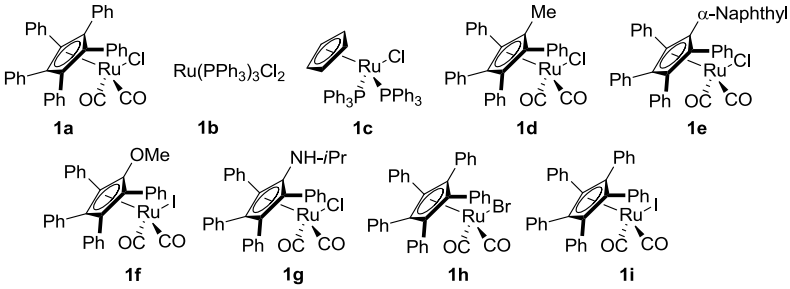

Figure 4. Ruthenium catalysts tested.

The complexes were activated with KO*t*Bu, which displaces the halide ligand to form catalytically active ruthenium *tert*-butoxide intermediates.[8m,8p,8t,9c]

While the commercially available ruthenium complexes **1b** and **1c** (Figure 4) afforded the desired aldol (**4**) in low yields (22–34%), along with large amounts of the ketone by-product (**5a**) (Table 1, entries 1–2), ruthenium complexes **1a** and **1d–1e**, containing pentasubstituted cyclopentadienyl ligands, gave good results (entries 3–10). In particular, catalyst **1a**, bearing five phenyl groups on the cyclopentadienyl ring, showed the highest activity (entry 3). Introduction of a MeO or NH*i*Pr group onto the cyclopentadienyl ligand (**1f**[46] and **1g**[47]) did not give better results (entries 7 and 8).

Further optimisation of the reaction conditions revealed that at a lower temperature, **1a** afforded quantitative yields of aldol **4** (Table 1, entry 5). Replacement of the Cl ligand in **1a** by Br or I (**1h**[48] and **1i**,[49] respectively), led to results comparable to those obtained with catalyst **1a** (entries 9–10 *vs.* 5).

Table 1. Catalyst screening.

2a **3a** **4** *syn* + *anti* **5a**

R = *p*-Cl-C_6H_4

Entry	Catalyst	Temperature (°C)	Conversion (%)[a]	Reaction time	**4** / **5a**[a]	*syn*/*anti*[a]
1	**1b**	50	73	16 h	43/57	71/29
2	**1c**	50	85	16 h	32/68	84/16
3	**1a**	50	> 99	13 min	85/15	65/35
4	**1d**	50	> 99	1.5 h	96/4	62/38
5	**1e**	50	> 99	40 min	63/37	62/38
6	**1a**	20	> 99	6 h	99/1	84/16
7[b]	**1f**	20	13	18 h	50/50	-
8	**1g**	20	57	18 h	91/9	75/25
9	**1h**	20	94	18 h	87/13	78/22
10	**1i**	20	70	18 h	97/3	77/23

[a] Determined by ^{1}H NMR spectroscopic analysis of the crude reaction mixtures. [b] Several decomposition products were formed along with **5a**.

2.3 Synthesis of *β*-hydroxy ketones – scope and limitations

Using the optimised reaction conditions (Table 1, entry 5), a variety of allylic alcohols (**2a–e**) were coupled with a number of aromatic and aliphatic aldehydes (**3a–p**), to give aldols **4**,**6–24** in excellent yields (Scheme 19, Table 2), and in most cases, under very mild reaction conditions. In general, the reaction of aromatic allylic alcohols (**2a–2c**) with aromatic aldehydes (**3a–f**) proceded smoothly, regardless of their electronic properties (Table 2, entries 1–6 and 9–10). The presence of certain potentially coordinating groups, such as 4-methoxy or 1-furyl, did not affect the reaction rates (Table 2, entries 4 and 6). On the other hand, reactions with aldehydes containing 4-cyano and 2-pyridyl moieties were slower and had to be performed at higher

temperatures (Table 2, entries 7 and 8). Aliphatic alcohols **2d** and **2e** (Table 2, entries 11–12) could also be used in the coupling. In general, allylic alcohols **2a–2d** which have no substituents on the terminal carbon of the double bond, reacted much faster than more substituted ones (*i.e.* alcohol **2e**).

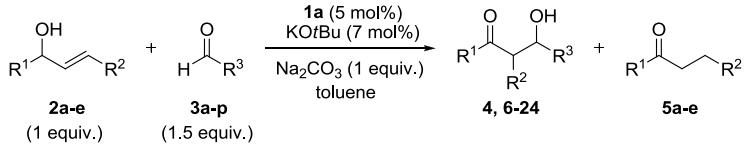

2a R^1 = Ph, R^2 = H
2b R^1 = *p*-MeO-C_6H_4, R^2 = H
2c R^1 = *p*-Cl-C_6H_4, R^2 = H
2d R^1 = C_5H_{11}, R^2 = H
2e R^1 = Me, R^2 = Ph

3a R^3 = *p*-Cl-C_6H_4
3b R^3 = *p*-F-C_6H_4
3c R^3 = Ph
3d R^3 = *p*-MeO-C_6H_4
3e R^3 = *β*-naphthyl
3f R^3 = 1-furyl
3g R^3 = 2-pirydyl
3h R^3 = *p*-CN-C_6H_4
3i R^3 = *i*-Pr
3j R^3 = Et

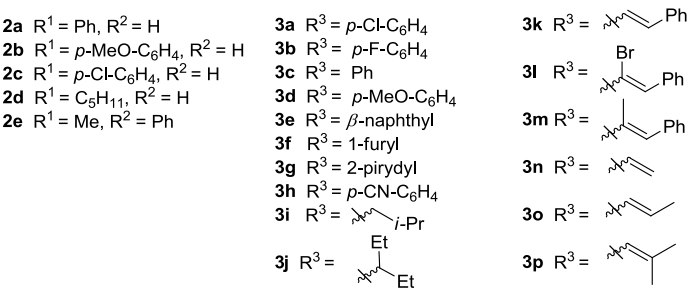

Scheme 19. Synthesis of *β*-hydroxy ketones **4,6**–**24** from allylic alcohols **2a**–**e** and aldehydes **3a**–**p**.

Table 2. Coupling of allylic alcohols with aldehydes catalysed by **1a**.[a]

Entry	**2** / **3**	Aldol	t (h)/ T (°C)	Aldol/**5** (%)[b]	*syn*/*anti* (%)[b]
1	**2a** / **3a**	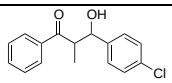 **4**	3.5/25	>99(88)/1	77/23
2	**2a** / **3b**	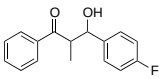 **6**	3.5/25	>99(78)/1	83/17
3	**2a** / **3c**	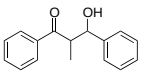 **7**	2.5/35	99(84)/1	69/31
4	**2a** / **3d**	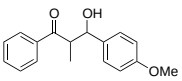 **8**	1/35	95(93)/5	60/40
5	**2a** / **3e**	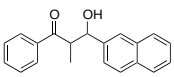 **9**	5/25	99(97)/1	82/18

6	**2a** / **3f**	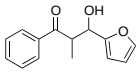 **10**	7/25	>99(78)/1	70/30
7	**2a** / **3g**	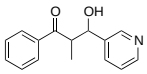 **11**	20/50	>99(91)/1	83/17
8	**2a** / **3h**	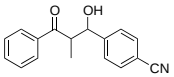 **12**	7/50	>99(80)/1	82/18
9	**2b** / **3a**	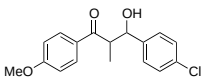 **13**	4/25	>99(79)/1	79/21
10	**2c** / **3a**	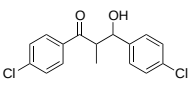 **14**	2/35	>99(75)/1	75/25
11	**2d** / **3a**	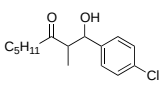 **15**	18/65	>99(59)/1	60/40
12[d]	**2e** / **3a**	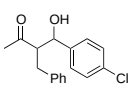 **16**	5/35	>99(79)/1	40/60

[a] Reaction conditions: KO*t*Bu (56 µL; 0.5 M in THF, 7 mol%) was added to a mixture of complex **1a** (13 mg, 0.020 mmol, 5 mol%) and Na_2CO_3 (42 mg, 0.4 mmol) in degassed toluene (1 mL) under a nitrogen atmosphere. The mixture was stirred for 3 min before a solution of the allylic alcohol (**2**, 0.4 mmol) and aldehyde (**3**, 0.6 mmol) in degassed toluene (1 mL) was added by syringe. [b] Determined by ^{1}H NMR spectroscopy of the crude mixture. In parentheses, isolated yield of aldols. [c] At room temperature, **16** was obtained in 75% yield, *syn*/*anti* 80:20 after 24 h.

Aliphatic aldehydes, which are generally considered to be difficult substrates[15m] could be successfully coupled with **2a** (Table 3, entries 1–2, to avoid self aldolisation of aldehyde 4Å MS were added instead of Na_2CO_3) to give the corresponding aldols in high yields and *syn*/*anti* ratios (up to 92:8). Such diastereoselectivity is among the highest observed for this transformation.

Table 3. Coupling of allylic alcohols with aldehydes catalysed by **1a**.[a]

Entry	**2** / **3**	Aldol	t (h)/ T (°C)	Aldol/**5** (%)[b]	*syn*/*anti* (%)[b]
1[c]	**2a** / **3i**	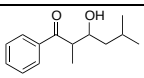 **17**	3/35	96(92)/4	92/8
2[c]	**2a** / **3j**	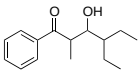 **18**	2.5/35	91(76)/9	89/11
3	**2a** / **3k**	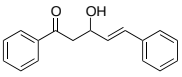 **19**	12/35	92(75)/8	54/46
4	**2a** / **3l**	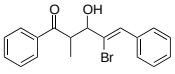 **20**	1/35	97(79)/3	87/13
5	**2a** / **3m**	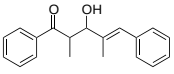 **21**	13/35	78(48)/22	50/50
6	**2a** / **3n**	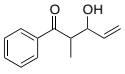 **22**	3/35	96(72)/4	56/44
7	**2a** / **3o**	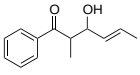 **23**	3/35	97(86)/3	48/52
8	**2a** / **3p**	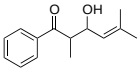 **24**	4.5/35	96(77)/4	73/27

[a] Reaction conditions: KO*t*Bu (56 μL; 0.5 M in THF, 7 mol%) was added to a mixture of complex **1a** (13 mg, 0.02 mmol, 5 mol%) and Na_2CO_3 (42 mg, 0.4 mmol) in degassed toluene (1 mL) under a nitrogen atmosphere. The mixture was stirred for 3 min before a solution of the allylic alcohol (**2**, 0.4 mmol) and aldehyde (**3**, 0.6 mmol) in degassed toluene (1 mL) was added by syringe. [b] Determined by ^{1}H NMR spectroscopy of the crude mixture. In parentheses, isolated yield of aldols. [c] 4Å MS were added instead of Na_2CO_3.

Catalyst **1a** could also be used for the coupling of α,β-unsaturated aldehydes. The resulting aldol products contain an allylic alcohol functionality that can potentially undergo further isomerisation (Table 3, entries 3-8). However, products **20**–**25** were formed exclusively, and no further isomerisation/aldolisation was observed under the reaction conditions

applied.[50] Only when the reaction temperature was maintained for 3 h at 35 °C and then raised to 100 °C for an additional 12 h, was aldol **20** transformed into a mixture of 1,3-diketone **25** and ketone **5a** (Scheme 20).

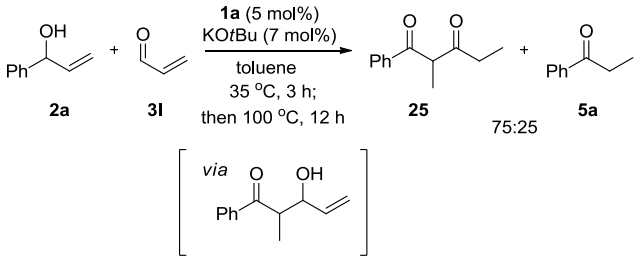

Scheme 20. Tandem isomerisation/aldol reaction/isomerisation leading to 1,3-diketone **25**.

As to the limitations of this synthetic procedure, neither primary nor substituted secondary allylic alcohols (Figure 5) gave any coupling product. Also the reaction did not work with endo and exocyclic cyclohexenols (Figure 5), that together with **1a** as the catalyst can be used for other transformations such as condensation to symmetric ethers and DKR, respectively.[51a,51b]

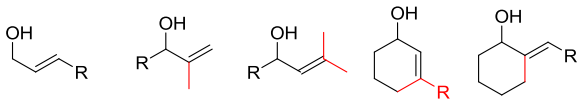

Figure 5. Alcohols that gave no isomerisation/coupling reaction with **1a** as catalyst

2.4 Synthesis of *β*-amino ketones – scope and limitations

Next, we investigated the use of imines as electrophilic coupling partners in the reaction catalysed by complex **1a**. The products obtained, *β*-amino ketones, are important intermediates in the synthesis of a variety of nitrogen-containing drugs and natural products.[52,53]

A number of substituted imines were evaluated for their reactivity under the conditions described above (Scheme 21 and Table 4). *N*-Aryl aldimines[15e,54] **26a–26c** were not converted into the desired products (Table 4, entries 1–3). Instead **2a** was quantitatively isomerised into **5a**. *N*-Boc-protected imine **26d** (entry 4)[55] gave by-products as a result of a nucleophilic attack of the hydroxy group in **2a** on the Boc moiety. *N*-Sulfonylaldimine **26e**,[15o,15p,15q,56] on the other hand, gave good results (Table 4, entry 5), producing *β*-amino ketone **31** in 90% yield. To examine a possible influence of the *N*-sulfonyl substituent on the diastereoselectivity, we tested two

additional *N*-sulfonyl imines: 6-methylnaphthyl- and 2-pyridylsulfonylimines (**26f** and **26g**, respectively). These attempts, however, were unsuccessful. The more bulky imine **26f** gave a similar *syn*/*anti* ratio to that obtained with **26e** (entry 6 *vs* entry 5), and the presence of an additional chelating group in imine **26g**[57] suppressed the coupling reaction completely (entry 7).

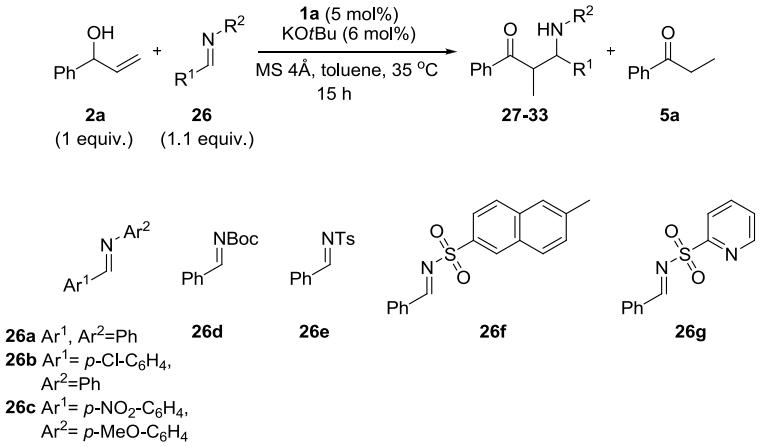

Scheme 21. Screening of different imines in the reaction with allylic alcohol **2a** catalysed by complex **1a**.

Table 4. Imine scope in the coupling with allylic alcohol **2a** catalysed by ruthenium complex **1a**.

Entry	Imine	*β*-Amino Ketone	*β*-Amino Ketone / **5a**[a]	*syn*/*anti*[a]
1	**26a**	**27**	0/100	-
2	**26b**	**28**	0/100	-
3	**26c**	**29**	0/100	-
4	**26d**	**30**	20/80[b]	n.d.[c]
5	**26e**	**31**	90/10	71/29
6	**26f**	**32**	92/8	73/27
7	**26g**	**33**	0/100	-

[a] Determined by ^{1}H NMR spectroscopy. [b] Formation of side products. [c] n.d. = not determined.

The optimised reaction conditions were used in the synthesis of a number of *β*-amino ketones (**31**, **34**-**43**, Scheme 22, Table 5).

Aromatic imines containing both electron-donating and electron-withdrawing substituents in *ortho*, *meta*, and *para* positions were coupled uneventfully with some of the allylic alcohols that were shown to work well in the aldol-type reactions described above. The diastereoselectivity, though, was however poor, with *syn*/*anti* ratios up to 3:1. Only bulky alcohol **2f**, containing a large *α*-naphthyl substituent, afforded a high diastereomeric ratio (86:14, Table 5, entry 9).

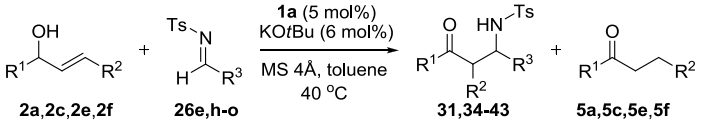

2a,**2c**,**2e**,**2f** (1 equiv.) + **26e**,**h**-**o** (1.1 equiv.) → **31**,**34**-**43** + **5a**,**5c**,**5e**,**5f**

2a R^1 = Ph, R^2 = H	**26e** R^3 = Ph	**26k** R^3 = *o*-Br-C_6H_4
2c R^1 = *p*-Cl-C_6H_4, R^2 = H	**26h** R^3 = *p*-F-C_6H_4	**26l** R^3 = *o*-Me-C_6H_4
2e R^1 = Me, R^2 = Ph	**26i** R^3 = *p*-Br-C_6H_4	**26m** R^3 = *p*-Me-C_6H_4
2f R^1 = α-naphthyl, R^2 = H	**26j** R^3 = *m*-Br-C_6H_4	**26n** R^3 = *β*-naphthyl

Scheme 22. Synthesis of *β*-amino ketones from allylic alcohols.

Table 5. Scope of the Mannich-type reaction catalysed by **1a**.[a]

Entry	**2** / **26**	Amino Ketone	Time (h)	Product/**5**[b]	*syn*/ *anti*[b]	Yield[c]
1	**2a** / **26e**	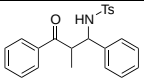 **31**	15	90/10	71/ 29	90 (80)
2	**2a** / **26h**	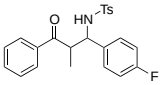 **34**	15	95/5	62/ 38	89 (78)
3[d]	**2a** / **26i**	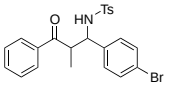 **35**	30	94/6	73/ 27	94 (78)
4	**2a** / **26j**	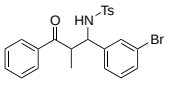 **36**	14	94/6	63/ 37	94 (83)
5[d]	**2a** / **26k**	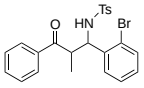 **37**	30	95/5	56/ 44	95 (75)
6	**2a** / **26l**	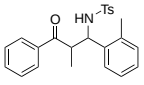 **38**	11	77/23	66/ 34	77 (70)
7	**2a** / **26m**	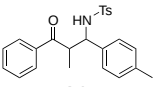 **39**	11	81/19	53/ 47	81 (70)
8	**2a** / **26n**	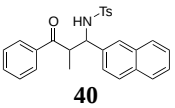 **40**	15	89/11	61/ 39	89 (76)
9	**2f** / **26e**	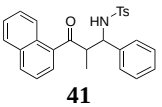 **41**	15	88/12	86/ 14	81 (68)
10	**2e** / **26e**	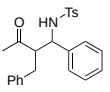 **42**	12	93/7	49/ 51	93 (79)
11	**2c** / **26e**	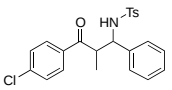 **43**	15	94/6	60/ 40	94 (80)

[a] Reaction conditions: KO*t*Bu (56 µL; 0.5M in THF, 7 mol%) was added to a mixture of complex **1a** (13 mg, 0.020 mmol, 5 mol%) and 4Å molecular sieves (20 mg) in degassed toluene (1 mL) under a nitrogen atmosphere. The mixture was stirred for 3 min before a solution of the allylic alcohol (**2**, 0.4 mmol) and imine (**26**, 0.44 mmol) in degassed toluene (1 mL) was added by syringe. The mixtures were stirred at 40 °C for the time indicated. [b] Determined by ^{1}H NMR spectroscopy. [c] Isolated yield in parentheses. [d] Reaction in THF.

2.5 Mechanistic investigations

Complex **1a** is known to catalyse the racemisation of secondary alcohols.[58] Its mechanism of action in this reaction has been extensively investigated. It was established that the key role in the catalytic cycle is played by ruthenium alkoxides, which undergo reversible β-hydride elimination to effect the racemisation.

Such a course of events resembles the first steps of the mechanism of isomerisation of allylic alcohols shown in Scheme 8. Therefore, we believe that this tandem process follows the alkoxide-type mechanistic pathway. The objective of the studies described in this section was to elucidate the details of the remaining steps of the mechanism.

2.5.1 Kinetics of the reaction

To obtain insight into the reaction mechanism, we followed the coupling reaction of **2a** and **3a** catalysed by ruthenium complex **1a** by ^{1}H NMR spectroscopy, at different temperatures (Scheme 23). The obtained kinetic profiles are presented in Figures 6a–c.

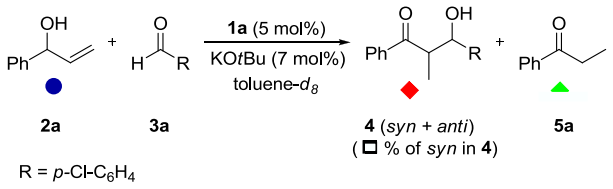

Scheme 23. Reaction of alcohol **2a** with aldehyde **3a** in toluene-d_8 catalysed by **1a** at different temperatures.

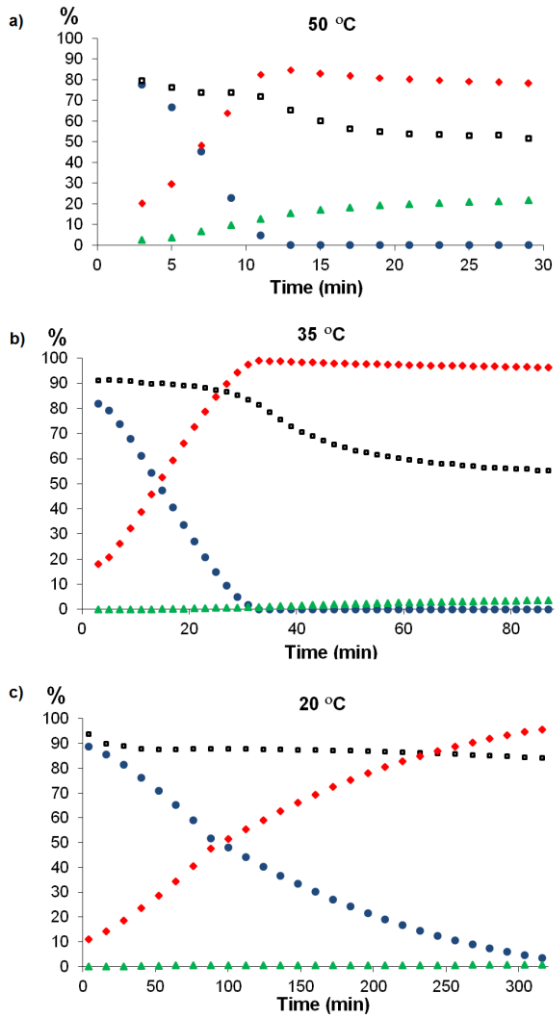

Figure 6. Reaction of alcohol **2a** with aldehyde **3a** in toluene-d_8 catalysed by **1a** at (a) 50 ºC, (b) 35 ºC, and (c) 20 ºC. Time = 4 min corresponds to the first ^{1}H NMR spectrum recorded.[● : **2a**; ♦ : aldol **4** (*syn* + *anti*); ▮: % of *syn* in **4**; ▲: propiophenone (**5a**)].

At 50 °C, alcohol **2a** had already been completely comsumed after 12 minutes (Figure 6a). At this moment, the yield of aldol product **4** was 83% and that of ketone **5a** was 17%. Interestingly, from this point on, the amount of aldol **4** decreased, with a simultaneous increase in the yield of ketone **5a**. This result indicates that ketone **5a** can be formed not only by Ru catalysed isomerisation of the allylic alcohol, but also from **4**, by retro-aldolisation.

The other important aspect, also apparent from Figure 6a, is that the *syn/anti* ratio of aldol **4** was *ca.* 80:20 at the beginning of the reaction, and that it later decreased with time, reaching a thermodynamic ratio of *ca.* 55:45 *syn*/*anti* after prolonged heating. Moreover, the rate of epimerisation increased considerably after the alcohol substrate had been fully consumed.

Similar plots were recorded at 35 °C and 20 °C (Figures 6b and 6c, respectively). In these cases, the reactions were slower, reaching full conversion after 30 min and 5 h, respectively. At these lower temperatures, the plots of alcohol consumption and product formation were sigmoidal in shape, suggesting a catalyst preactivation period. Ketone **5a** was formed in much lower amounts, even after prolonged reaction times, and in the case of the reaction carried out at 20 °C, its formation could be almost completely suppressed. Also at this temperature, the rate of epimerisation was significantly reduced.

Similarly, the reaction plots obtained for the Mannich-type reaction between allylic alcohol **2a** and imine **26h** was followed by ^{1}H NMR spectroscopy (Scheme 24, Figure 7). In comparison to the aldol reaction, which was finished within 30 min at 35 °C, the Mannich-type process was much slower, and required 3 h at 40 °C to reach full conversion. The formation of *β*-amino ketone **34** was found to be irreversible. The ketone (**5a**) was thus formed exclusively by direct isomerisation of the allylic alcohol, and it was already detected in small quantities after short reaction times. The *syn*/*anti* ratio was moderate from the beginning of the reaction, but in contrast to the aldol reactions, the epimerisation proceeded at a lower rate in this case.

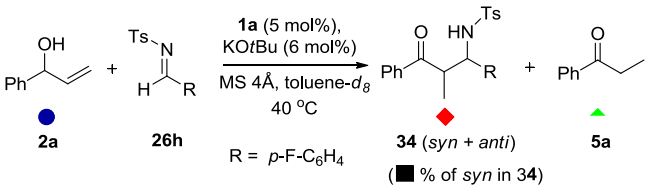

Scheme 24. Reaction of alcohol **2a** and imine **26h** in toluene-d_8 catalysed by **1a** at 40 °C.

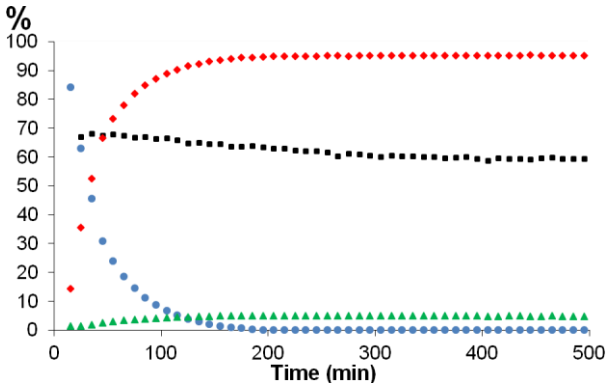

Figure 7. Coupling of alcohol **2a** and imine **26h** in toluene-d_8 catalysed by **1a** at 40 °C. Time = 4 min corresponds to the first ^{1}H NMR spectrum recorded. [● : **2a**; ♦ : *β*-amino ketone **34** (*syn* + *anti*); ▪: % of *syn* in **34**; ▲ : propiophenone **5a**].

2.5.2 Additional stoichiometric mechanistic investigations

We wanted to confirm the involvement of ruthenium alkoxides formed from allylic alcohol **2a** in the mechanism of the reaction, and also to identify other reaction intermediates.

Activation of complex **1a** with KO*t*Bu followed by addition of **2a** was carried out in a stoichiometric fashion and monitored by NMR spectroscopy (Scheme 25).

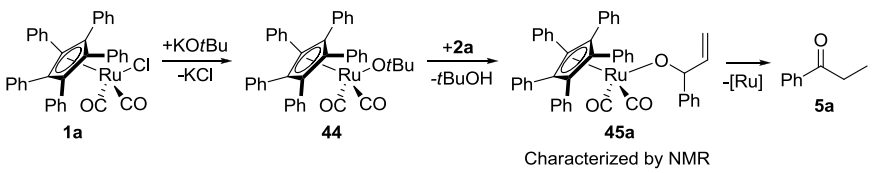

Scheme 25. Stoichiometric activation of catalyst **1a** and formation of alkoxide complex **45a**.

The *tert*-butoxide complex **44** was smoothly transformed into alkoxide **45a** under such reaction conditions. With time (5 h), the latter complex was

converted into ketone **5a**. However, no intermediates of this process could be observed by NMR spectroscopy.

In an attempt to characterise enolate intermediates, we decided to generate alkoxide **45a** in an absence of any protic species *i.e.* *t*BuOH, which could possibly protonate and thus decompose these transient species. Hence, complex **1a** was transformed directly into ruthenium allylic alkoxide **45a** by reacting it with lithium or sodium allylic alkoxides (**46** and **47**, respectively; Scheme 26). Although alkoxide complex **45a** was successfully obtained in both cases, it did not react further to form any other species (except for minute amounts of ketone **5a**, probably formed by reaction of enolate intermediate with traces of water).

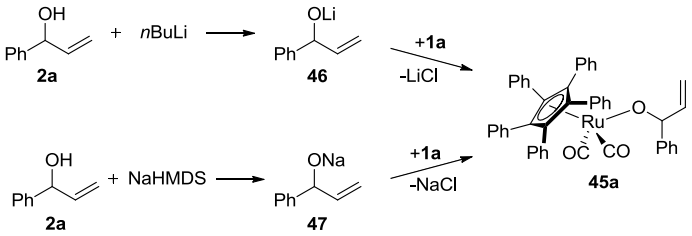

Scheme 26. Formation of ruthenium alkoxide **45a** from lithium or sodium allylic alkoxides.

Complex **45a**, generated as described above (Scheme 26), proved to be a competent catalyst for the isomerisation of allylic alcohol **2a** into propiophenone (**5a**). Therefore, it seems that ruthenium alkoxide **45a** is reversibly transformed into a highly reactive intermediate (enolate), which is present in the reaction mixture in an amount undetectable by NMR spectroscopy. This enolate species, in the presence of proton sources (alcohol **2a**, *t*BuOH), undergoes protonation, leading eventually to ketone **5a**.

In a final attempt to observe the elusive enolate intermediate, ruthenium chloride **1a** was reacted with potassium enolate **48** (Scheme 27).[59] Interestingly, under such conditions a ruthenium C-bound enolate (**49a**) was formed in about 35% yield. The structure of **49a** was confirmed by a number of NMR experiments (Figure 8). The diagnostic signals enabling characterisation of **49a** include: (i) ^{1}H NMR chemical shift of the α-hydrogen (Ru-C*H*-(COPh)CH_3) at 3.91 ppm; (ii) ^{13}C NMR chemical shift of the α-carbon (Ru-*C*H-(COPh)CH_3) at 27.1 ppm;[60] (iii) ^{13}C NMR chemical shift of the carbonyl carbon at 203.8 ppm.[61]

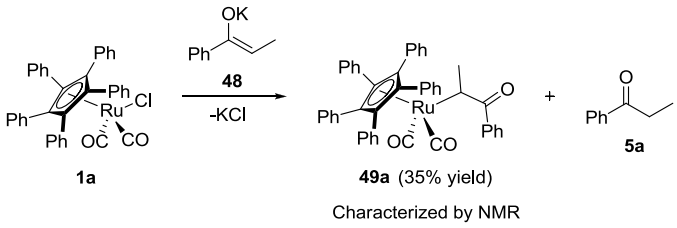

Scheme 27. Generation of ruthenium C-bound enolate.

Complex **49a** was found to be very stable in the reaction mixture, at temperatures ranging from –50 to +50 °C. Most importantly, **49a** catalysed neither the isomerisation of allylic alcohol **2a** to **5a**, nor the tandem isomerisation/aldolisation. Hence, it can be concluded that the ruthenium C-bound enolate **49a** is not an intermediate in the catalytic cycle. However the possibility of that a C-enolate complex **49c** having only one CO ligand is an intermediate in the catalytic cycle cannot be excluded.

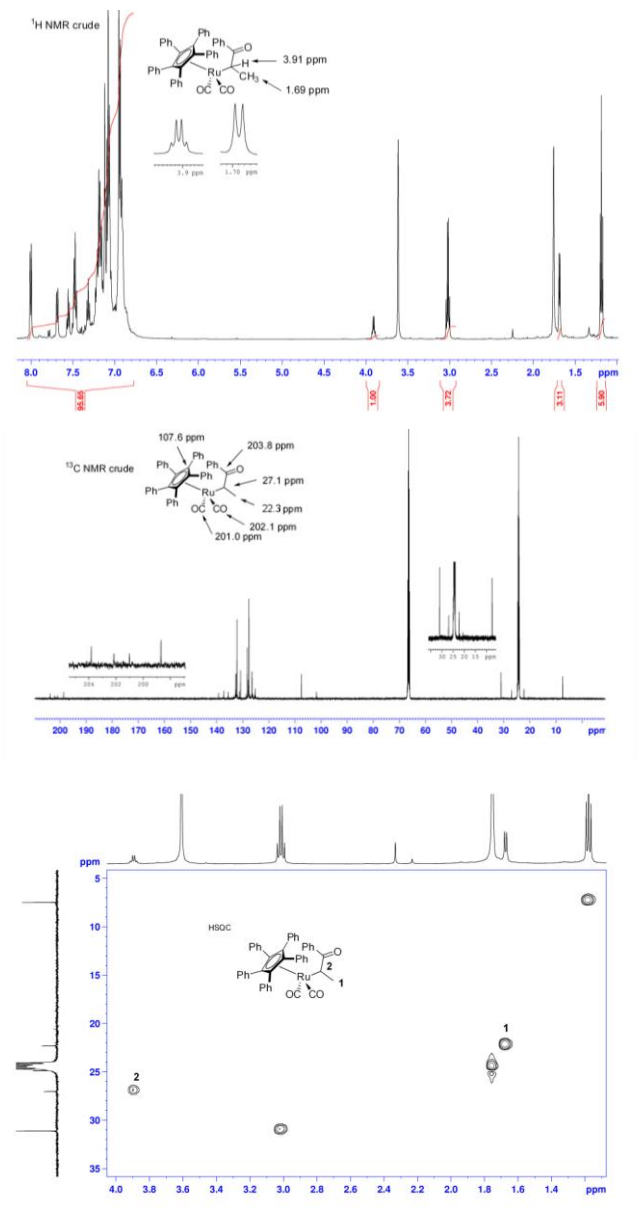

Figure 8. NMR characterisation of *in situ* formed ruthenium C-bound enolate **49a**.

To obtain further support for the 1,4-addition step, an experiment employing deuterated allylic alcohol **2a**-d_1 was carried out (Scheme 28). The coupling reaction with **3a** gave monodeuterated aldol **4**-d_1, with the deuterium label incorporated exclusively into the methyl group (Scheme 33).

This deuterium distribution is in agreement with the proposed mechanism shown in Scheme 8, path a.

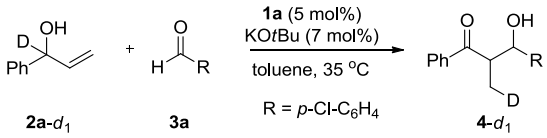

Scheme 28. Coupling of a deuterium-labelled allylic alcohol.

To verify whether the enone intermediate remains coordinated to the ruthenium centre throughout the tandem process, we performed a cross-over experiment, in which the reaction between **2b** and **3a** was carried out in the presence of phenyl vinyl ketone (Scheme 29). Aldol **15** was formed as the sole product, indicating that the intermediate enone, produced within the coordination sphere of the metal, is reduced before it can diffuse into the reaction mixture. Further support for coordination of the α,β-unsaturated ketone to the Ru hydride comes from the fact that the aldehydes used as electrophiles are not reduced to the corresponding alcohols during the reaction.

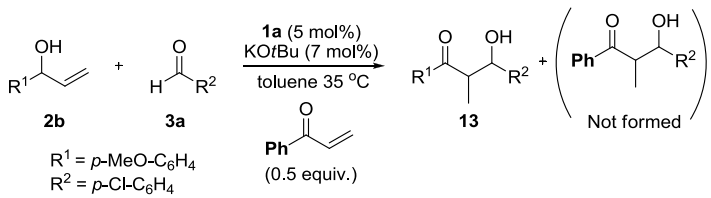

Scheme 29. Cross-over experiment.

Due to the transient nature of the putative ruthenium O-bound enolate intermediate, it is difficult to investigate the details of the C–C bond-formation step of the reaction. In particular, as discussed in Section 1.5, the identity of the nucleophilic species involved in the reaction with the aldehyde (Ru-enolate or free enol) is the most interesting feature of this process.

However, the observation of retro-aldolisation during the NMR experiments (Figure 5) inspired us to examine whether this reaction is catalysed by ruthenium. If this turned out to be the case, it would mean that ruthenium is directly involved in the C–C bond-breaking step of the retro-aldolisation. Hence, according to the principle of microscopic reversibility,[62] the C–C bond formation should also be mediated by ruthenium. When aldol **4** was subjected to the reaction conditions at 50 °C, it underwent a fast decomposition into aldehyde **3a** and ketone **5a** (Scheme 30). Importantly, the retro-aldolisation required the presence of **1a**, and did not occur with KO*t*Bu alone. This result supports the involvement of ruthenium, and in

particular a ruthenium O-bound enolate, in the C–C bond-forming step of the mechanism.

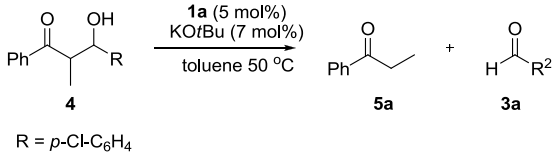

Scheme 30. Ruthenium-catalysed retro-aldol reaction.

2.5.2 Reaction mechanism

Based on the results presented in the previous sections as well as the known pathway for activation of catalyst **1a**[63] and its mechanism of action in the racemisation of secondary alcohols,[64] the mechanism for the tandem isomerisation/aldol reaction shown in Scheme 25 is proposed.[65,66]

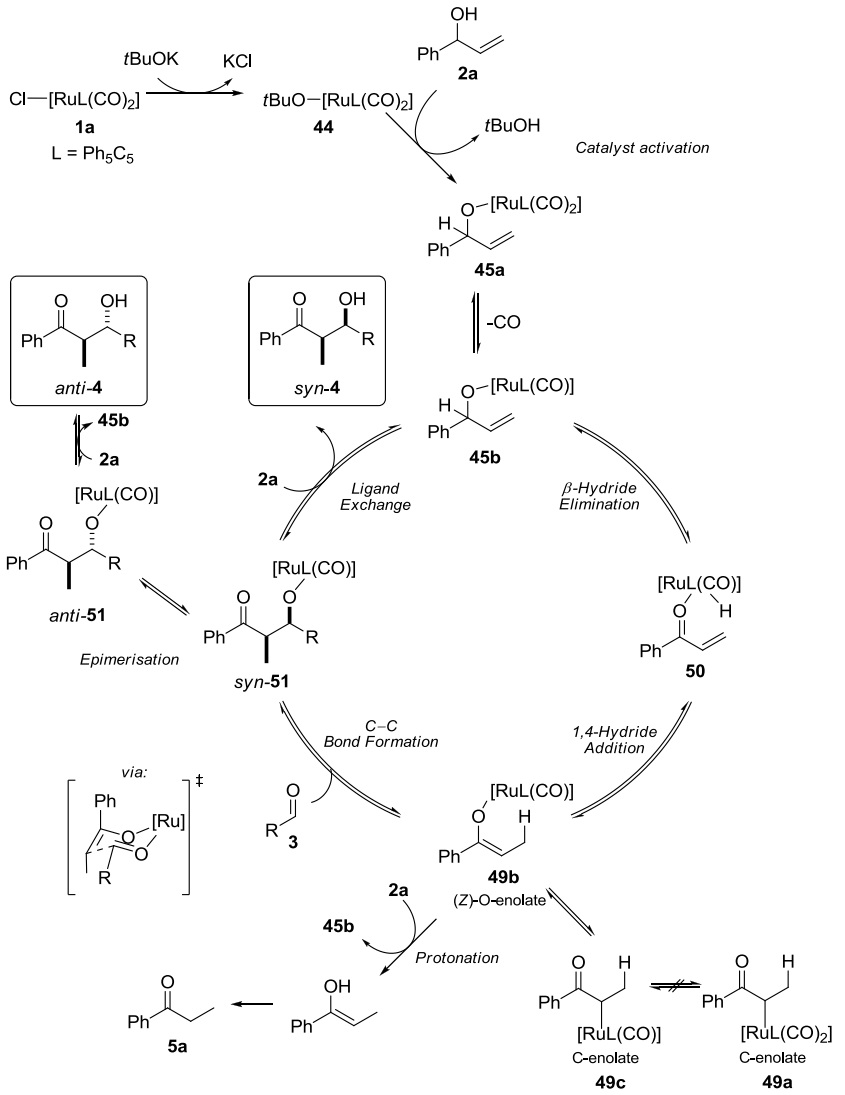

Scheme 31. Proposed mechanism for the tandem isomerisation/aldol reaction catalysed by ruthenium complex **1a**.

The mechanism begins with activation of catalyst **1a** with potassium *tert*-butoxide, followed by the exchange of the *t*BuO ligand, to give ruthenium alkoxide **45a**. The details of this process have been studied before, both experimentally and computationally, by Bäckvall and co-workers.[63,64] These studies have also shown that removal of one of the CO ligands has to occur in order to create an empty coordination site on the metal, which is necessary for the subsequent steps. The CO dissociation has high energy barrier (22.6 kcal) and thus it can account for the preactivation period observed in the NMR experiments (Figure 6c).[63,64] The CO dissociation process is faster in

Ru-alkoxide complexes **44** and **45a** than in the Ru-chloride precursor (**1a**). This is explained by a weaker Ru–CO bond in alkoxide complexes due to the strong σ and π electron-donating properties of this type of ligands.

The next step of the mechanism is the *β*-hydride elimination, leading to ruthenium hydride **50**. Then, a 1,4-readdition of the hydride produces the key ruthenium O-bound enolate **49b**. Based on the results of the cross-over experiment shown in Scheme 29, we propose that the 1,4-hydride addition occurs intramolecularly with the enone intermediate in an s-*cis* conformation. This results in the stereospecific formation of (*Z*)-O-enolate **49b**. As shown before, C-bound Ru-enolate **49a** is not in equilibrium with the ruthenium O-bound enolate **49b**. However the possibility of the C-enolate complex **49c** with one CO ligand being an intermediate in the catalytic cycle cannot be excluded. The difficulties in dissociation of CO from **49a** to form **49c** can be explained by the fact that the alkyl ligand is less electron donating than an alkoxide ligand which results in a stronger bond between the Ru centre and the carbonyl ligand.[64b]

Enolate **49b** may undergo protonation by another molecule of alcohol **2**, regenerating the active form of the catalyst, and eventually leading to ketone **5**. However, if an aldehyde is present in the reaction mixture, **49b** participates in C–C bond formation. This step is most likely to take place *via* a Zimmerman–Traxler six-membered transition state.[19] Such a course for the C–C bond formation would explain the preferential formation of the *syn*-configured aldol from a (*Z*)-O-bound enolate, as discussed in Section 1.5 (Scheme 13).

However, a direct product of the C–C bond formation is (predominantly) ruthenium-alkoxide *syn*-**51**. In order to release the final product, it must undergo a ligand exchange with a molecule of alcohol **2a**. In the final stages of the reaction, however, this process is slow, and after reaching full conversion, it stops completely. Hence, the ruthenium remains in the form of **51**, and catalyses its epimerisation by consecutive *β*-hydride elimination and 1,2-hydride addition.[66] In this way, the diastereoemeric ratio of the final product decreases to the thermodynamic limit, as seen in Figure 5.

The final aspect of the mechanism is the retro-aldolisation. Apparently, enolate **49b** displays a kinetic preference for coupling with aldehyde **3** instead of protonation with alcohol **2**. Hence, aldol **4** is the kinetic product of the reaction. However, ketone **5** must be thermodynamically more stable than aldol **4**, hence, with time, a transformation of **4** into **5** takes place. Fortunately, it was possible to obtain the kinetic product in high yields (and diastereoselectivities) by lowering the reaction temperature.

The mechanism of the tandem isomerisation/Mannich reaction is essentially identical to that shown in Scheme 31, but it involves imines instead of aldehydes in the role of the electrophile. For the Mannich reaction, the retro-process was, however, not observed and the epimerisation of the product (by reversible *β*-hydride elimination on amino group) was

considerably slower. On the other hand, the stereoselectivity of the C–C bond-formation was generally lower in this case.

2.6 Conclusions

We have developed an efficient tandem process combining allylic alcohol isomerisation and C–C bond formation, catalysed by $Ru(\eta^5\text{-}C_5Ph_5)(CO)_2Cl$ (**1a**). An array of *β*-hydroxy ketone and *β*-amino ketone products were obtained in excellent yields and in most cases with good *syn*/*anti* diastereoselectivities.

Mechanistic investigations support a mechanism involving ruthenium allylic alkoxide intermediates. Several new aspects of the reaction mechanism were identified for the first time, such as epimerisation of the product and retro-aldolisation. Also, a ruthenium C-bound enolate has been prepared and characterised by NMR spectroscopy, and was shown to be a catalytically inactive species.

The results obtained here give a general framework for understanding processes involving ruthenium-catalysed tandem allylic alcohol isomerisation combined with C–C coupling reactions, as well as provide aid for developing other catalytic reactions based on this transformation.

Chapter 3

Building molecular complexity through tandem ruthenium catalysed isomerisation/ C–H activation/C–C coupling reaction. (Paper III)

3.1 Introduction

The transformation of allylic alcohols into ketones can broaden the scope of the Murai reaction (see section 1.7), if the carbonyl functional group generated *in situ* can assist with the cleavage and functionalisation of the *ortho* C–H bond in an attached aromatic ring by chelation. Ideally, both reactions could be catalysed by the same ruthenium complex. In this way, the molecular complexity would increase in just two synthetic steps (Scheme 32). Thus, the aim of this project was to develop a new tandem process namely isomerisation of allylic alcohols combined with *ortho* C–H bond activation and C–C bond formation directed by the carbonyl group formed *in situ*.

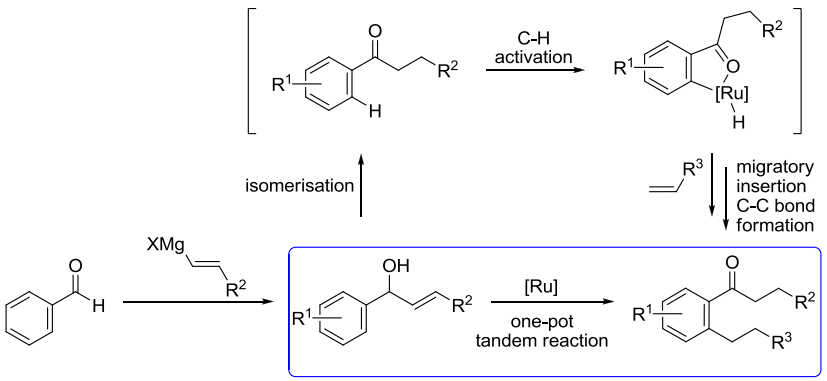

Scheme 32. Ru-catalysed tandem isomerisation/C–H activation/C–C bond formation.

3.2 Optimisation of the reaction conditions

A variety of ruthenium complexes, such as $RuH_2(CO)(PPh_3)_3$, $RuH_2(PPh_3)_4$, $Ru_3(CO)_{12}$, and $RuH_2(H_2)(CO)(PCy_3)_2$, have been used in aromatic C–H activations.[25] These complexes show very high selectivity and reactivity. On the other hand, they are expensive, and some of them, in particular the hydrides, are sensitive to moisture and oxygen. Recently, $[Ru(p\text{-cymene})Cl_2]_2$ (**52c**) and $RuCl_3$ from which the active Ru hydrides were generated *in situ*, were also used for aromatic C–H activation, and excellent reactivity was observed.[27]

The first task in this project was to find an optimal catalyst capable of catalysing the two transformations, *i.e*. the isomerisation of an allylic alcohol and the subsequent C–H functionalisation. Allylic alcohol **2a** and olefin **53** were selected as model substrates (Table 6).

Table 6. Screening of the reaction conditions.

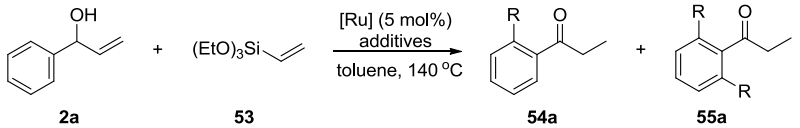

Entry	Catalyst	Additives (mol%)	Time (h)	**54a**+**55a** (%)[a]
1	$RuH_2CO(PPh_3)_3$ (**52a**)	-	2	>99 (92/8)
2	$RuH_2(PPh_3)_4$ (**52b**)	-	2	86 (93/7)
3	$[Ru(p\text{-cymene})(Cl)_2]_2$ (**52c**)	HCO_2Na (30), PPh_3 (15)	2	>99 (62/38)
4	$RuCl_2(PPh_3)_3$ (**52d**)	HCO_2Na (30)	2	>99 (67/33)
5[b]	**52d**	-	2	-
6	**52d**	Na_2CO_3 (30)	12	49 (96/4)
7[c]	**52d**	KO*t*Bu (7)	12	-
8	**52c**	Na_2CO_3 (30), PPh_3 (15)	12	90 (83/17)
9	**52c**	Na_2CO_3 (30), *i*PrOH (30), PPh_3 (15)	12	>99 (80/20)
10	**52d**	Na_2CO_3 (30), *i*PrOH (30)	6	>99 (83/17)

[a] Yields measured by ^{1}H NMR spectroscopy (**54a** + **55a**); **54a**:**55a** ratio in parentheses. [b] Propiophenone was produced in 100% yield. [c] Complex reaction mixture.

In a systematic study, we found that a number of commercially available Ru complexes efficiently catalyse both the isomerisation and the aromatic C–H activation (Table 6). We observed that the isomerisation occurs within the first few minutes of the reaction. $RuH_2CO(PPh_3)_3$ (**52a**) and $RuH_2(PPh_3)_4$ (**52b**) both gave high conversion of the starting material into a mixture of the

products (1:1 and 1:2 adducts, **54a** and **55a**, respectively) after only 2 h (Table 5, entries 1 and 2). The commercially available ruthenium chloride complexes $[Ru(p\text{-cymene})Cl_2]_2$ (**52c**) and $RuCl_2(PPh_3)_3$ (**52d**), in the presence of sodium formate as a hydride donor, were also highly active catalysts (entries 3 and 4).[27] In the absence of the hydride source, treatment with complex **52d** resulted only in the isomerisation of the allylic alcohol, and no C–H functionalisation product was detected (entry 5).

Since HCO_2Na acts not only as a hydride donor but also as a base, we decided to screen other bases. When complex **52d** was combined with Na_2CO_3, the product was formed in a low yield after 12 h (entry 6), and when it was used with KO*t*Bu, complex mixtures were observed (entry 7). For ruthenium complex **52c**, however, formate was not necessary, and full conversion was also reached when Na_2CO_3 was used as the base (entry 8). We then combined Na_2CO_3 as base with *i*PrOH as a hydride donor and obtained excellent results with both ruthenium complexes (**52c** and **52d**, Table 6 entries 9 and 10 respectively). However, much longer reaction times were needed with Na_2CO_3/*i*PrOH than with formate as an additive (entries 9 and 10 vs. 3 and 4). We continued our studies with catalyst **52d** since it could easily be prepared from cheap starting materials.[27]

Despite the excellent results obtained with **52c** and **52d** (Table 6, entries 3 and 4), we observed that the reactions sometimes lacked reproducibility (>99% yield could always be obtained, but it took variable reaction times, *e.g.* from 2 to 4 h). We thought that decomposition of the catalyst may be occuring, and that the addition of a phosphine could prevent these undesirable processes. On the other hand, the phosphine could make the complex more hindered, by blocking the metal centre, which could slow down the overall reaction. Furthermore, the electronic and steric properties of the added ligand could also change the outcome of the reaction.

A number of phosphines were evaluated (Table 7). We decided to examine the influence of phosphine additives only on the slower C–H activation/C–C coupling reaction step, so ketone **3a** was used as the substrate.

Table 7. Screening of phosphine additives.

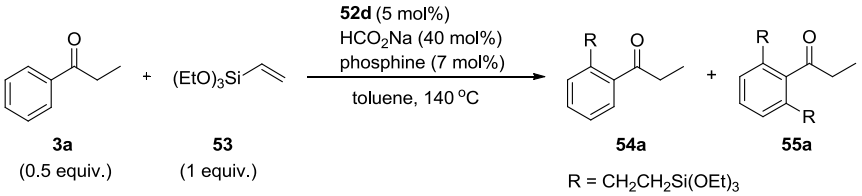

Entry	Phosphine	Time (h)	Yield (%) [a]	**54a**/**55a**[a]
1[b]	None	1	>99	89/11
2	P(*t*Bu)$_3$	0.5	>99	58/42
3	P(*p*-OMe-C$_6$H$_4$)$_3$	0.5	>99	88/12
4	PPh$_2$Me	0.5	>99	57/43
5	PPh$_3$	1	>99	85/15
6	P(Cy)$_3$	1	>99	89/11
7	P(Mes)$_3$	1	98	90/10
8	P(*t*Bu)$_2$(biph)	2	>99	88/12
9	P(*p*-Cl-C$_6$H$_4$)$_3$	2	95	91/9
10	P(2-furyl)$_3$	2	70	87/13
11	P(OEt)$_3$	2	67	95/5
12	P(C$_6$F$_5$)$_3$	2	38	98/2
13	P(Cy)$_2$(biph)	2	20	95/5
14	P(OPh)$_3$	4	traces	n.d.
15	DPPE	4	5	n.d.
16	DPPF	4	10	n.d.
17	*rac*-BINAP	4	10	n.d.

[a] measured by ^{1}H NMR analysis of crude reaction mixture; [b] lacked reproducibility. BINAP = 2,2'-*bis*(diphenylphosphino)-1,1'-binaphthyl, biph = biphenyl, DPPE = 1,2-*bis*(diphenylphosphino)ethane, DPPF = 1,1'-*bis*(diphenylphosphino)ferrocene, Mes = mesityl.

With electron-rich phosphines, such as P*t*Bu$_3$ (Table 7, entry 2) or P(*p*-MeO-C$_6$H$_4$)$_3$ (entry 3), the reaction times decreased, and the results became more reproducible. On the other hand, electron-poor phosphines slowed the reaction down (Table 7, entries 9–14), and bidentate phosphines completely suppressed the reaction (Table 7, entries 15–17).

The final optimised reaction conditions consisted of catalyst RuCl$_2$(PPh$_3$)$_3$ (**52d**) used together with sodium formate and tri-*tert*-butylphosphine additives.

3.3 Scope of the reaction

We examined the scope of the reaction, and the results are shown in Table 7. The tandem process worked very well for a variety of aromatic allylic alcohols. The 1:1/1:2 adduct ratio (*i.e.* **54**:**55** ratio) could be influenced in favour of **54** by using less triethoxyvinylsilane, although this meant that the reactions required longer times (entries 3, 6, 8). A lower temperature of 100 °C could also be used, but once again, this meant that a longer reaction time was needed (entry 2). More substituted substrates gave good results as well (entries 14 and 15). A homoallylic alcohol could also be used as a substrate in the reaction (entry 16).

Table 7. Tandem isomerisation/C–H activation/C–C coupling reaction – substrate scope.

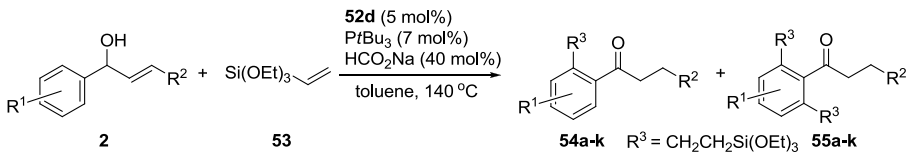

Entry	Substrate	Major product	Time (h)	Yield (**54** + **55**)[b]	**54**/**55** (%)[c]
1		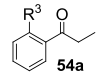 **54a**	2	>99 (86)	40/60
2[d]			7	>99	80/20
3[e]			4	94	92/8
4	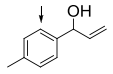	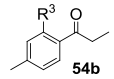 **54b**	5	>99 (83)	84/16
5	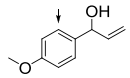	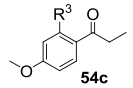 **54c**	1	>99 (90)	70/30
6[e]			4	>99	84/16
7	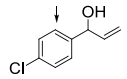	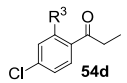 **54d**	3	>99 (85)	60/40
8[e]			6	80	95/5
9	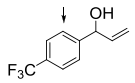	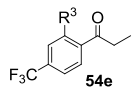 **54e**	7	96 (76)	84/16
10	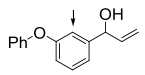	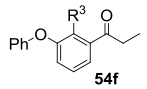 **54f**	3	>99 (92)	79(57/43)/ 21
11		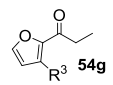 **54g**	3	95 (80)	–
12	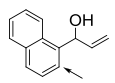	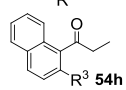 **54h**	3	91 (85)	–
13	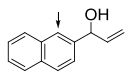	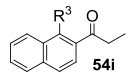 **54i**	2	>99 (90)	100/0
14	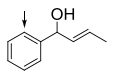	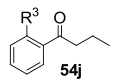 **54j**	18	91	92/8
15	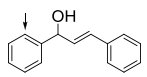	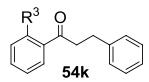 **54k**	24	64 (45)	100/0
16	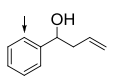	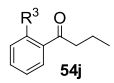 **54j**	14	90 (74)	94/6

[a] Alcohols **2** (0.5 mmol) and triethoxyvinylsilane (2 equiv.) were added to a suspension of HCO_2Na (30 mol %), **54d** (5 mol %), and P*t*Bu_3 (7 mol %) in toluene (0.5 mL) under a N_2 atmosphere. The flask was quickly introduced into an oil bath at 140 °C, and stirred for the time indicated. The arrows indicate the position where substitution took place. [b] Measured by ^{1}H NMR spectroscopy, isolated yields (**54**+**55**) in parentheses. [c] Measured by ^{1}H NMR spectroscopy.[d] In an oil bath at 100 °C. [e] (1.4 equiv.) Triethoxyvinylsilane was used.

The scope of reaction was further extended by using styrene (**56**) as the olefin coupling partner (Scheme 33). In this case, only the mono-substituted product was formed. However, in contrast to what we had seen with olefin **53**, the insertion of styrene was not regioselective, and a mixture of linear (**54l**) and branched (**55l**) products in an 80:20 ratio was obtained (> 95% conversion by ^{1}H NMR spectroscopy).

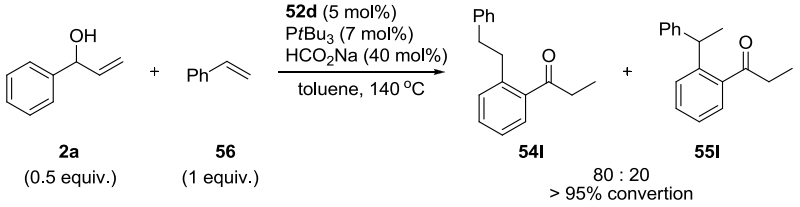

Scheme 33. Coupling with styrene.

3.4 Mechanistic investigations

To obtain some insight into the isomerisation process, the reaction was performed with α-deuterated allylic alcohol **2a**-d_1 without the coupling substrate (Scheme 34). The reactions were stopped after a few minutes (< 5 min).

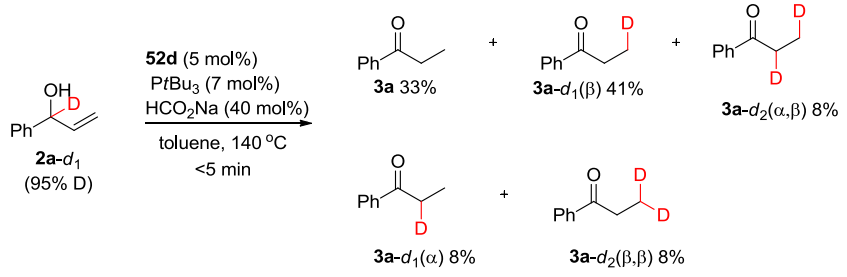

Scheme 34. Isomerisation of **2a**-d_1.

Analysis by HRMS spectrometry and ^{1}H NMR spectroscopy indicated that a mixture of non-deuterated, mono-deuterated and di-deuterated ketones **3a** was produced in >95% yield. Traces of unsaturated ketones (<2%) were also detected by ^{1}H NMR spectroscopy. Analysis by quantitative ^{13}C NMR spectroscopy helped us to estimate the ratio and structure of the mono-deuterated and di-deuterated ketones. More than one isomerisation mechanism must be considered to explain the deuterium distribution obtained in the isomerisation of **2a**-d_1 (see section 1.4). We believe that the isomerisation is most probably catalysed by Ru(II) complexes. The use of HCO_2Na for the formation of the active ruthenium hydride species can account for some of the deuterium loss. The non-regioselective or reversible

insertion of the olefins into the Ru–H/D bonds can explain the ratio of non-deuterated, mono-deuterated and di-deuterated ketones observed. Further support for the intermediacy of Ru dihydrides comes from the fact that $RuH_2(PPh_3)_4$ (**52b**) was found to be an efficient catalyst for the reaction (Table 5, entry 2). Since isomerisation of **2a** to ketone **3a** took place in a very short reaction time (<5 min), it was impossible to carry out more detailed studies using standard spectroscopic techniques.

A Ru(0)/Ru(II) mechanism previously described in the literature[20a] is probably involved in the C–H activation (Scheme 35). Ru(0) complexes can be produced by the reaction of Ru(II) dihydrides with a hydride acceptor. We did not detect formation of alcohol by-products in the ^{1}H NMR spectra of the crude reaction mixtures. These could have been formed by the reduction of ketones by ruthenium hydrides. Therefore, we propose that triethoxyvinyl silane, which is used in excess, can also act as a hydride acceptor and mediate the reduction of Ru(II) to Ru(0).[29a,67] This suggestion was also supported by the observation by NMR spectroscopy of traces of triethoxy(ethyl)silane in the crude reaction mixtures. The role of the phosphine additives is unclear, since it was found by mechanistic studies that only two phosphine ligands are bound to the metal in the catalytically active species.[30] It might be either to protect a highly unsaturated Ru(0) species or to act as an oxygen scavenger. A similar observation was made by Genêt and Darses,[27] who found that four equivalents of phosphine ligands for each [Ru] was the optimal amount under their reaction conditions for a similar ortho C–H functionalisation reaction.

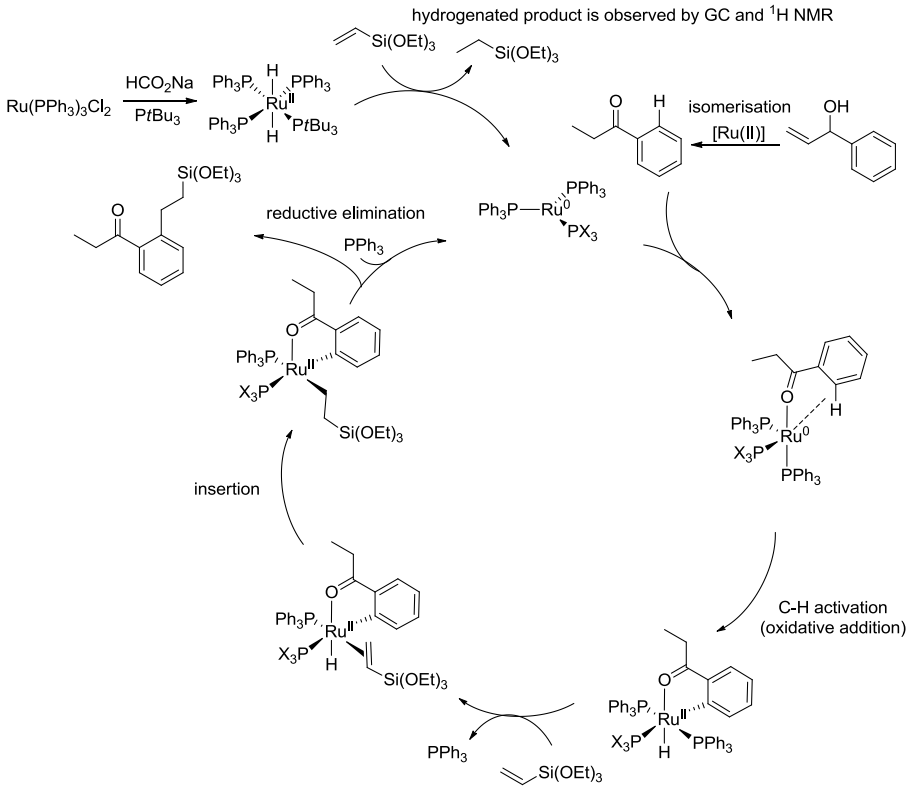

Scheme 35. Plausible mechanism for the tandem isomerisation/C–H functionalisation.

3.5 Summary

In conclusion, we have described a tandem process comprising isomerisation of allylic alcohols and a Murai reaction, using $RuCl_2(PPh_3)_3$ as the catalyst precursor. The tandem process gives the products in excellent yields and in very short reaction times. A broad scope of α-aryl allylic alcohols is tolerated, and homoallylic alcohols could also be used in the reaction. In most cases of coupling of alcohols with triethoxy(vinyl)silane, good selectivity for the monosubstituted product was obtained. The scope of the coupling substrate was extended to styrene. Good conversion and moderate selectivity was obtained with this substrate, but lower reaction rates were observed. The catalytically active Ru hydride intermediates and Ru(0) are generated under the reaction conditions, which allows the use of stable and commercially available ruthenium(II) precursors. The experiments with a deuterium-labelled substrate revealed that the isomerisation can occur by more than one mechanism.

Chapter 4

A bifunctional iridium complex with an alcohol/alkoxide-tethered *N*-Heterocyclic carbene ligand for alkylation of amines with alcohols – synthetic and mechanistic studies (Paper IV and Appendix 1).

4.1 Introduction

N-Heterocyclic carbenes (NHCs) constitute a very important family of ligands for the synthesis of transition metal complexes.[40] The robustness of metal complexes bearing NHC ligands can be attributed to a strong σ-donation ability and steric properties of these ligands. The strong metal–NHC bond often makes carbene complexes more stable to heat, oxygen, moisture and in some instances more active than those containing phosphine ligands.[40] Another advantage of NHCs is their straightforward synthesis, which allows easy access to an array of structures.

A special group of NHCs are those that are functionalised with an extra donor moiety. Such a modification introduces a stabilising chelating effect. [68] Depending on the nature of this donor functionality, bidentate NHCs may behave as hemilabile ligands, which would enable the creation of vacant coordination sites.[69] The bidentate NHCs with a donor function having a proton donor/acceptor capability may have a beneficial influence in catalytic reactions involving hydrogen transfer by protonating/deprotonating reactants and intermediates. This metal–ligand cooperation is called bifunctional catalysis (see section 1.3).[5,6] Additionally, secondary hydrogen bonding between the ligand and the substrate, may enhance the reaction rate and/or improve selectivity.[70] A number of complexes containing NHCs functionalised with alcohol, alkoxide, phenoxide, ether, *N*-heteroaryl, oxazoline, amino, amido, and other donor groups have been reported.[71] In several instances, potential hemilability of the donor group or metal–ligand bifunctionality has been proposed.[72]

Most of the cooperative catalytic systems contain amine or phenol moieties, *e.g.* Ikariya/Noyori[5] or Shvo catalysts.[6] In contrast, the

alcohol/alkoxide bifunctional system has never been tested in hydrogen-transfer reactions or hydrogenations.[73]

In this project, we aimed to prepare of such alcohol/alkoxide bifunctional metal complexes and to use them in reactions involving hydrogen transfer.[74,75] In particular, we were interested in the synthesis of iridium complexes that could be used in the alkylation of amines with alcohols (section 1.8). This reaction is very interesting from a synthetic viewpoint, since it makes use of simple and abundant starting materials. It has been shown before that iridium complexes are efficient catalyst for this transformation (Figure 2).[35,36,37] We envisioned that application of a complex capable of cooperative metal–ligand action may further improve the reactivity.

4.2 Ligand design and synthesis of the complexes

The new carbene ligand (Figure 9) was designed bearing in mind the following points: First, a chelate structure could provide higher complex stability. One of the most stable, a six-membered chelate, was chosen as the most promising. Second, the weakly binding OH group was expected to be labile and dissociate during the catalytic cycle, creating a vacant coordination site on iridium. Reverse coordination of the hydroxyl group could also help in a decordination of the amine product, which has been proposed to be a turnover-limiting step.[76] We chose a tertiary alcohol function, to avoid undesired β-hydride elimination processes on the ligand. Finally, the alcohol/alkoxide pair has the proton donor/acceptor properties required for the bifunctional catalysis.

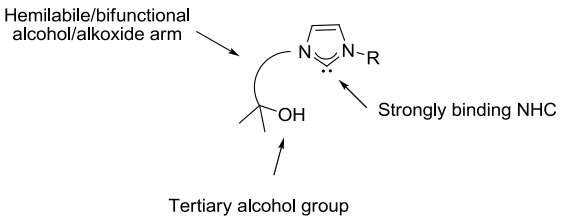

Figure 9. The design of a hemilable alcohol/alkoxide ligand.

Complexes **61a–d** were synthesised following a short reaction sequence shown in Scheme 36. Salt **58** was prepared in three steps starting from imidazole.[77] To obtain iridium complex **60**, we first prepared the corresponding silver carbene complex (**59**) by addition of Ag_2O to a solution of **58** in CH_2Cl_2 under light-free conditions. The formation of **59** was confirmed by NMR spectroscopy, which showed the characteristic Ag-$C_{carbene}$ signal at 180.4 ppm in the ^{13}C NMR spectrum. Complex **60** was

prepared by transmetallation of the carbene ligand to $[IrCp^*Cl_2]_2$. The presence of the O*H* proton in **60** was confirmed by ^1H NMR spectroscopy in an exchange experiment with D_2O, as well as with two-dimensional ^1H-^{13}C (HSQC) correlation spectra. Single-crystal X-ray diffraction analysis of **60** (Figure 10, left) additionally proved its structure to be correct, and revealed that the OH group of the ligand was not coordinated to the iridium centre.

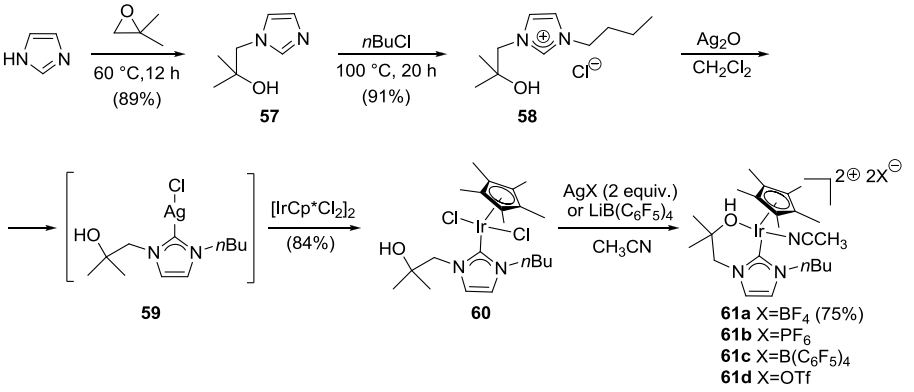

Scheme 36. Synthesis of complexes **1a-d**.

Dicationic iridium complexes **61a–d** were prepared by addition of two equivalents of AgX (X = BF_4, PF_6, OTf; for complexes **61a**, **61b**, and **61d**, respectively) or $LiB(C_6F_5)_4$ (for **61c**) to a solution of **60** in CH_3CN. Complex **61a** was characterised by ^1H, ^{13}C NMR spectroscopy and high-resolution mass spectrometry (HRMS). The presence of the acidic O*H* proton was further confirmed by an exchange experiment with D_2O. Additionally, the structure of complex **61a** was characterised by a single crystal X-ray diffraction analysis (Figure 10, right). In contrast to complex **60**, the hydroxyl group in **61a** is coordinated to iridium. The average $Ir–C_{carbene}$ (2.07 Å) and Ir–O distances (2.17 Å), are both in the expected range.[78]

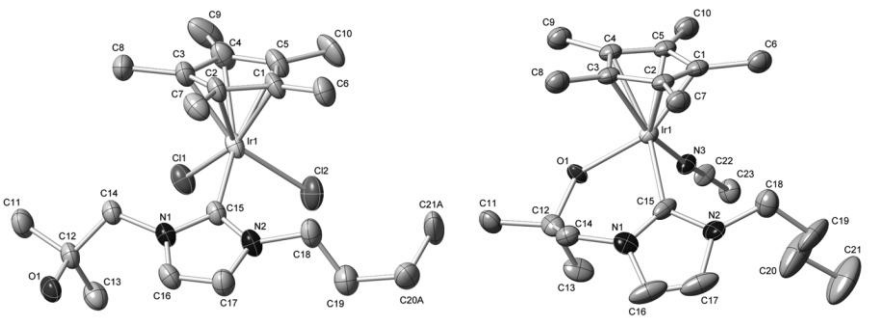

Figure 10. X-ray molecular structures of **60** (left) and **61a** (right, BF_4 anion is omitted for clarity).

We have also synthesised some structurally similar complexes (**63**, **67**, and **68**). Initially, the synthesis of monocationic complex **62**, an intermediate structure between complexes **60** and **61**, was attempted (Scheme 37). Despite several attempts to prepare **62** by treatment of **60** with $AgBF_4$ (1 equiv.), a mixture of different complexes was always formed. Since the acidic proton of **62** (as well as those of **61a–d**) is expected to be abstracted under the reaction conditions (*vide infra*), we prepared complex **63** instead, a deprotonated version of **62**. The reaction of complex **60** with KHMDS at low temperature gave alkoxide **63** that could be characterised by NMR spectroscopy, HRMS, and single crystal X-ray diffraction analysis (Scheme 38 and Figure 11).

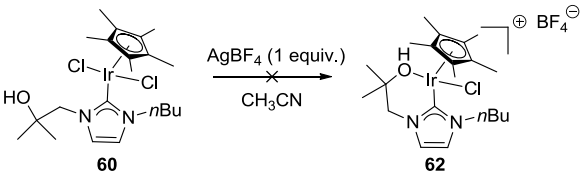

Scheme 37. Attempted synthesis of mono-cationic complex **62**.

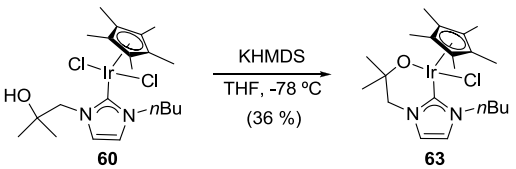

Scheme 38. Synthesis of neutral complex **63**.

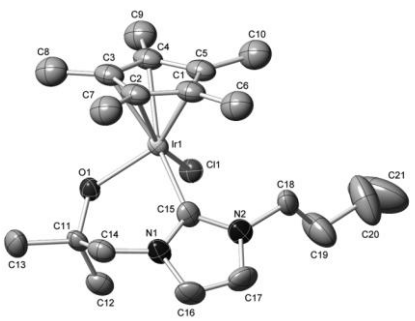

Figure 11. X-Ray molecular structure of complex **63**.

In addition, complexes **67** and **68,** which contain a methoxy group in the pendant chain were synthesised (Scheme 39). The precursor imidazolium salt **65** was prepared by treatment of **57** with MeI under basic conditions in THF, followed by reaction with *n*-butyl chloride. Complexes **67** and **68** were obtained following a synthetic route similar to that used for the synthesis of for **60** and **61** (*i.e.* by through transmetallation of the carbene from silver to

the iridium, followed by chloride abstraction). In the crystal structures, the methoxy group is not coordinated to iridium in the case of neutral complex **67** (Figure 12, left), while in biscationic complex **68** (Figure 12, right), the ether group is bound to the metal.

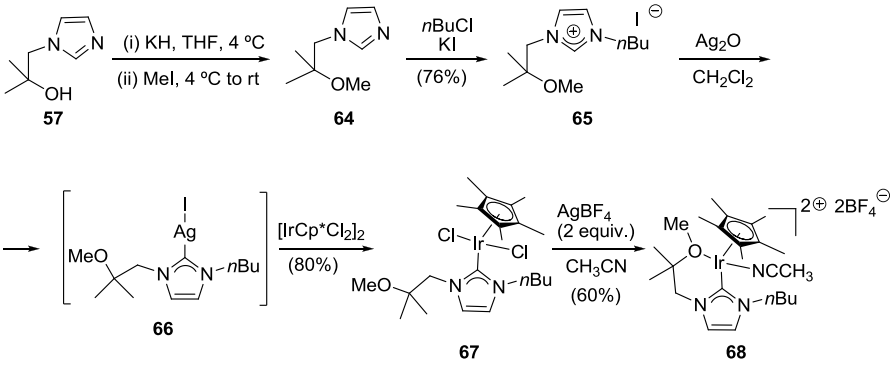

Scheme 39. Synthesis of complexes **67** and **68**.

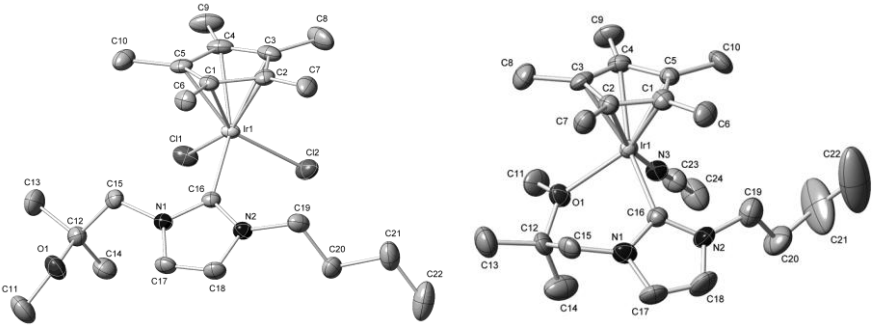

Figure 12. X-ray molecular structures of complexes **67** (left) and **68** (right).

4.3 Catalytic activity

The activity of NHC-iridium complexes **60**, **61a–d**, **63**, and **68** in the *N*-alkylation of amines with alcohols was explored. For comparison, we also tested $[IrCp^*Cl_2]_2$. The coupling of aniline with benzyl alcohol was investigated as a model reaction (Table 8). All the reactions were carried out with a 1.0 mol% catalyst loading, in toluene, under an argon atmosphere, using a 1:1 ratio of amine/alcohol.

Table 9. *N*-Alkylation of aniline with benzyl alcohol – catalyst screening.[a]

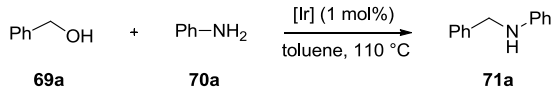

69a **70a** **71a**

Entry	Catalyst	Time (h)	Yield (%)[b]
1	none	14	0
2	$[IrCp^*Cl_2]_2$	14	12
3	$[IrCp^*Cl_2]_2/2AgBF_4$	14	5
4	**60**	2 / 14	11 / 47
5	**61a**	1 / 2	76 / >99
6	**61b**	1 / 2	78 / >99
7	**61c**	1 / 2	78 / >99
8	**61d**	2 / 5	50 / >99
9	**63**	2 / 14	33 / >99
10[c]	**63** + $AgBF_4$	1	>99
11[d]	**68**	2	72

[a] Unless otherwise noted: BnOH (1.0 mmol), $PhNH_2$ (1.0 mmol), [Ir] (1 mol%, 0.01 mmol) in toluene (0.5 mL) at 110 ºC. [b] Yield of *N*-benzylaniline determined by ^1H NMR spectroscopy using 1,4-di-*tert*-butylbenzene as an internal standard. [c] The active catalyst was prepared *in situ* from **9** and $AgBF_4$ (1 equiv.) in CH_2Cl_2 (0.1 mL), AgCl was separated by centrifugation and the remaining solution was used in the reaction. [d] 1.5 mol% Ir was used. When the reaction was performed using 1.0 mol%, 10% conversion was obtained (monitored from 2 h to 24 h).

No conversion was observed in the absence of any catalyst (entry 1), and with $[IrCp^*Cl_2]_2$ the reaction gave very low yield (entry 2).[79] The combination of $[IrCp^*Cl_2]_2$ with $AgBF_4$ also led to formation of traces of product (entry 3). The yield of *N*-benzylaniline was significantly improved using complex **60** (entry 4), which suggests the importance of the carbene ligand for the catalytic activity.

A dramatic increase in the catalytic activity was observed when the chloride ligands in **60** were substituted by less coordinating counter ions such as BF_4^- (**61a**), PF_6^- (**61b**), $B(C_6F_5)_4^-$ (**61c**), and OTf^- (**61d**) (entries 5-8, respectively). The results obtained with catalysts **61a-c** bearing BF_4^-, PF_6^- and $B(C_6F_5)_4^-$ anions were among the best. The reaction with complex **61d**, containing a more coordinating anion (OTf), needed slightly longer time to reach full conversion (entry 8).

Monochloride complex **63** gave a slightly better yield than dichloride **60** (entry 9 *vs.* 4), but it was clearly inferior to *bis*cationic catalysts **61a–d**. This suggests that the higher activity is obtained with increased electrophilic character of iridium center and cationic character of the complex. When

alkoxide complex **63** was used together with 1 equiv. $AgBF_4$, the reaction was complete in only 1 h (entry 10), indicating that the alkoxide complex might be the active intermediate in the reaction.

Finally, the activity of complex **68** (entry 11), containing a methyl ether moiety, was lower than that of catalyst **61a** bearing a hydroxyl group. Furthermore, catalyst **68** was less stable than catalysts **61a–d** and the catalyst loading had to be increased from 1 mol% to 1.5 mol% in order to reach high conversion levels. This result may be an indication that the presence of a ligand bearing an acidic proton in the catalyst increases the reaction rate.

Due to its high reactivity, complex **61a** was chosen for further optimisation studies (Table 10). An attempt to lower the catalyst loading below 1 mol% resulted in a drastic decrease of the catalytic activity (entry 1 *vs.* 2). The temperature of the reaction was found to have a high impact on the reaction rate (entries 3 and 4). It could be lowered to 90 °C, but a longer reaction time was needed to obtain a high conversion (6 h, 93% conv., entry 5).

Generation of the active catalyst **61a** *in situ* from the more stable precursor **60** (entry 5) afforded the *N*-alkylated product in an excellent yield and using same reaction time as when the isolated catalyst **61a** was used (entry 1 *vs.* 5).[80] Even better results were achieved when the acetonitrile used to prepare the catalyst stock solutions was replaced by a non-coordinating solvent (CH_2Cl_2). In this case, the temperature could be decreased down to 50 °C without diminishing the yields, albeit requiring longer reaction times and a higher catalyst loading (entries 6–9). To the best of our knowledge, this is first time that the alkylation of amines with alcohols has been performed at temperatures below 70 °C.[81]

Table 10. Optimisation of the reaction temperature and catalyst loading.[a]

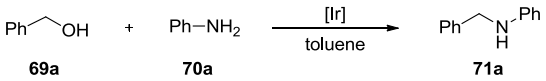

69a **70a** **71a**

Entry	Catalyst loading (mol%)	Temp (°C)	Time (h)	Yield (%)[b]
1	1	110	2	>99
2	0.5	110	6	21
3	1	100	6	>99
4	1	90	6	93
5[c]	1	110	2	>99
6[d]	2	80	3	>99
7[d]	1	80	36	92
8[d]	2	60	24	95
9[d]	2	50	48	>99

[a] Reaction conditions: BnOH (1.0 mmol), $PhNH_2$ (1.0 mmol), toluene (0.5 mL). [b] Yield of *N*-benzylaniline determined by ^1H NMR using 1,4-di-*tert*-butylbenzene as an internal standard. [c] **61a** was prepared *in situ* from **60** and $AgBF_4$ (2 equiv.) in MeCN and used in the reaction after filtration through Celite® to remove AgCl. The reaction was carried out in a mixture of MeCN/toluene (1:2). [d] The active catalyst was prepared *in situ* from **60** and $AgBF_4$ (2 equiv.) in CH_2Cl_2, after AgCl was separated by centrifugation and the remaining solution was used in the reaction. The reaction was carried out in a mixture of CH_2Cl_2/toluene (1:4).

4.4 Substrate scope

The optimised conditions, (*in situ* generation of the active catalyst, Table 9, entry 5) were applied to the coupling of various amines and alcohols (Tables 11 and 12).

A number of primary and secondary alcohols could be coupled with aniline to produce monoalkylated amines in high yields (Table 11). Benzyl alcohols (entries 1–2), primary aliphatic alcohols (entries 3–5) and secondary alcohols bearing alkyl and aryl substituents (entries 6–7) afforded the corresponding higher order amines in excellent yields. When 1,5-pentanediol was reacted with aniline, the cyclic 1-phenylpiperidine was the major product (entry 4). Coupling of the most reactive alcohols (Table 10, entry 9 and Table 11, entry 4) with aniline could be done at a reaction temperature as low as 50 °C, but to obtain reasonable reaction rates, 2 mol% of catalyst was necessary.

Table 11. *N*-alkylation of aniline with alcohols catalysed by **61a.**[a]

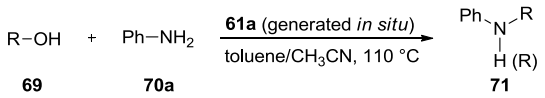

69 **70a** **71**

Entry	Alcohol	Amine product	Catalyst (mol%)	Time (h)	Yield (%)[b]
1			1	2	>99
2[c]	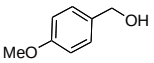	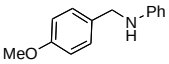	1.5	2	91
3	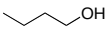	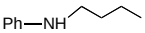	2.5	4	84
4			2.5	5	75
5	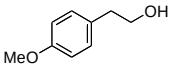	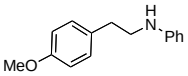	1.5	8	88
6			2.5	16	87
7		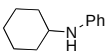	2.5	18	83

[a] Reaction conditions: alcohol (1.0 mmol), aniline (1.0 mmol), **61a** in toluene (0.3 mL) at 110 ºC. **61a** was prepared *in situ* as in Table 9, entry 5. [b] Isolated yield after flash chromatography. [c] When the reaction was carried out in a mixture of CH_2Cl_2/toluene (1:4) at 50 °C, 95% NMR yield of *N*-(4-methoxybenzyl)aniline product was obtained in 60 h. The active catalyst was prepared in same way as in Table 10, entry 9.

As for the amine substrate scope, various anilines with aromatic rings with different electronic properties were successfully alkylated with benzyl alcohol in high yields (Table 11, entries 1–5). Sterically hindered 2,4,6-trimethylaniline could be used as well, although a longer reaction time was necessary to reach a high conversion (entry 3). No cleavage of the halogen atoms was observed when 4-bromo or 4-chloro substituted substrates were used (entries 4 and 5). Moreover, the heteroaromatic moiety in 2-aminopyridine was also well tolerated (entry 6). Secondary amines, such as *N*-alkyl-*N*-arylamines, reacted efficiently under similar conditions in 15-16 h (entries 7–8). The reaction of benzyl alcohol with 4-amino-*N*-benzylbenzenesulfonamide resulted in a selective alkylation of the sulfonamide group (entry 9).[82] The coupling of the most reactive anilines (entry 9, Table 10, and entry 4, Table 12) with benzyl alcohol could be done at 50 °C.

Table 12. *N*-Alkylation of amines with benzyl alcohol catalysed by **61a**.[a]

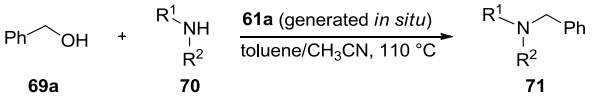

69a **70** **71**

Entry	Amine	Amine product	Catalyst (mol%)	Time (h)	Yield (%)[b]
1	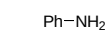	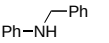	1	2	>99
2	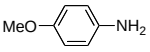	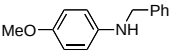	1.5	5	93
3	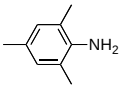	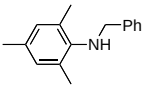	1.5	12	71
4[c]	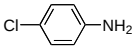	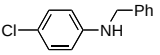	1	2.5	85
5	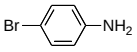	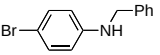	1	3	86
6	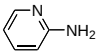	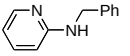	1.5	16	88
7			1.5	16	74
8			1.5	15	84
9	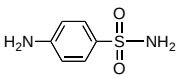	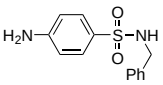	2.5	16	80

[a] Reaction conditions: **69a** (1.0 mmol), amine (1.0 mmol), **61a** in toluene (0.3 mL) at 110 ºC. **61a** was prepared *in situ* as in Table 9, entry 5. [b] Isolated yield after flash chromatography. [c] When the reaction was carried out in a mixture of CH_2Cl_2/toluene (1:4) at 50 °C, a >99% NMR yield of *N*-benzyl-4-chloroaniline product was obtained in 60 h. The active catalyst was prepared in same way as in Table 10, entry 9.

The catalytic system has also been tested with aliphatic amines, such as benzylamine, *n*-hexylamine, and cyclohexylamine, but in all cases, less than 10% conversion was observed. The lower activity obtained with aliphatic amines compared to aromatic amines might be due to the higher nucleophilicity and basicity of the aliphatic amines. A strong coordination of the aliphatic amines would prevent the binding of the alcohol substrate and result in deactivation of the complex.

4.5 Mechanistic investigations

The general mechanism of the alkylation of amines with alcohols was described in section 1.8. It consists of three major steps: (i) oxidation (dehydrogenation) of the alcohol to an aldehyde, (ii) condensation of the aldehyde with an amine to form an imine, and (iii) reduction (hydrogenation) of the imine (section 1.8, Scheme 17). Thus, the catalyst oscillates between two forms: dehydrogenated and hydrogenated.

To obtain insight into the mechanism of the studied reaction we used a combination of experimental and theoretical approaches. The former provides general information on the structure of the active form of the catalyst as well as relative rates of the respective mechanistic steps. The latter enables elucidation of the fine details of the catalytic cycle, such as distinguishing between the inner and outer sphere hydrogen-transfer mechanisms (section 1.3, Scheme 3).

4.5.1 Experimental studies

The first aspect of interest is the structure of an active form of the catalyst. Important conclusions in this regard can be drawn from the results shown in Table 8. All the most active catalytic systems, *i.e.* **61a**–**d** and **63**+$AgBF_4$, contain two common features: (1) a chelate structure with an alcohol (**61a**–**d**) or alkoxide (**63**+$AgBF_4$) coordinating group, and (2) a weakly bound (CH_3CN in **61a**–**d**) or no extra ligand (**63**+$AgBF_4$). Where either of these two attributes was lacking, a significant drop in catalytic activity was seen, as in the case of complexes **68** (methyl instead of proton on the chelating oxygen), **63** (strongly coordinating chloride), or **60** (no alcohol coordination, two chloride ligands). Also, the two other iridium(III) NHC complexes, that have been used before as catalysts for the reaction (Figure 2), contain only either the proton-accepting N-site (pyridine in Crabtree system)[36] or two weakly coordinating triflate ligands (Peris system),[37] which can account for their lower activity compared to our system.

The results presented above support the bifunctional mechanism of action of the iridium system studied: in order to efficiently catalyse the hydrogen transfer, the complex requires binding sites for both the proton and hydride binding sites (iridium and oxygen, respectively). The former is created by abstraction of the proton from the OH group in **61**, and the latter by dissociation of the CH_3CN ligand.[83]

The acidity of the OH group in **61** is expected to be increased due to the coordination to the metal centre. Therefore, its deprotonation should be facile under the reaction conditions due to the presence of a high excess of

the amine (*i.e.* aniline). To support this assumption, we studied the deprotonation by ^{1}H NMR spectroscopy. Unfortunately, titration of **61a** with aniline, resulted in complex NMR spectra, due to equilibria between differently coordinated iridium species. Instead, **61a** could be deprotonated with *N*,*N*,*N*',*N*'-tetramethylnaphthalene-1,8-diamine (**72**, proton sponge) in acetone-d_6 (Scheme 40). Due to the low nucleophilicity of **72**, a well-resolved spectrum of complex **73**, containing an acetone ligand, was recorded.

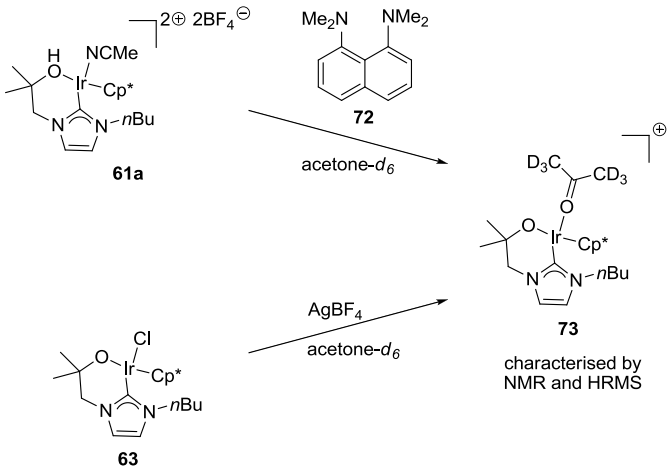

Scheme 40. Generation of the deprotonated complex **73**.

Complex **73** was also prepared by an alternative method from complex **63** and $AgBF_4$ in acetone-d_6 (Scheme 40). Complex **73** could be characterised by NMR spectroscopy and HRMS. Importantly, complex **73** generated *in situ* from **63** and $AgBF_4$ as shown in Table 9, entry 10, is the most efficient catalytic system for the studied reaction.

The second important aspect of the reaction mechanism that we decided to study was the relative rates of the three reaction steps. To address this issue, a measurement of a primary kinetic isotope effect was performed. Thus the progress of two separate reactions: (1) between aniline (**70a**) and benzyl alcohol (**69a**), and (2) aniline (**70a**) and α-d_2-benzyl alcohol (**69a**-d_2), was followed by GC and NMR spectroscopy (Scheme 41). Figure 13 shows the decay of the alcohol substrate in the two experiments. The resulting plots overlay, hence there is no primary isotope effect. This result clearly suggests that the alcohol dehydrogenation step (which would give a high KIE) is not the turnover-limiting step. In the second step, *i.e.* the hydrogenation of imine with iridium hydride, only a small primary KIE is expected, due to a low force constant of the Ir-H/Ir-D bond. The complete lack of a visible KIE is thus difficult to account for at the moment and needs further investigation.

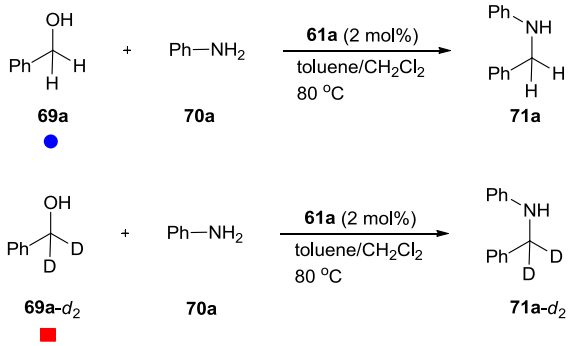

Scheme 41. The coupling reactions with non-deuterated (**69a**) and dideuterated (**69a**-d_2) benzyl alcohols catalysed by **61a**.

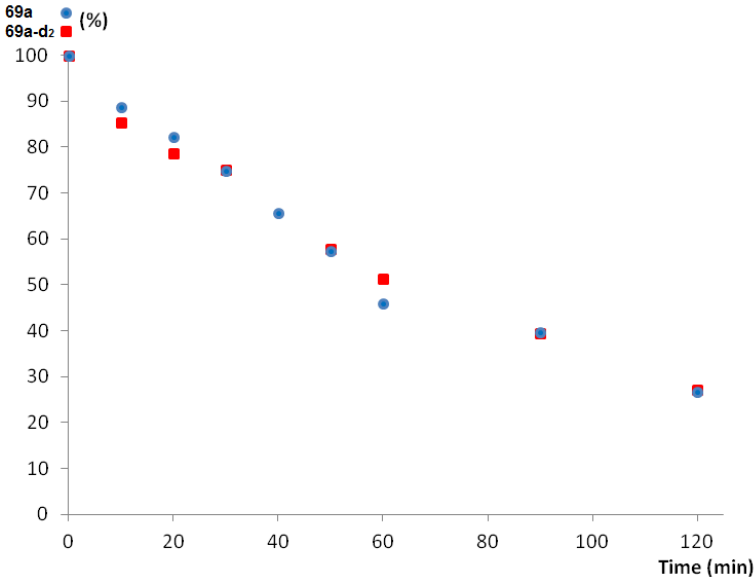

Figure 13. Consumption of non-deuterated (**69a**) and dideuterated (**69a**-d_2) benzyl alcohols during separate reactions with aniline (**70a**) catalysed by **61a**.

To obtain additional insights into the mechanism, a crossover experiment was carried out. In this reaction, a 1:1 mixture of **69a** and **69a**-d_2 was subjected to the coupling with aniline (Scheme 42). The reaction was stopped after 90% conversion and the resulting mixture was analysed by ^{1}H and ^{13}C NMR spectroscopy, combined with GC analysis. It was found that deuterium/hydrogen scrambling occurred in both the reaction product and the remaining starting material (*i.e.* all of **69a**, **69a**-d_1, **69a**-d_2, **71a**, **71a**-d_1, and **71a**-d_2 were present in the reaction mixture). This result implies that at least some portion of the intermediate aldehyde produced in the dehydrogenation step leaves the coordination sphere of the iridium hydride(deuteride) intermediate. After condensation with the amine in

solution, the resulting imine may undergo hydrogenation by another molecule of the catalyst, containing a different isotope of hydrogen, resulting in the monodeuterated product **71a**-d_1. Additionally, the formation of small amounts of monodeuterated benzyl alcohol **69a**-d_1 suggests that the alcohol dehydrogenation step is reversible.

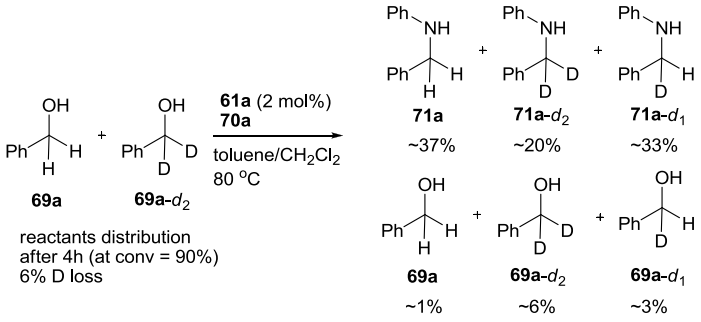

Scheme 42. Cross-over experiment.

Based on the results presented above, we propose a general mechanism for the alkylation of amines with alcohols catalysed by **61a** (Scheme 43).

In order to become catalytically active, complex **1a** must undergo a two-step activation. First, the OH proton is abstracted by the amine substrate, present in abundance in the reaction mixture. In the second activation step, the weakly coordinated CH_3CN ligand dissociates, forming the active bifunctional 16-electron complex **75**.

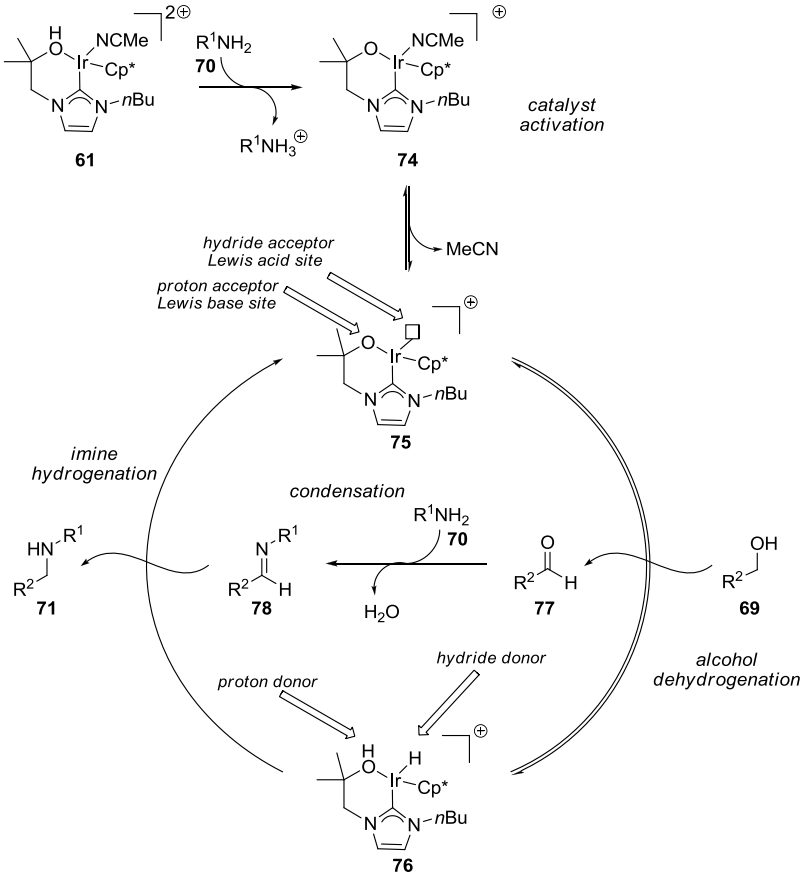

Scheme 43. Plausible general mechanism for the alkylation of amines with alcohols catalysed by complex **61**.

Complex **75** contains Lewis basic (oxygen) and Lewis acidic (iridium) sites, capable of accepting a proton and a hydride, respectively. Thus, **75** can dehydrogenate the alcohol substrate to give the hydrogenated form **76** with concomitant formation of aldehyde intermediate **77**. According to the results described above, this process is reversible and not rate-determining. Aldehyde **77** condenses with the amine, forming an imine intermediate **78**. Subsequently, bifunctional complex **76**, which contains both the hydride-donating and the proton-donating sites, re-hydrogenates the imine closing the catalytic cycle. Dehydrogenation and hydrogenation steps might occur either *via* outer or inner sphere mechanism (see section 1.3).

4.5.2 Theoretical studies

The details of the catalytic cycle shown in Scheme 43 were elucidated using density functional theory (DFT) calculations. The aim of these

investigations was to determine which of the two possible mechanisms, inner or outer sphere, that is more likely to operate (Scheme 44). We were also interested in investigating whether the alkoxide/alcohol ligand facilitates the key steps of the reaction, *i.e*. that **61** works as a metal-ligand bifunctional catalyst.

The calculations were performed on a model structure representing the catalyst, in which the *n*-butyl substituent was replaced with an ethyl group. The substrates were first modelled by methanol and aniline. The free energy profile was then recalculated for benzyl alcohol, which was the actual starting material used in the mechanistic experiments. Such an approach is advantageous on two accounts. First, the calculations with methanol as a substrate proceed faster and thus the reaction mechanism can be quickly established. Second, despite that the benzyl alcohol was the substrate we were interested in, the obtained free energy profile for methanol itself is also of value, since it enables comparison between the different alcohols.

The detailed mechanistic pathways obtained from the calculations are shown in Scheme 44. First, the calculations employing methanol and aniline as substrates will be presented. Later the critical points of the reaction pathway with methanol will be compared to those obtained with benzyl alcohol. The corresponding free energy profiles for methanol and benzyl alcohol as the substrates are given in Figures 16 and 17, respectively.

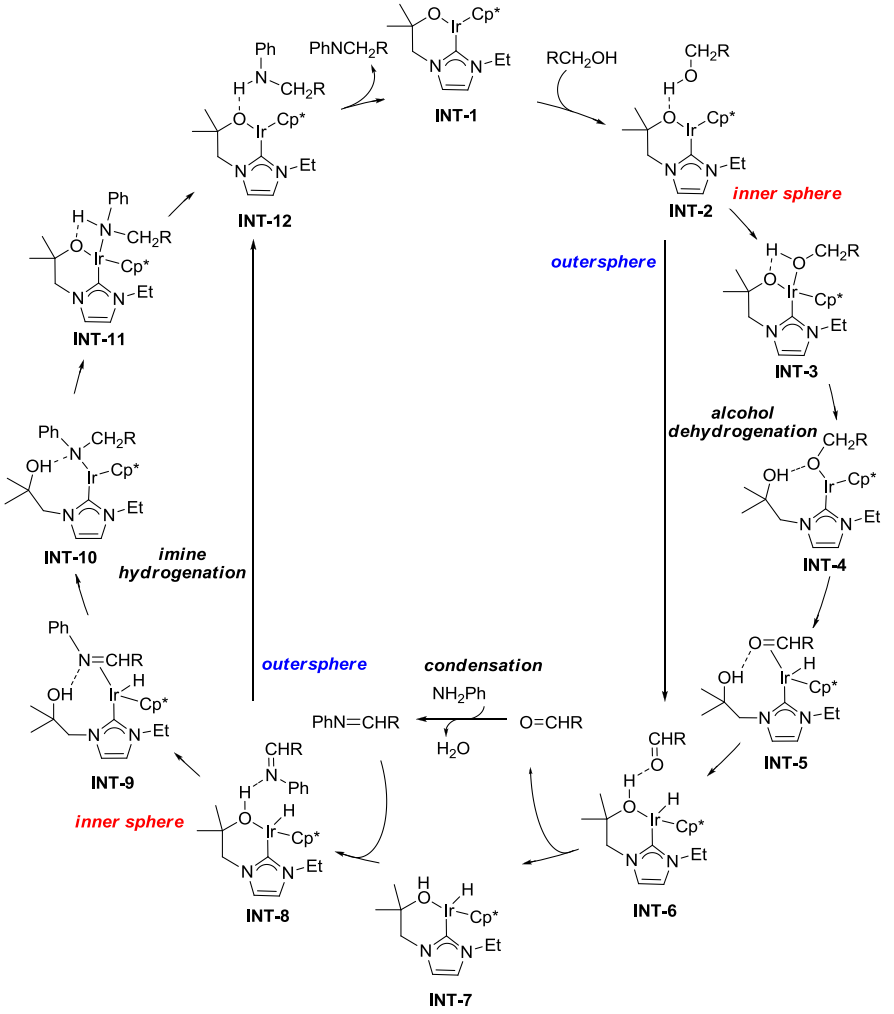

Scheme 44. Detailed mechanism for the alkylation of amines with alcohols catalysed by **INT-1**, showing outer and inner sphere pathway.

The experimental studies suggested that the catalytically active species is the iridium complex **INT-1**, formed by deprotonation and dissociation of CH_3CN from complexes **61**. According to the calculations, **INT-1** has a planar structure, with significant π-donation from the alkoxide group to the metal centre. This results in a short Ir–O distance (see Figure 15 for this and other key structures).

The mechanism (Scheme 44) starts with hydrogen bond formation between the alcohol substrate and the oxygen of **INT-1**. At this point, the outer and inner sphere pathways of the alcohol dehydrogenation diverge, to merge later at the stage of the hydrogenated catalyst (**INT-6**).

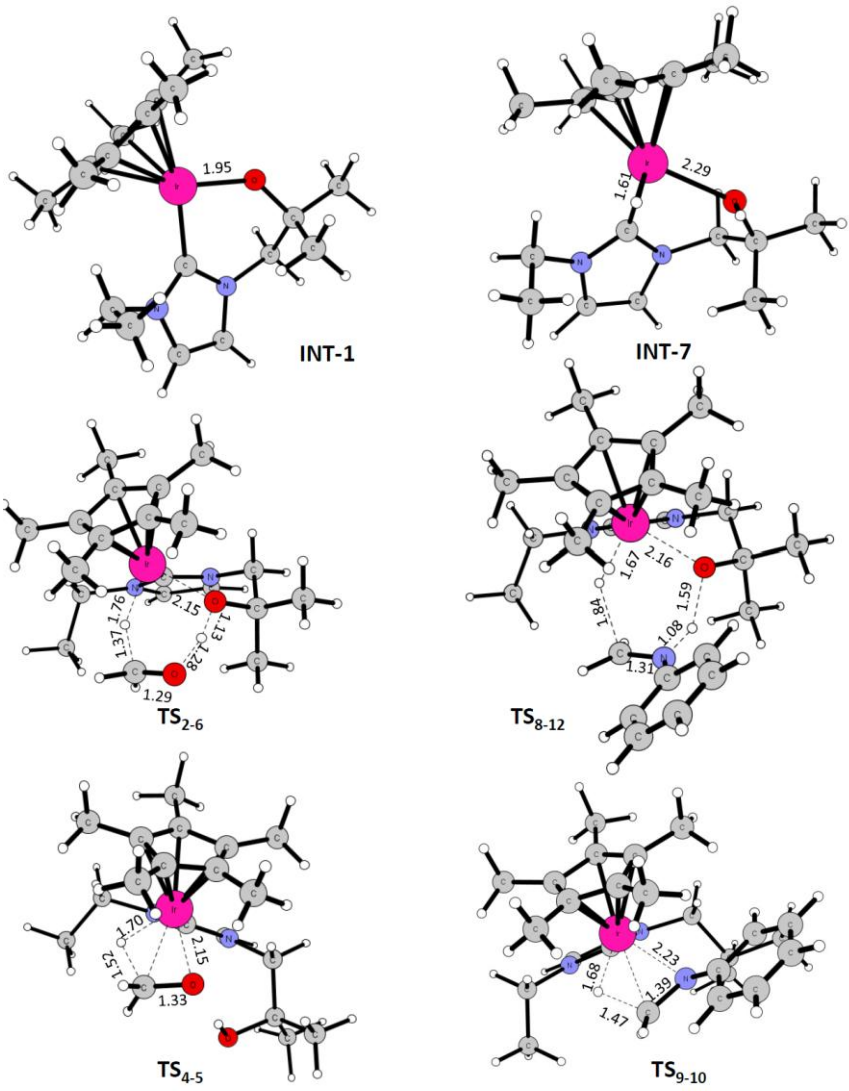

Figure 15. Selected key intermediates and transition-state structures.

From **INT-2** to **INT-6**, the outer sphere route involves only a single step, in which the dehydrogenation of methanol is realised by a concerted synchronous transfer of the hydride and the proton from methanol to the metal centre and the alkoxide oxygen atom, respectively, in a six-membered cyclic transition state $\mathbf{TS_{2\text{-}6}}$ (Figure 15). On the other hand, a inner sphere mechanism consists of several steps. The first of them is the coordination of the oxygen atom of methanol to iridium ($\mathbf{TS_{2\text{-}3}}$), followed by a proton transfer from the methanol oxygen to the alkoxide tether ($\mathbf{TS_{3\text{-}4}}$). Upon protonation, the tether dissociates from iridium, resulting in a planar iridium methoxide complex **INT-4**.[84] The energy barriers for both the methanol

coordination and the proton transfer are relatively low (16 and 9 kJ/mol, respectively), and the formation of **INT-4** from **INT-1** and methanol is practically thermoneutral. From **INT-4,** the *β*-hydride elimination can occur *via* $\mathbf{TS_{4\text{-}5}}$, which is the highest energy point of the inner sphere pathway. The product after the *β*-elimination step is **INT-5**, containing a formaldehyde molecule π-bonded to iridium. This compound evolves into a more stable intermediate (**INT-6**), in which the oxygen of the alcohol moiety on the ligand is coordinated to the metal centre and formaldehyde is hydrogen-bonded.

Overall, the calculations show that the inner sphere mechanism for the alcohol dehydrogenation is more favourable than the outer sphere alternative, although the energy difference between $\mathbf{TS_{2\text{-}6}}$ and $\mathbf{TS_{4\text{-}5}}$ is only 7 kJ/mol.

The cross-over experiment (Scheme 42) suggested that the aldehyde dissociates from the iridium-hydride complex. This result corresponds well with the data obtained from the calculations that show that **INT-6** and **INT-7** are very close in energy.

The next step is imine formation. There are a number of mechanistic possibilities for this condensation step, which can occur outside or inside the coordination sphere of iridium, and which can be mediated by **INT-5**, **INT-6**, or **INT-7** acting as Lewis or Brønsted acid catalysts. In any case, the condensation of formaldehyde with aniline itself is expected to have low barriers and thus was not explicitly studied.

After the condensation step, the hydrogen-bonded iridium hydride intermediate (**INT-8**) is formed. In the following step, the imine may undergo hydrogenation *via* either the outer or inner sphere pathway. Again, the first alternative involves only a single step. The corresponding transition state ($\mathbf{TS_{8\text{-}12}}$) is analogous to $\mathbf{TS_{2\text{-}6}}$, however in this case, a concerted asynchronous transfer of the proton and the hydride occurs. The barrier for this step is 80 kJ/mol, relative to **INT-6**.

The inner sphere route for the imine hydrogenation consists of a number of steps analogous to the first part of the cycle, but taking place in the reverse order. Specifically, **INT-8** must first undergo a ligand exchange (*i.e.* dissociation of the alcohol ligand and coordination of the imine), to form **INT-9**, so that the subsequent migratory insertion step can occur. A hydrogen bond of the OH group in **INT-8** makes the imine more electrophilic, which makes the hydride addition easier. $\mathbf{TS_{8\text{-}9}}$ is the highest point of the second part of the catalytic cycle in the inner sphere mechanism. Similar to the first part of the reaction, it is lower in energy than the corresponding transition state in the outer sphere pathway ($\mathbf{TS_{8\text{-}12}}$) by 21 kJ/mol.[85] Therefore, the calculations clearly rule out the outer sphere pathway for the amine hydrogenation part of the mechanism.

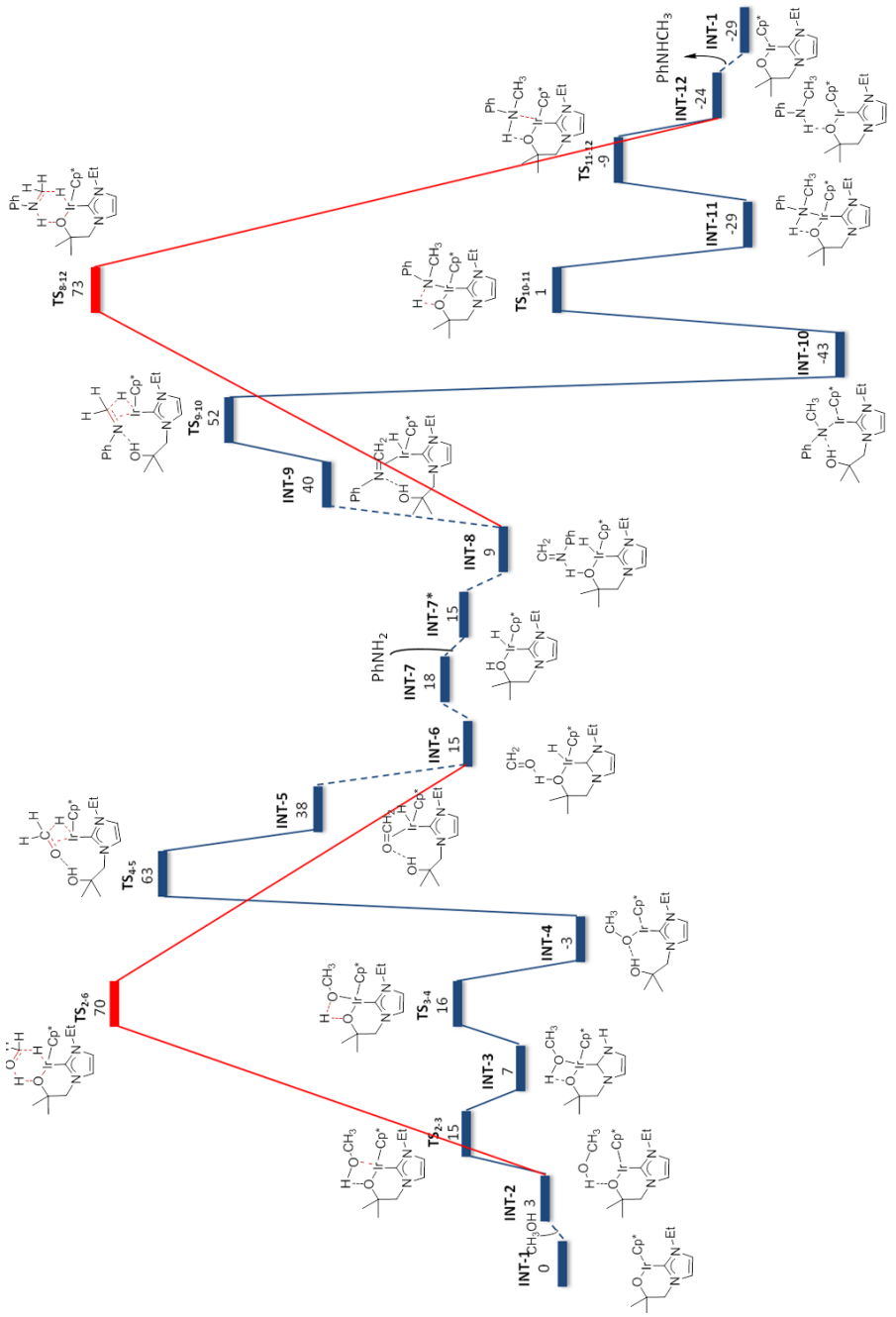

Figure 16. Complete free-energy diagram for the outer and inner sphere mechanisms with methanol and aniline as the substrates.

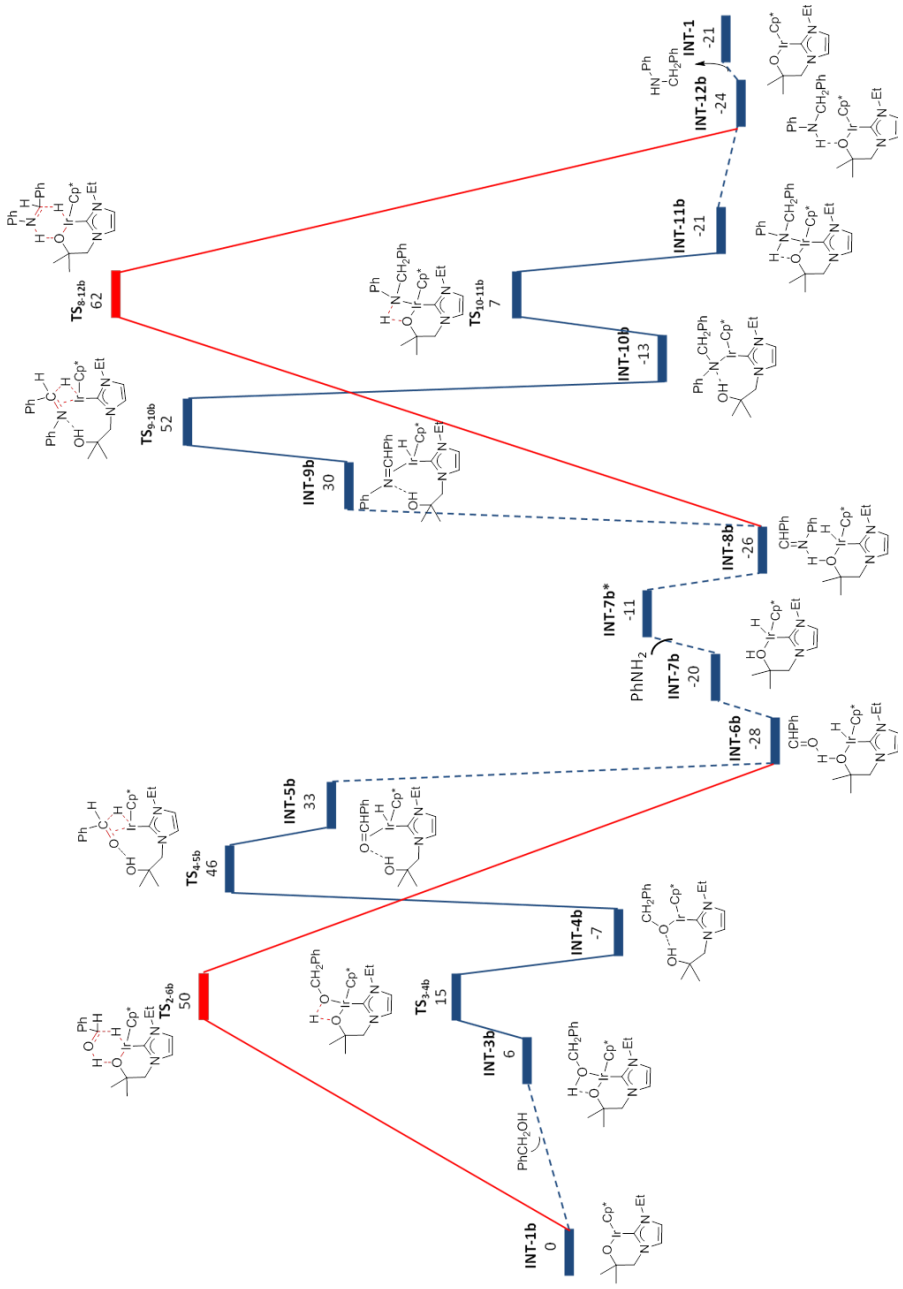

Figure 17. Complete free-energy diagram for the outer and inner sphere mechanisms with benzyl alcohol and aniline as the substrates.

The addition of hydride to the imine results in amido complex **INT-10**, which is the most stable intermediate of the whole catalytic cycle. From

INT-10, sequential proton transfer (**$TS_{10\text{-}11}$**) and decoordination of the amine from the iridium (**$TS_{11\text{-}12}$**) occur, producing intermediate **INT-12**, with the amine hydrogen-bonded to the oxygen atom of the ligand. Finally, the product is released, and the catalyst (**INT-1**) is regenerated. The overall reaction was calculated to be exergonic by 29 kJ/mol.

The calculated free energy profile obtained for methanol does not agree with the experimental results obtained with benzyl alcohol on several points which suggests that the exact reaction mechanism is significantly influenced by the substrate used. First, the calculations predict that the alcohol dehydrogenation should be turnover-limiting step of the reaction. Its overall barrier is 77 kJ/mol (in the favoured inner sphere pathway) counting from the lowest preceding intermediate (**INT-10**) to the highest transition state (**$TS_{4\text{-}5}$** in the next cycle). This is much higher than the barrier for the imine hydrogenation (43 kJ/mol from **INT-8** to **$TS_{9\text{-}10}$**). Also, the transition state of the *β*-hydride elimination step from the alcohol (**$TS_{4\text{-}5}$**) lies 11 kJ/mol above the TS for the migratory insertion of the imine (**$TS_{9\text{-}10}$**). Hence, the alcohol dehydrogenation is predicted to be irreversible by the calculations.

To get better agreement between the experimental and computational data, the structures of the critical intermediates and transition states were reoptimised and their free energies recalculated for benzyl alcohol. The resulting profile is shown in Figure 17.

Similarly to the reaction involving methanol, the inner sphere mechanism is favoured for both the alcohol dehydrogenation and the imine hydrogenation (by 4 and 10 kJ/mol, respectively). Also, dissociation of the transient benzaldehyde from complex **INT-6b** was found to be relatively facile, which agrees well with the experimental results. Several significant differences between the behaviour of the alcohols can be observed. First, for benzyl alcohol, the dehydrogenation step has a much lower energy barrier (53 kJ/mol for benzyl alcohol *vs.* 77 kJ/mol for methanol). This difference originates from a combination of a lower intrinsic barrier for the oxidation of benzyl alcohol and a lack of product inhibition (by the formation of stable amino, amido-iridium complexes), which raises the ground state for this step. In contrast to methanol, the overall dehydrogenation of benzyl alcohol is an exergonic process (by 20 kJ/mol). This correlates well with a general trend in the electroxidation potentials of alcohols.[86] On the other hand, the hydrogenation of the imine is the turnover-limiting step in the benzyl alcohol cycle, with an activation energy barrier of 80 kJ/mol from **INT-6b** to **$TS_{9b\text{-}10b}$**. Hence, in this case, the results of the calculations correspond well with the experiments – the alcohol dehydrogenation is not the turnover-limiting step. Additionally, **$TS_{9b\text{-}10b}$** has a higher energy than **$TS_{4b\text{-}5b}$**, so the alcohol dehydrogenation is reversible, as indeed was observed experimentally in the crossover experiment (Scheme 42).

In summary, the mechanism of the alkylation of amines with alcohols catalysed by complex **61** was studied in detail by DFT calculations. It was

shown that the inner sphere mechanism is slightly favoured in the alcohol dehydrogenation and dominant in the imine reduction. The calculations revealed significant differences between the reactions involving methanol and benzyl alcohol as the substrates. The critical points in the outer and inner sphere mechanisms are close in the free energy profile for benzyl alcohol substrate, which suggests that the operating mechanism will be dependent on the electronic and steric properties of the substrates. In the case of benzyl alcohol, the experimental findings were very well reproduced by the calculations. Most importantly, the theoretical studies clearly demonstrated the involvement of the alcohol/alkoxide ligand in almost every step of the catalytic cycle, thus confirming the bifunctional mode of action of the catalyst.

4.7 Conclusions

In summary, we have synthesised new *N*-Heterocyclic carbene ligands containing a hydroxyl moiety, which allowed for the first time the preparation of iridium complexes bearing chelating NHC-alcohol ligands. The unique properties of the complexes account for their high catalytic activity in the *N*-alkylation of amines with alcohols. The best catalyst shows a broad substrate scope and is one of the most active catalysts known to date, being able to catalyse the reaction at temperatures as low as 50 °C.

A combination of experimental and theoretical approaches has been used to elucidate the mechanism of the reaction. It has been shown that metal–ligand cooperation (bifunctionality) can account for the high activity of the catalyst.

Concluding Remarks

The work described in this thesis was aimed at development of transfer hydrogen processes to make C–C and C–N bond and investigating their mechanisms.

In the first two projects, it was demonstrated that allylic alcohols can be successfully used as synthetic enolate or ketone equivalents. Two tandem processes that begin with isomerisation of allylic alcohols were developed. In the first part, a new catalytic system for the synthesis of β-hydroxy ketones and β-amino ketones from allylic alcohols was described. The aldol and Mannich products could be synthesized by reacting enolates intermediates formed during the isomerisation of allylic alcohols. Excellent yields and good *syn*/*anti* diastereoselectivities were obtained. Several new aspects of the reaction mechanism were identified for the first time, such as epimerisation of the product and retro-aldolisation. The results obtained give a general framework for understanding processes involving ruthenium-catalysed tandem allylic alcohol isomerisation/C–C coupling reactions, as well as provide aid for developing other catalytic reactions based on this transformation. In the second part of this thesis, it was demonstrated that ruthenium catalysed allylic alcohol isomerisation can be combined with aromatic C–H activation. In this case, the allylic alcohol substrate was isomerised into ketone, and the carbonyl group of this intermediate served as directing group for further C–H activation and C–C bond formation reaction.

The last part of the thesis shows a possible extension of metal-ligand bifunctional systems to those containing alcohol/alkoxy ligand. The design and synthesis of iridium(III) complexes bearing the alcohol/alkoxide ligands were described. The synthesised complexes were used as catalyst in the alkylation of anilines using alcohols as latent electrophiles. It has been shown by experimental and theoretical studies that the metal-ligand cooperation is the key for the high activity of the catalyst.

Appendix 1

Alkylation of aamines with alcohols catalysed by a bifunctional iridium complex: a mechanistic investigation

Agnieszka Bartoszewicz, Rocío Marcos, Per-Ola Norrby, and Belén Martín-Matute

Experimental details

General

All reactions were carried out under argon atmosphere in oven-dried glassware. The sealable tubes used were Biotage microwave vials. Reagents were of analytical grade, obtained from commercial suppliers and used as purchased. CH_2Cl_2 was dried over CaH_2 and distilled under nitrogen. Anhydrous toluene was obtained using VAC solvent purifier system. ^{1}H and ^{13}C NMR spectra were recorded at 400 MHz and at 100 MHz, respectively, on a Bruker Avance spectrometer. Chemical shifts (δ) are reported in ppm, using the residual solvent peak in $CDCl_3$ (δ_H 7.26). Gas chromatography GC was performed on a Varian 3800 GC with a CP-CHIRASIL-DEX CB chiral column (30 m) with FID detector and naphthalene as internal standard.

Preparation of 73

To an oven-dried sealed tube containing the corresponding pre-catalyst **60** (45 mg, 0.075 mmol) in CH_2Cl_2 (0.5 mL) under argon, a solution a solution of $AgBF_4$ (28.8 mg, 0.15 mmol) in anhydrous and degassed CH_2Cl_2 (0.25 mL) was added. The reaction mixture was stirred for 15 min at room temperature. AgCl was separated by centrifugation and the resulting solution containing **70** was used as the stock solution for catalysis.

Primary KIE determination

Two parallel reactions: one with benzyl alcohol and another with benzyl alcohol-α-d_2 were prepared (Scheme 41). The solutions of either benzyl

alcohol (1 mmol) or benzyl alcohol-α-d_2 (1 mmol) and amine (1 mmol) in anhydrous and degassed toluene (0.3 mL) containing naphthalene as internal standard (32 mg, 0.25 mmol) were stirred under argon at 80 °C. The solution of catalyst **70** (0.2 mL, 2 mol%) was added to each of preheated reaction mixtures. Crude reaction samples were taken every 10-15 min and consumption of the non-deuterated (**69a**) and dideuterated (**69a**-d_2) was followed by GC (Figure 13).

Cross-over experiment

A solution of benzyl alcohol (0.5 mmol), benzyl alcohol-α-d_2 (0.5 mmol), and aniline (1 mmol) in anhydrous and degassed toluene (0.3 mL) containing naphthalene as internal standard (32 mg, 0.25 mmol) was stirred at 80 °C under an argon atmosphere. The solution of catalyst **70** (0.2 mL, 2 mol%) was added to the preheated mixture (Scheme 42). Reaction aliquots were taken after 4 h and analysed by of GC and ^{1}H NMR spectroscopy.

Computational details

The calculations were performed using Jaguar package.[87] Geometries were optimized using B3LYP functional[88] with LACVP* basis set.[89] These were then characterized with frequency calculations to confirm their character as minima (no imaginary frequencies) or transition states (one single imaginary frequency). The connections between transition states and their corresponding reactants and products were verified by fully optimizing structures derived from the transition states with a small displacement following the transition vector in both directions (QRC). The final Gibbs free energies were obtained from single-point calculations using M06 functional[90] with the larger basis set LACV3P**$^+$, corrected for zero-point and thermal effects at 353.15 K and 325.0 atm from the frequency calculations,[91] and solvation free energy. The latter was calculated using self-consistent reaction field (SCRF) polarized continuum model (PCM) with parameters for benzene,[92] as implemented in Jaguar.

Acknowledgements

I would like to thank the following people:

My Supervisor, *Associate Prof. Belén Martín-Matute* for accepting me as a PhD student and for excellent guidance.

Prof. Jan–Erling Bäckvall for his interest in this thesis.

My present and past group members: *Nanna Ahlsten, Dr. Rocío Marcos, Dr. Santosh Agrawal, Dr. Mikaela Gustafsson, Dr. Suman Sahoo, Fabian Carson, Tove Slagbrand, Martina Jeżowska, Kévin Laymand, Madeleine Livendahl, Dr. Antonio Bermejo, Vlad Pascanu, Helena Lundberg, Asraa Ziadi, Debasree Saha, María Batuecas, Jose Ignacio Martínez, Maud Lenormand, Dr. Eduardo Busto, Liu Baoyan* for good collaboration and creating a great atmosphere in lab.

Dr. Marcin Kalek, Nanna Ahlsten, Dr. Ian Cumpstey, Dr. Rocío Marcos and Dr. Antonio Bermejo for proof-reading of this thesis.

Prof. Per-Ola Norrby for collaboration on theoretical studies on the bifunctional complex.

Prof. M. A. Pericàs from ICIQ in Spain for providing me the lab space during my short exchange project in flow chemistry.

All the people at the Department of Organic Chemistry.

TA-staff

K & A Wallenberg's Foundation, Swedish Chemical Society, Ångpanneföreningen (ÅF), Astra Zeneca, and Berzelii Center Exselent for travel grants.

Berzelii Center Exselent & people from Inorganic and Structural Chemistry Department: *Prof. Xiaodong Zou, Dr. Mikaela Gustafsson, Fabian Carson, Dr. Suman Sahoo and Dr. A. Ken Inge,* for collaboration on projects involving heterogenous catalysis.

My friends back in Poland, and the ones in Sweden

My family

Marcin for patience and constant support – dzięki.

References

(1) In this thesis ACS Standard Abbreviations/Acronyms are followed. *The ACS Style Guide*;3 ed.; American Chemical Society: Washington, DC, 2006.

(2) Selected reviews: a) Malacria, M. *Chem. Rev.* **1996**, *96*, 289-306; b) Tietze, L. F. *Chem. Rev*. **1996**, *96*, 115-136; c) Molander, G. A.; Harris, C. R. *Chem. Rev*. **1996**, *96*, 307-338; d) Eilbracht, P.; Bärfacker, L.; Buss, C.; Hollmann, C.; Kitsos-Rzychon, B. E.; Kranemann, C. L.; Rische, T.; Roggenbuck, R.; Schmidt, A. *Chem. Rev.* **1999**, *99*, 3329-3365; e) Ikeda, S.–I. *Acc. Chem. Res.* **2000**, *33*, 511-519; f) Mayer, S. F.; Kroutil, W.; Faber, K. *Chem. Soc. Rev*. **2001**, *30*, 332-339; g) Fogg, D. E.; dos Santos, E. N. *Coord. Chem. Rev*. **2004**, *248*, 2365-2379; h) Lee, J. M.; Na, Y.; Han, H.; Chang, S. *Chem. Soc. Rev*. **2004**, *33*, 302-312; i) Wasilke, J.–C.; Obrey, S. J.; Baker, R. T.; Bazan, G. C. *Chem. Rev.* **2005**, *105*, 1001-1020; j) D'Souza, D. M.; Mueller, T. J. J. *Chem. Soc. Rev*. **2007**, *36*, 1095-1108; k) Felpin, F.–X.; Fouquet, E. *ChemSusChem* **2008**, *1*, 718-724; l) Godineau, E.; Landais, Y. *Chem. Eur. J*. **2009**, *15*, 3044-3055; m) Hugel, H. M. *Molecules* **2009**, *14*, 4936-4972; n) Kumaravel, K.; Vasuki, G. *Curr. Org. Chem.* **2009**, *13*, 1820-1841; o) Tambade, P. J.; Patil, Y. P.; Bhanage, B. M. *Curr. Org. Chem.* **2009**, *13*, 1805-1819; p) Toure, B. B.; Hall, D. G. *Chem. Rev*. **2009**, *109*, 4439-4486; q) Alonso, F.; Foubelo, F.; González-Gómez, J. C.; Martínez, R.; Ramón, D. J.; Riente, P.; Yus, M. *Mol. Divers.* **2010**, *14*, 411-424; r) Bariwal, J. B.; Trivedi, J. C.; Van, d. E. E. V. *Top. Heterocycl. Chem*. **2010**, *25* 169-230; s) Estévez, V.; Villacampa, M.; Menéndez, J. C. *Chem. Soc. Rev*. **2010**, *39*, 4402-4421; t) Fustero, S.; Sánchez-Roselló, M.; del Pozo, C.*Pure Appl. Chem.* **2010**, *82*, 669-677; u) Ruijter, E.; Scheffelaar, R.; Orru, R. V. A. *Angew. Chem. Int. Ed.* **2011,** *50*, 6234-6246; v) de Graaff, C.; Ruijter, E.; Orru, R. V. A. *Chem. Soc. Rev.* **2012**, *41*, 3969-4009; w) Domling, A.; Wang, W.; Wang, K. *Chem. Rev*. **2012**, *112*, 3083-3135; x) Eckert, H. *Molecules* **2012**, *17*, 1074-1102.

(3) a) Hamid, M. H. S. A.; Slatford, P. A.; Williams, J. M. J. *Adv. Synth. Catal.* **2007**, *349*, 1555-1575; b) Guillena, G.; Ramón, D. J.; Yus, M. *Angew. Chem. Int. Ed*. **2007**, *46*, 2358-2364; c) Nixon, T. D.; Whittlesey, M. K.; Williams, J. M. J. *Dalton Trans*. **2009**, 753-762.

(4) a) Roundhill, D. M. *Chem. Rev*. **1992**, *92*, 1-27; b) Guillena, G.; Ramón, D. J.; Yus, M. *Chem. Rev*. **2010**, *110*, 1611-1641; c) Dobereiner, G. E.; Crabtree, R. H. *Chem. Rev*. **2010**, *110*, 681-703; d) Watson, A. J. A.; Williams, J. M. J. *Science* **2010**, *329*, 635-636; e) Bähn, S.; Imm, S.; Neubert, L.; Zhang, M.; Neumann, H.; Beller, M. *ChemCatChem* **2011**, *3*, 1853-1864.

(5) Selected reviews: a) Noyori, R.; Yamakawa, M.; Hashiguchi, S. *J. Org. Chem*. **2001**, *66*, 7931-7944; b) Muñiz, K. *Angew. Chem. Int. Ed*. **2005**, *44*, 6622-6627; c) Kuwata, S.; Ikariya, T. *Dalton Trans*. **2010**, *39*, 2984-2992; d) Ikariya, T.; Gridnev, I. D. *Top. Catal.* **2010**, *53*, 894-901; e) Ikariya, T.; Kuwata, S.; Kayaki, Y. *Pure Appl. Chem.* **2010**, *82*, 1471-1483; f) Ikariya, T. *Bull. Chem. Soc. Jpn.* **2011**, *84*, 1-16; g) Ikariya, T. *Topics* in *Organometallic Chemistry*,

Vol. 37, (Eds: Ikariya, T.; Shibasaki, M.), Springer Verlag, Berlin / Heidelberg, **2011**, pp. 31-53.

(6) Selected examples: a) Blum, Y.; Czarkie, D.; Rahamim, Y.; Shvo Y. *Organometallics* **1985**, *4*, 1459-1461; b) Shvo, Y.; Czarkie, D.; Rahamim, Y.; Chodosh, D. F. *J. Am. Chem. Soc.* **1986**, *108*, 7400-7402; c) Mays, M. J.; Morris, M. J.; Raithby, P. R.; Shvo, Y.; Czarkie, D. *Organometallics* **1989**, *8*, 1162-1167; d) Menashe, N.; Salant, E.; Shvo, Y. *J. Organomet. Chem.* **1996**, *514*, 97-102; e) Casey, C. P.; Singer, S. W.; Powell, D. R.; Hayashi, R. K.; Kavana, M. *J. Am. Chem. Soc.* **2001**, *123*, 1090-1100; f) Casey, C. P.; Johnson, J. B.; Singer, S. W.; Cui, Q. *J. Am. Chem. Soc.* **2005**, *127*, 3100-3109; g) Fujita, K.; Tanino, N.; Yamaguchi, R. *Org. Lett.* **2007**, *9*, 109-111; h) Yamaguchi, R.; Ikeda, C.; Takahashi, Y.; Fujita, K. *J. Am. Chem. Soc.* **2009**, *131*, 8410-8412; i) Conley, B. L.; Pennington-Boggio, M. K.; Boz, E.; Williams, T. J. *Chem. Rev.* **2010**, *110*, 2294-2312; j) Nieto, I.; Livings, M. S.; Sacci, J. B.; Reuther, L. E.; Zeller, M.; Papish, E. T. *Organometallics* **2011**, *30*, 6339-6342; k) Bauer, G.; Kirchner, K. A. *Angew. Chem. Int. Ed.* **2011**, *50*, 5798-5800; l) Li, H.; Lu, G.; Jiang, J.; Huang, F.; Wang, Z.–X. *Organometallics* **2011**, *30*, 2349-2363; m) Casey, C. P.; Guan H. *Organometallics* **2012**, *31***,** 2631-2638; n) Warner, M. C.; Casey, C. P.; Bäckvall J.–E. *Topics in Organometallic Chemistry*, Vol. 37, (Eds: Ikariya, T.; Shibasaki, M.), Springer Verlag, Berlin / Heidelberg, **2011**, pp. 31-53.

(7) Reviews: a) Van der Drift, R. C.; Bouwman, E.; Drent, E. J. *J. Organomet. Chem.* **2002**, *650*, 1-24; b) Uma, R.; Crévisy, C.; Grée, R. *Chem. Rev.* **2003**, *103*, 27-51; c) Cadierno, V.; Crochet, P.; Gimeno, J. *Synlett* **2008**, *8*, 1105-1124; d) Mantilli L.; Mazet C. *Chem. Lett.* **2011**, *40*, 341-344; e) Ahlsten, N.; Bartoszewicz, A.; Martín-Matute, B. *Dalton Trans.* **2012**, *41*, 1660-1670; f) Lorenzo-Luis, P.; Romerosa, A.; Serrano-Ruiz, M. *ACS Catal.* **2012**, *2*, 1079-1086.

(8) Selected examples of transition-metal-catalysed allylic alcohol isomerisations: a) Ruthenium in Organic Synthesis (Ed.: Murahashi S.–I.), Wiley–VCH, Weinheim, **2004**, 309-315; b) Tanaka, K. *Comprehensive Organometallic Chemistry III*, **2007**, Chapter 10.02, 71-100; c) Trost, B. M., Kulawiec, R. J. *Tetrahedron Lett.* **1991**, *32*, 3039-3042; d) Bäckvall, J.–E.; Andreasson, U. *Tetrahedron Lett.* **1993**, *34*, 5459-5462; e) Trost, B. M., Kulawiec, R. J. *J. Am. Chem. Soc.* **1993**, *115*, 2027-2036; f) McGrath, D. V.; Grubbs, R. H. *Organometallics* **1994**, *13*, 224-235; g) Wang, D.; Chen, D.; Haberman, J. X.; Li, C.–J. *Tetrahedron* **1998**, *54*, 5129-5142; h) Markó, I. E.; Gautier, A.; Tsukazaki, M.; Llobet, A.; Plantalech-Mir, E.; Urch, C. J.; Brown. S. M. Angew. *Chem. Int. Ed.* **1999**, *38*, 1960-1962; i) Slugovc, C.; Rüba, E.; Schmid, R.; Kirchner, K. O*rganometallics* **1999**, *18*, 4230-4233; j) Van der Drift, R. C.; Vailati, M.; Bouwman, E.; Drent, E. *J. Mol. Catal. A: Chem.* **2000**, *159*, 163-177; k) Doppiu, A.; Salzer, A. *Eur. J. Inorg. Chem.* **2004**, *11*, 2244-2252; l) Ganchegui, B.; Bouquillon, S.; Hénin, F.; Muzart, J. *J. Mol. Cat. A: Chem.* **2004**, *214*, 65-69; m) Martín-Matute, B.; Bogàr, K.; Edin, M.; Kaynak, F. B.; Bäckvall, J.–E. *Chem. Eur. J.* **2005**, *11*, 5832-5842; n) Trost, B. M.; Frederiksen, M. U.; Rudd, M. T. *Angew. Chem. Int. Ed.* **2005**, *44*, 6630-6666; o) Van der Drift, R. C.; Gagliardo, M.; Kooijman, H.; Spek, A. L.; Bouwman, E.; Drent, R. C. *J. Organomet. Chem.* **2005**, *690*, 1044-1055; p) Crochet, P.;

Fernández-Zúmel, M. A.; Gimeno, J.; Scheele, M. *Organometallics* **2006**, *25*, 4846-4849; q) Bouziane, A.; Carboni, B.; Bruneau, C.; Carreaux, F.; Renaud, J.–L. *Tetrehedron* **2008**, *64*, 11745-11750; r) Ahlsten, N.; Lundberg, H.; Martín-Matute, B. *Green Chem.* **2010**, *12*, 1628-1633; s) Batuecas, M.; Esteruelas, M. A.; García-Yebra, C.; Oñate, E. *Organometallics* **2010**, *29*, 2166-2175; t) García-Álvarez, J.; Gimeno J.; Suárez, F. J. *Organometallics* **2011**, *30*, 2893-2896; u) Liu, P. N.; Ju, K. D.; Lau, C. P. *Adv. Synth. Cat.* **2011**, *353*, 275-280; v) Mantilli, L.; Gerard, D.; Besnard, C.; Mazet, C. *Eur. J. Inorg. Chem.* **2012**, 3320-3330; w) Bizet, V.; Pannecoucke, X.; Renaud, J.-L.; Cahard, D. *Angew. Chem. Int. Ed.* **2012**, *51*, 6467-6470; x) Sahoo, S.; Lundberg, H.; Eden, M.; Ahlsten, N.; Wan, W.; Zou, X.; Martín-Matute, B. *ChemCatChem* **2012**, *4*, 243-250; y) Bellarosa, L.; Díez, J.; Gimeno, J.; Lledós, A.; Suárez, F. J.; Ujaque, G. *Chem. Eur. J.* **2012**, *18*, 7749-7765; z) Bellarosa, L.; Díez, J.; Gimeno, A.; Lledós, F. J.; Suárez, G.; Vincent, C. *ACS Catal.* **2012**, *2*, 2087-2099.

(9) Carey, F. A.; Sundberg, R. J. *Advanced Organic Chemistry*. Part A: Structure and Mechanisms, Plenum Press, New York, **1991**, p. 12.

(10) a) Trost, B. M. *Science*, **1991**, *254*, 1471-1477; b) Trost, B. M. *Angew. Chem. Int. Ed.* **1995**, *34*, 259-281; c) Trost, B. M. *Acc. Chem. Res.* **2002**, *35*, 695-705; d) Eissen, M.; Mazur, R.; Quebbemann, H.–G.; Pennemann, K.–H. *Helv. Chim. Acta* **2004**, *87*, 524-535.

(11) Díaz-Álvarez, A. E.; Cadierno, V. *Recent Patents on Catalysis*, **2012**, *1*, 43-50.

(12) Selected examples of asymmetric isomerisations: a) Tani, K. *Pure Appl. Chem.* **1985**, *57*, 1845-1854; b) Tanaka, K.; Qiao, S.; Tobisu, M.; Lo M. M. C.; Fu, G. C. *J. Am. Chem. Soc.* **2000**, *122*, 9870-9871; c) Ito, S. M.; Kitahara, T.; Ikariya, J. *J. Am. Chem. Soc.* **2005**, *127*, 6172-6173; d) Mantilli, L.; Gérard, D.; Torche, S.; Besnard, C.; Mazet, C. *Angew. Chem. Int. Ed*. **2009**, *48*, 5143-5147 e) Mantilli L.; Mazet, C. *Tetrahedron Lett.* **2009**, *50*, 4141-4144; f) Li, J.–Q.; Peters B.; Andersson, P. G. *Chem. Eur. J.* **2011**, *17*, 11143-11145.

(13) a) Chowdhury, R. L.; Bäckvall, J.–E. *J. Chem. Soc. Chem. Commun*. **1991**, 1063-1064; b) Attila, A.; Csjernyik, G.; Szabó, K. J.; Bäckvall, J.–E. *Chem. Commun.* **1999**, 351-352.

(14) For related 1,4-addition of active methylene compounds across enones, see: a) Watanabe, M.; Murata, K.; Ikariya, T. *J. Am. Chem. Soc.* **2003**, *125*, 7508-7509; b) Ikariya, T.; Wang, H.; Watanabe, M.; Murata, K. *J. Organomet. Chem.* **2004**, *689*, 1377-1381; c) Wang, H.; Watanabe, M.; Ikariya, T. *Tetrahedron Lett*. **2005**, *46*, 963-966; d) Guo, R.; Morris, R. H.; Song, D. *J. Am. Chem. Soc*. **2005**, *127*, 516-517.

(15) a) Gazzard, L. J.; Motherwell, W. B.; Sandham, D. A. *J. Chem. Soc. Perkin Trans.* **1999**, *1*, 979-993; b) Crévisy, C.; Wietrich, M.; Le Boulaire, V.; Uma, R.; Grée, R. *Tetrahedron Lett.* **2001**, *42*, 395-398; c) Uma, R.; Davies, M.; Crévisy, C.; Grée, R. *Tetrahedron Lett*. **2001**, *42*, 3069-3072; d) Wang, M.; Li, C.–J. *Tetrahedron Lett*. **2002**, *43*, 3589-3591; e) Wang, M.; Yang, X.–F.; Li, C.–J. *Eur. J. Org. Chem.* **2003**, 998-1003; f) Yang, X.–F.; Wang, M.; Varma, R. S.; Li, C.–J. *Org. Lett.* **2003**, 5657-5660; g) Uma, R.; Gouault, N.; Crévisy, C.; Grée, R. *Tetrahedron Lett.* **2003**, *44*, 6187-6190; h) Yang, X.–F.; Wang, M.; Varma, R. S.; Li, C.–J. *J. Mol. Catal. A: Chem.* **2004**, *214*, 147-154; i) Cuperly, D.; Crévisy, C.; Grée, R. *Synlett* **2004**, 93-96; j) Branchadell, V.;

Crévisy, C.; Grée, R. *Chem. Eur. J.* **2004**, *10*, 5795-5803; k) Kiyooka, S.–I.; Ueno, M.; Ishiii. E. *Tetrahedron Lett.* **2005**, *46*, 4639-4642; l) Petrignet, J.; Roisnel, T.; Grée, R. *Tetrahedron Lett.* **2006**, *47*, 7745-7748; m) Cuperly, D.; Petrignet, J.; Crévisy, C.; Grée, R. *Chem. Eur. J.* **2006**, *12*, 3261-3274; n) Bartoszewicz, A.; Livendahl, M.; Martín-Matute, B. *Chem. Eur. J.* **2008**, *14*, 10547-10550; o) Ahlsten, N.; Martín-Matute, B. *Adv. Synth. Catal.* **2009**, *351*, 2657-2666; p) Cao, H. T. Roisnel, T. Grée, R. *Lett. Org. Chem.* **2009**, *6*, 507-510; q) Cao, H. T.; Roisnel, T. Valleix A. Grée, R. *Eur. J. Org. Chem.* **2011**, 3430-3436; r) Bartoszewicz, A.; Jeżowska, M. M.; Laymand, K.; Möbus, J.; Martín-Matute B. *Eur. J. Inorg. Chem.* **2012**, 1517-1530.

(16) a) Ahlsten N.; Martín-Matute, B. *Chem. Commun.* **2011**, *47*, 8331-8333; b) Ahlsten, N.; Bartoszewicz, A.; Agrawal S.; Martín-Matute, B. *Synthesis* **2011**, 2600-2608; c) Ahlsten, N.; Bermejo, A.; Martín-Matute, B. *submitted*; d) Martín-Matute, B.; Bermejo, A.; Ahlsten, N. patent application P-76116-USP.

(17) a) Geary, L. M; Pultin, P. G. *Tetrahedron: Asymm.* **2009**, *20*, 131-173; b) Mukherjee, S.; Yang, J. W.; Hoffmann, S.; List, B. *Chem. Rev.* **2007**, *107*, 5471-5569; c) Nishiyama, H.; Shiomi, T. *Topics in Current Chemistry* **2007**, *279*, 105-137.

(18) Recent examples of transition-metal-catalysed reductive aldol reactions: a) Taylor, S. J.; Duffey, M. O.; Morken, J. P. *J. Am. Chem. Soc.* **2000**, *122*, 4528-4529; b) Zhao, C.–X.; Duffey, M. O.; Taylor, S. J.; Morken, J. P. *Org. Lett.* **2001**, *3*, 1829-1831; c) Baik, T.–G.; Luis, A. L.; Wang, L.–C.; Krische, M. J. *J. Am. Chem. Soc.* **2001**, *123*, 5112-5113; d) Emiabata-Smith, D.; McKillop, A.; Mills, C.; Motherwell, W. B.; Whitehead, A. J. *Synlett* **2001**, 1302-1304; e) Han, S. B.; Hassan, A.; Krische, M. J. *Synthesis* **2008**, 2669-2679; f) Garner, S.; Han, S. B.; Krische, M. J. *Modern Reductions*; (Eds. Andersson, P.; Munslow, I.) Wiley-VCH: Weinheim, **2008**, 387-408.

(19) Zimmerman, H. E.; Traxler, M. D. *J. Am. Chem. Soc.* **1957**, *79*, 1920-1923.

(20) a) Murai, S.; Kakiuchi, F.; Sekine, S.; Tanaka, Y.; Kamatani, A.; Sonoda, M.; Chatani, N.; *Nature* **1993**, *366*, 529-531; b) Bercaw, J. E. *Angew. Chem., Int. Ed.* **1998**, *37*, 2181-2192; c) Kakiuchi, F.; Murai, S. *Topics in Organometallic Chemistry* (Ed. Murai, S.) Springer, Berlin, **1999**, vol. 3, 47-79; d) Labinger, J. A.; Bercaw, J. E. *Nature* **2002**, *417*, 507-514; e) Ritleng, V.; Sirlin. C.; Pfeffer, M. *Chem. Rev*. **2002**, *102*, 1731-1769; f) Godula, K.; Sames, D. *Science* **2006**, *312*, 67-72; g) Dick, A. R.; Sanford, M. S. *Tetrahedron* **2006**, *62*, 2439-2463; h) Alberico, D., Scott, M. E.; Lautens, M. *Chem. Rev.* **2007**, *107*, 174-238; i) Herrerías, C. I.; Yao, X.; Li, Z.; Li, C.–J. *Chem. Rev*. **2007**, *107*, 2546-2562; j) Bergman, R. G. *Nature* **2007**, *446*, 391-393; k) Lin, Z. *Coord. Chem. Rev*. **2007**, *251*, 2280-2291; l) Hartwig, J. F. *Nature* **2008**, *455*, 314-322; m) Colby, D. A.; Bergman, R. G.; Ellman, J. A. *Chem. Rev*. **2010**, *110*, 624-655; n) Lyons, T. W.; Sanford, M. S. *Chem. Rev.* **2010**, *110*, 1147-1169; o) Balcells, D.; Clot, E.; Eisenstein, O. *Chem. Rev*. **2010**, *110*, 749-823.

(21) C–H functionalisation by 1,2-addition to metal carbenoids/nitrenoids: a) Walsh, P. J.; Hollander, F. J.; Bergman, R. G. *J. Am. Chem. Soc.* **1988**, *110*, 8729-8731; b) Bennett, J. L.; Wolczanski, P. T. *J. Am. Chem. Soc.* **1997**, *119*, 10696-10719; c) Tran, E.; Legzdins, P. *J. Am. Chem. Soc.* **1997**, *119*, 5071-5072; d) Schafer, D. F.; Wolczanski, P. T. *J. Am. Chem. Soc.* **1998**, *120*, 4881-4882; e) Davies, H. M. L.; Manning, J. R. *Nature* **2008**, *451*, 417-424, Metalloradical

activation: f) Sherry, A. E.; Wayland, B. B. *J. Am. Chem. Soc.* **1990**, *112*, 1259-1261; g) Wayland, B. B.; Ba, S.; Sherry, A. E. *J. Am. Chem. Soc*. **1991**, *113*, 5305-5311.

(22) Metalloradical activation of aryl C–H: Rice, J. E.; Cai, Z.–W. *J. Org. Chem*. **1993**, *58*, 1415-1424.

(23) Mota, A. J.; Dedieu, A.; Bour, C.; Suffert, J. *J. Am. Chem. Soc.* **2005**, *127*, 7171-7182.

(24) a) Lapointe, D.; Fagnou, K. *Chem. Lett*. **2010**, *39*, 1118-1126; b) Ackermann, L. *Chem. Rev.* **2011**, *111*, 1315-1345.

(25) For a review using Ru complexes, see: a) Murai, S.; Kakiuchi, F.; Sekine, S.; Tanaka, Y.; Kamatani, A.; Sonoda, M.; Chatani, N. *Pure App. Chem*. **1994**, *66*, 1527-1534; b) Kakiuchi, F.; Murai, S. *Acc. Chem. Res*. **2002**, *35*, 826-834; c) Park, Y. J.; Jun, C.–H. *Bull. Korean Chem. Soc.* **2005**, *26*, 871-877; d) Kakiuchi, F.; Kochi, T. *Synthesis* **2008**, 3013-3039; For other metals, see: e) Ackermann, L. *Topics* in *Organometallic Chemistry*, Vol. 24, (Ed.: Chatani, N.), Springer, Berlin / Heidelberg**, 2007**, pp. 35-60; f) Satoh, T.; Miura, M. *Chem. Lett.* **2007**, *36*, 200-205; g) Seregin, I. V.; Gevorgyan, V. *Chem. Soc. Rev*. **2007**, *36*, 1173-1193; h) Bergman, R. G. *Nature* **2007**, *446*, 391-393; i) Campeau, L.–C.; Stuart, D. R.; Fagnou, K. *Aldrichim. Acta* **2007**, *40*, 35-41;

(26) Sonoda, M.; Kakiuchi, F.; Chatani, N.; Murai, M. *Bull. Chem. Soc. Jpn.* **1997**, *70*, 3117-3128.

(27) a) Martinez, R.; Chevalier, R.; Darses, S.; Genêt, J.–P. *Angew. Chem. Int. Ed.* **2006**, *45*, 8232-8235; b) Martinez, R.; Simon, M.–O.; Chevalier, R.; Pautigny, C.; Genêt, J.–P.; Darses, S. *J. Am. Chem. Soc*. **2009**, *131*, 7887-7895; c) Simon, M.–O.; Martinez, R.; Genêt, J.–P.; Darses, S. *Adv. Synth. Catal.* **2009**, *351*, 153-157; d) Simon, M.–O.; Martinez, R.; Genêt, J.–P.; Darses, S. *J. Org. Chem.* **2010**, *75*, 208-210; e) Simon, M.–O.; Genêt, J. –P.; Darses, S. *Org. Lett*. **2010**, *12*, 3038-3041.

(28) a) Guari, Y.; Sabo-Etienne, S.; Chaudret, B. *J. Am. Chem. Soc*. **1998**, *120*, 4228-4229; b) Toner, A. J.; Gründemann, S.; Clot, E.; Limbach, H. –H.; Donnadieu, B.; Sabo-Etienne, S.; Chaudret, B. *J. Am. Chem. Soc*. **2000**, *122*, 6777-6778; c) Guari, Y.; Castellanos, A.; Sabo-Etienne, S.; Chaudret, B. *J. Mol. Catal. A: Chem.* **2004**, *212*, 77-82; d) Grellier, M.; Vendier, L.; Chaudret, B.; Albinati, A.; Rizzato, S.; Mason, S.; Sabo-Etienne, S. *J. Am. Chem. Soc*. **2005**, *127*, 17592-17593; e) Toner, A. J.; Matthes, J.; Gründemann, S.; Limbach, H.–H.; Chaudret, B.; Clot, E.; Sabo-Etienne; S. *Proc. Natl. Acad. Sci.* **2007**, *104*, 6945-6950; f) Helmstedt, U.; Clot, E. *Chem. Eur. J.* **2012**, *18*, 11449-11458.

(29) a) Matsubara, T.; Koga, N.; Musaev, D. G.; Morokuma, K. *J. Am. Chem. Soc.* **1998**, *120*, 12692-12693; b) Matsubara, T.; Koga, N.; Musaev, D. G.; Morokuma, K. *Organometallics* **2000**, *19*, 2318-2329.

(30) a) Lu, P.; Paulasaari, J.; Jin, K.; Bau, R.; Weber, W. P. *Organometallics* **1998**, *17*, 584-588; b) Jazzar, R. F. R.; Mahon, M. F.; Whittlesey, M. K. *Organometallics* **2001**, *20*, 3745-3751; c) Drouin, S. D.; Amoroso, D.; Yap, G. P. A.; Fogg, D. E. *Organometallics* **2002**, *21*, 1042-1049; d) Guari, Y.; Castellanos, A.; Sabo-Etienne, S.; Chaudret, B. *J. Mol. Catal. A: Chem.* **2004**, *212*, 77-82; e) Grellier, M.; Vendier, L.; Chaudret, B.; Albinati, A.; Rizzato, S.; Mason, S.; Sabo-Etienne, S. *J. Am. Chem. Soc.* **2005**, *127*, 17592-17593.

(31) Kakiuchi, F.; Kochi, T.; Mizushima, E.; Murai, S. *J. Am. Chem. Soc*. **2010**, *132*, 17741-17750.
(32) a) Müller, T. E.; Beller, M. *Chem. Rev*. **1998**, 675-703; b) Mizuta, T.; Sakagushi, S.; Ishii, Y. J. *Org. Chem.* **2005**, *70*, 2195-2199; c) Müller, T. E.; Hultzsch, K. C.; Yus, M; Foubelo, F.; Tada, M. *Chem. Rev.* **2008**, *108*, 3795-3892; b) Nugent, T. C.; El-Shazly, M. *Adv. Synth. Catal*. **2010**, *352*, 753-819; d) Krueger, K.; Tillack, A.; Beller, M. *ChemSusChem* **2009**, *2*, 715-717; e) Ward, J.; Wohlgemuth, R. *Curr. Org. Chem*. **2010**, *14*, 1914-1927; f) Crozet, D.; Urrutigoity, M.; Kalck, P. *ChemCatChem* **2011**, *3*, 1102-1118.
(33) Grigg, R.; Mitchell, T. R. B.; Sutthivaiyakit, S.; Tongpenyai, N. *J. Chem. Soc. Chem. Commun*. **1981**, 611-612.
(34) a) Watanabe, Y.; Tsuji, Y.; Ohsugi, Y. *Tetrahedron Lett.* **1981**, *22*, 2667-2670.
(35) Blank, B.; Michlik, S.; Kempe, R. *Chem. Eur. J*. **2009**, *15*, 3790-3799.
(36) Gnanamgari, D.; Sauer, E. L. O.; Schley, N. D.; Butler, C.; Incarvito, C. D.; Crabtree, R. H. *Organometallics* **2009**, *28*, 321-325.
(37) Prades, A.; Corberán, R.; Poyatos, M.; Peris, E. *Chem. Eur. J*. **2008**, *14*, 11474-11479.
(38) a) Cumpstey, I.; Agrawal, S.; Borbas, E. K.; Martín-Matute, B. *Chem. Commun.* **2011**, *47*, 7827-7829; b) Agrawal, S.; Lenormand, M.; Martín-Matute, B. *Org. Lett.* **2012**, *14*, 1456-1459.
(39) An alternative mechanism: Zhao, Y.; Foo, S. W.; Saito, S. *Angew. Chem. Int. Ed.* **2011**, *50*, 3006-3009.
(40) a) *N-Heterocyclic Carbenes in Synthesis*, (Ed: Nolan, S. P.), Wiley-VCH: Weinheim, **2006**, pp. 1-304; b) *N-Heterocyclic Carbenes in Transition Metal Catalysis*; Topics in Organometallic Chemistry, Vol. 21 (Ed: Glorius, F.); Springer-Verlag, **2007**, pp. 1-218; c) Díez-González, S.; Marion, N.; Nolan, S. P. *Chem. Rev.* **2009**, *109*, 3612-3676; d) Jacobsen, H.; Correa, A.; Poater, A.; Constabile, C.; Cavallo, L. *Coord. Chem. Rev.* **2009**, *253*, 687-703; e) Corberán, R.; Mas-Marzá, E.; Peris, E. *Eur. J. Inorg. Chem*. **2009**, 1700-1716; f) Albrecht M. *Science* **2009**, *326*, 532-533; g) Schuster, O.; Yang, L.; h) Raubenheimer, H. G.; Albrecht, M. *Chem. Rev*. **2009**, *109*, 3445-3478; i) Krüger, A.; Albrecht, M. *Aust. J. Chem.* **2011**, *64*, 1113-1117.
(41) Wanzlick, V. H. W.; Schonher, H.–J. *Angew. Chem. Int. Ed*. **1968**, *7*, 141-142.
(42) Arduengo, A. J.; Dias, H. V. R.; Kline, M. *J. Am. Chem. Soc.* **1992**, *114*, 9724-9725.
(43) a) Mukaiyama, T. *Pure Appl. Chem.* **1983**, *55*, 1749-1758; b) Arya, P. Qin, H. *Tetrahedron* **2000**, *56*, 917-947.
(44) Sheppard, T. D. *Synlett*, **2011**, 1340-1344.
(45) Recent reviews on transition-metal-catalysed reductive aldol and Mannich reactions: a) Nishiyama, H. Shiomi, T. *Top. Curr. Chem*. **2007**, *279*, 105-137; b) Han, S. B. Hassan, A. Krische, M. J. *Synthesis*, **2008**, 2669-2679; c) Garner, S. Han, S. B. Krische, M. J. In *Modern Reduction Methods* (Eds.: P. Andersson, I. Munslow), Wiley-VCH, Weinheim, **2008**; pp. 387-408.
(46) Schneider, B.; Goldberg, I.; Reshef, D.; Stein, Z.; Shvo, Y. *J. Organomet. Chem.* **1999**, *588*, 92-98.
(47) Choi, J. H.; Kim, Y. H.; Nam, S. H.; Shin, S. T.; Kim, M. J.; Park, J. *Angew. Chem. Int. Ed.* **2002**, *41*, 2373-2376.
(48) Connelly, N. G.; Manners, I. *J. Chem. Soc. Dalton Trans.* **1989**, 283-288.

(49) Nelson, G. O.; Sumner, C. E. *Organometallics* **1986**, *5*, 1983-1986.
(50) Mizuno, A.; Kusama, H.; Iwasawa, N. *Chem. Eur. J.* **2010**, *16*, 8248-8250.
(51) a) Warner, M.; Nagendiran, A.; Bogár, K; Bäckvall J.–E. *manuscript*; b) Lihammar, R.; Millet, R.; Bäckvall J.–E. *manuscript.*
(52) a) Kleinmann E. F. in *Comprehensive Organic Synthesis*, vol. 2, (Eds.: Trost, B. M. Fleming I.), Pergamon Press, New York, **1991**, ch. 4.1.-4.3; b) Arend, M.; Westermann, B.; Risch, N. *Angew. Chem. Int. Ed.* **1998**, *37*, 1044-1070.
(53) a) Bohme, H.; Haake, M. *Advances in Organic Chemistry*, (Ed.: E. C. Taylor), John Wiley and Sons, New York, **1976**; pp. 107-223; b) Muller, R. Goesmann, H. Waldmann, H. *Angew. Chem. Int. Ed.* **1999**, *38*, 184-187; c) Notz, W.; Tanaka, F.; Watanabe, S.–I.; Chowdari, N. S.; Turner, J. M.; Thayumanavan, R.; Barbas, C. F. *J. Org. Chem.* **2003**, *68*, 9624-9634 and references cited there in; d) Ting, A.; Suginome, M.; Uehlin, L.; Murakami, M. *J. Am. Chem. Soc.* **2004**, *126*, 13196-13197; e) Marques, M. M. B. *Angew. Chem. Int. Ed.* **2006**, *45*, 348-352; f) Schaus, S. E. *Eur. J. Org. Chem.* **2007**, *35*, 5797-5815.
(54) Recent examples of the use of *N*-aryl aldimines in reductive Mannich reactions: a) Townes, J. A.; Evans, M. A.; Queffelec, J.; Taylor, S. J.; Morken, J. A. *Org. Lett.* **2002**, *4*, 2537-2540; b) Nishiyama, H.; Ishikawa, J.; Shiomi, T. *Tetrahedron Lett.* **2007**, *48*, 7841-7844.
(55) Recent examples of transition-metal-catalysed Mannich reactions with Boc-protected imines: a) Kim, E. J;. Kang, Y. K.; Kim, D. Y. *Bull. Kor. Chem. Soc*. **2009**, *30*, 1437-1438; b) Shepherd, N. E.; Tanabe, H.; Xu, Y.; Matsunaga, S.; Shibasaki, M. *J. Am. Chem. Soc.* **2010**, *132*, 3666-3667; c) Zhao, Q.–Y.; Shi, M. *Tetrahedron* **2011**, *67*, 3724-3732; d) Kang, Y. K.; Kim, D. Y.; *Tetrahedron Lett.* **2011**, *52*, 2356-2358.
(56) Recent examples of the use of *N-t*osyl imines in reductive Mannich reactions: a) Muraoka, T.; Kamiya, S.–I.; Matsuda, I.; Itoh, K. *Chem. Commun.* **2002**, 1284-1285; b) Garner, S. A.; Krische, M. J. *J. Org. Chem.* **2007**, *72*, 5843-5846; c) Prieto, O.; Lam, H. W. *Org. Biomol. Chem*. **2008**, *6*, 55-57.
(57) For some recent examples on the use of heteroarylsulfonyl imines in organometallic catalysis, see: a) Esquivias, J.; Gómez Arrayás, R.;. Carretero, J. C. *J. Am. Chem. Soc.* **2007**, *129*, 1480-1481; b) Morimoto, H.; Lu, G.; Aoyama, N.; Matsunaga, S.; Shibasaki, M. *J. Am. Chem. Soc.* **2007**, *129*, 9588-9589; c) Nakamura, S.; Nakashima, H.; Sugimoto, H.; Sano, H.; Hattori, M.; Shibata, N.; Toru, T. *Chem. Eur. J.* **2008**, *14*, 2145-2152; d) Nakamura, S.; Nakashima, H.; Yamamura, A.; Shibata, N.; Toru, T. *Adv. Synth. Catal.* **2008**, *350*, 1209-1212.
(58) a) Martín-Matute, B.; Edin, M.; Bogár, K.; Bäckvall, J.–E. *Angew. Chem. Int. Ed.* **2004**, *43*, 6535-6539; b) Martín-Matute, B.; Edin, M.; Bogár, K.; Kaynak, F. B.; Bäckvall, J.–E. *J. Am. Chem. Soc.* **2005**, *127*, 8817-8825.
(59) a) Hartwig, J. F.; Andersen, R. A.; Bergman, R. G. *J. Am. Chem. Soc.* **1990**, *112*, 5670-5671; b) Hartwig, J. F.; Bergman, R. G.; Anderson, R. A. *Organometallics* **1991**, *10*, 3326-3244; c) Tasley, B. T.; Rapta, M.; Kulawiec, R. J. *Organometallics* **1996**, *15*, 2852-2854.
(60) This signal is similar to that obtained for other ruthenium C-bound enolates (see reference 59c) and clearly different from that of ruthenium O-bound enolates (*e.g.* 76 ppm, see reference 59b)

(61) In published NMR data for O-enolates, the α carbon, as part of the double bond, appears at 169 ppm (see reference 59b).
(62) Tolman, R. C. *Proc. Natl. Acad. Sci. U.S.A.* **1925**, *11*, 436-439.
(63) a) Åberg, J. B.; Nyhlén, J.; Martín-Matute, B.; Privalov, T.; Bäckvall, J.–E. *J. Am. Chem. Soc.* **2009**, *131*, 9500-9501; b) Warner, C.; Verho, O.; Bäckvall, J.–E. *J. Am. Chem. Soc.* **2011,** *133*, 2820-2823.
(64) a) Nyhlén, J.; Privalov, T.; Bäckvall, J.–E. *Chem. Eur. J.* **2009**, *15*, 5220-5229; b) Steward, B.; Nyhlén, J.; Martín-Matute, B.; Bäckvall, J.–E.; Privalov, T. *Dalton Trans*. DOI: 10.1039/c2dt31919e
(65) Ruthenium alkoxide complexes: a) Loren, S. D.; Campion, B. K.; Heyn, R. H.; Tilley, T. D.; Bursten, B. E.; Luth, K. W. *J. Am. Chem. Soc.* **1989**, *111*, 4712-4718; b) Daley, C. J. A.; Bergens, S. H. *J. Am. Chem. Soc.* **2002**, *124*, 3680-3691.
(66) a) Martín-Matute, B.; Edin, M.; Bogár, K.; Bäckvall, J.–E. *Angew. Chem. Int. Ed.* **2004**, *43*, 6535-6539; b) Martín-Matute, B.; Edin, M.; Bogár, K.; Kaynak, F. B.; Bäckvall, J.–E. *J. Am. Chem. Soc.* **2005**, *127*, 8817-8825.
(67) For direct arylations without involving Ru(0) species, see: a) Özdemir, I.; Demir, S.; Çetinkaya, B.; Gourlaouen, C.; Maseras, F.; Bruneau,C.; Dixneuf, P. H. J. *Am. Chem. Soc*. **2008**, *130*, 1156-1157; b) Ackermann, L.; Vicente, R.; Althammer, A. *Org. Lett*. **2009**, *102*, 2299-2302.
(68) a) Chung, C.–S. *Inorg. Chem*. **1979**, *18*, 1318-1321; b) Myers, R. T. *Inorg. Chem*. **1978**, *17*, 952-958; c) Hancock, R. D.; Martell, A. E. *Comm. Inorg. Chem*. **1988**, *6*, 237-284; d) Martell, A. E.; Hancock, R. D.; Motekaitis, R. J. *Coord. Chem. Rev*. **1994**, *133*, 39-65; e) Breslow, R.; Belvedere, S.; Gershell, L.; Leung, D. *Pure Appl. Chem*. **2000**, *72*, 333-342.
(69) Concept of ligand hemilability: a) Braunstein, P.; Naud, F. *Angew. Chem. Int. Ed.* **2001**, *40*, 680-699; b) Werner, H. *Dalton Trans.* **2003**, 3829-3837; c) Braunstein, P. *J. Organomet. Chem*. **2004**, *689*, 3953-3967; d) Slone, C. S.; Weinberger, D. A.; Mirkin, C. A. in *The Transition Metal Coordination Chemistry of Hemilabile Ligands*, in Progress in Inorganic Chemistry, Vol. 48 (Ed: Karlin K. D.), John Wiley & Sons, Inc., Hoboken, NJ, **2007**, pp. 233-350.
(70) a) Rocha Gonsalves, A. M. d'A.; Bayón, J. C.; Pereira, M. M.; Serra, M. E. S. Pereira, J. P. R. *J. Organomet. Chem.* **1998**, *553*, 199-204; b) Quirmbach, M.; Holz, J.; Tararov, V. I.; Börner, A. *Tetrahedron* **2000**, *56*, 775-780; c) Börner, A. *Eur. J. Inorg. Chem.* **2001**, 327-337.
(71) Reviews on donor-functionalized *N*-heterocyclic carbene complexes: a) Liddle, S. T.; Edworthy, I. S.; Arnold, P. L. *Chem. Soc. Rev.* **2007**, *36*, 1732-1744; b) Gade, L. H.; Bellemin-Laponnaz, S. *Coord. Chem. Rev.* **2007**, *251*, 718-725; c) Kühl, O. *Chem. Soc. Rev.* **2007**, *36*, 592-607; d) Pugh, D.; Danopoulos, A. A. *Coord. Chem. Rev.* **2007**, *251*, 610-641; e) Lee, H. M.; Lee, C. C.; Cheng, P. Y. *Curr. Org. Chem.* **2007**, *11*, 1491-1524; f) Normand, A. T.; Cavell, K. J. *Eur. J. Inorg. Chem.* **2008**, 2781-2800; g) Poyatos, M.; Mata, J. A.; Peris, E. *Chem. Rev.* **2009**, *109*, 3677-3707; h) John, A.; Ghosh, P. *Dalton Trans.* **2010**, *39*, 7183-7206; i) Bierenstiel, M.; Cross, E. D. *Coord. Chem. Rev.* **2011**, *255*, 574-590.
(72) a) Yang, X.; Fei, Z.; Geldbach, T. J.; Phillips, A. D.; Hartinger, C. G.; Li, Y.; Dyson, P. J. *Organometallics* **2008**, 27, 3971-3977; b) Jiménez, M. V.; Pérez-Torrente, J. J.; Bartolomé, M. I.; Gierz, V.; Lahoz, F. J.; Oro, L. A.

Organometallics **2008**, *27*, 224-234; c) Gnanamgari, D.; Sauer, E. L. O.; Schley, N. D.; Butler, C.; Incarvito, C. D.; Crabtree, R. H. *Organometallics* **2009**, *28*, 321-325; d) Lu, C.; Gu, S.; Chen, W.; Qiu, H. *Dalton Trans.* **2010**, *39*, 4198-4204; e) Specht, Z. G.; Cortés-Llamas, S. A.; Tran, H. N.; van Niekerk, C. J.; Rancudo, K. T.; Golen, J. A.; Moore, C. E.; Rheingold, A. L.; Dwyer, T. J. ; Grotjahn, D. B. *Chem. Eur. J.* **2011**, *17*, 6606-6609; f) Gulcemal, S.; Daran, J.–C.; Çetinkaya, B. *Inorg. Chim. Acta* **2011**, *365*, 264-268; g) Topf, C.; Hirtenlehner, C.; Zabel, M.; List, M.; Fleck, M.; Monkowius, U. *Organometallics* **2011**, *30*, 2755-2764; h) Cross, W. B.; Daly, C. G.; Boutadla, Y.; Singh, K. *Dalton Trans.* **2011**, *40*, 9722-9730; i) Kumar, S.; Narayanan, A.; Rao, M. N.; Shaikh, M. M.; Ghosh, P. *J. Organomet. Chem.* **2012**, *696*, 4159-4165.

(73) For pendant hydroxyl group in Pt-catalysed hydration of nitriles, see; a) Ghaffar, T.; Parkins, A. W. *Tetrahedron Lett*. **1995**, *36*, 8657-8660; b) Ghaffar, T.; Parkins, A. W. *J. Mol. Catal. A: Chem.* **2000**, *160*, 249-261; c) Jiang, X.–B.; Minnaard, A. J.; Feringa, B. L.; De Vries, J. G. *J. Org. Chem.* **2004**, *69*, 2327-2331; For the influence of a hydroxyl group on the ligand in a Rh catalysed asymmetric hydrogenation of olefins, see: d) Gunanathan, C.; Milstein, D. *Angew. Chem. Int. Ed.* **2008**, *47*, 8661-8664; e) Kim, J. W.; Yamaguchi, K.; Mizuno, N. *J. Catal.* **2009**, *263*, 205-208; f) Yamaguchi, K.; He, J.; Oishi, T.; Mizuno, N. *Chem. Eur. J.* **2010**, *16*, 7199-7207.

(74) Bartoszewicz, A.; Marcos, R.; Sahoo, S.; Inge, A. K.; Zou, X.; Martín-Matute, B. *Chem. Eur. J.* **2012**, *18*, 14510-14519.

(75) Recently reported system that could be considered as metal-ligand bifunctional: Peñafiel, I.; Pastor, I. M.; Yus, M.; Esteruelas, M. A.; Oliván, M. *Organometallics* **2012**, *31*, 6154-6161.

(76) Balcells, D.; Nova, A.; Clot, E.; Gnanamgari, D.; Crabtree, R. H.; Eisenstein, O. *Organometallics* **2008**, *27*, 2529-2535.

(77)Arnold, P. L.; Rodden, M.; Davis, K. M.; Scarisbrick, A. C.; Blake, A. J.; Wilson, C. *Chem. Commun*. **2004**, 1612-1613.

(78) a) Feng, Y. Jiang, B. Boyle, P. A. Ison, E. A. *Organometallics*, **2010**, *29*, 2857-2867; b) Albrecht, M.; Miecznikowski, J. R.; Samuel, A.; Faller, J. W.; Crabtree, R. H. *Organometallics* **2002**, *21*, 3596-3604.

(79) Addition of K_2CO_3 gives 77% conversion after 17 h. Fujita, K.–I.; Li, Z.; Ozeki, N.; Yamaguchi, R. *Tetrahedron Lett*. **2003**, *44*, 2687-2690.

(80) The reactions in which AgCl was not filtered-off afforded the same conversions at the same rate.

(81) a) Michlik, S. Kempe, R. *Chem. Eur. J.* **2010**, *16*, 13193-13198; b) Michlik, S. Hille, T.; Kempe, R. *Adv. Synth. Catal*. **2012**, *354*, 847-862.

(82) The opposite selectivity, aromatic amine alkylation, was reported with the catalytic system from reference 39.

(83) It is important to mention that the relatively high catalytic activity of complex **68** (Table 9, entry 11), containing a methyl substituent on the oxygen atom, indicates that this complex operates *via* a different mechanism, in which the proton accepting capability is not crucial for catalysis.

(84) The methanol coordination and deprotonation could theoretically occur simultaneously by a σ-bond metathesis, directly connecting **INT-1** and **INT-4**.

However, despite multiple attempts, we were not able to locate the corresponding transition state.
(85) Hydrogenation of Z-imine *via* both the inner and outer sphere mechanisms was also tested. The obtained energy barriers were however higher than those for the E-imine, therefore involvement of the Z-imine in the reaction was ruled out.
(86) Wang, D.; Liu, J.; Wu, Z.; Zhang, J.; Su, Y.; Liu, Z.; Xu, C. *Int. J. Electrochem. Sci.* **2009**, *4*, 1672-1678.
(87) *Jaguar*, *version* 7.8, Schrödinger, LLC, New York, NY, 2011.
(88) a) Becke, A. D. *J. Chem. Phys.* **1993**, *98*, 5648-5652 ; b) Becke, A. D. *J. Chem. Phys.* **1993**, *98*, 1372-1377; c) Lee, C.; Yang W.; Parr, R. G. *Phys. Rev. B*, **1988**, *37*, 785-789.
(89) LACVP* uses the 6-31G* basis set for all light elements and the Hay–Wadt ECP and basis set for Ir, see: Hay P. J.; Wadt, W. R. J. *J. Chem. Phys.* **1985**, *82*, 299-310.
(90) a) Zhao Y.; Truhlar, D. G. *Theor. Chem. Acc.* **2008**, *120*, 215-241, b) Zhao Y.; Truhlar, D. G. *Acc. Chem. Res.* **2008**, *41*, 157-167.
(91) Sieffert, N.; Bühl, M. *J. Am. Chem. Soc*. **2010**, *132*, 8056-8070.
(92) a) Marten, B.; Kim, K.; Cortis, C.; Friesner, R. A.; Murphy, R. B.; Ringnalda, M. N.; Sitkoff, D.; Honig, B. *J. Phys. Chem.* **1996**, *100*, 11775-11788; b) Tannor, D. J.; Marten, B.; Murphy, R.; Friesner, R. A.; Sitkoff, D.; Nicholls, A.; Ringnalda, M.; Goddard, III, W. A.; Honig, B. *J. Am. Chem. Soc.* **1994**, *116*, 11875-11882.